Pathological Astrocyte Morphology and Dysregulated Glutamate Homeostasis in a Preclinical Phenotyping Model of Methamphetamine Addiction

Timothy Justin Hill

Bachelor of Psychology – Honours

Supervisors: Prof Jennifer Cornish and Dr Sarah Baracz

Empirical thesis submitted in partial fulfillment of the requirements for the degree of

Master of Research

Department of Psychology, Macquarie University, December 2019

Abstract

Methamphetamine (METH) remains one of the most abused illicit substances in Australia with only 10-20% of METH-users developing METH-addiction. Glutamate homeostasis and astrocyte-mediated neuroinflammation may be responsible for addiction behaviours. Therefore, this study aimed to distinguish between the role of astrocyte hypertrophy and glutamate activity in the neurocircuitry of addiction-vulnerable, compared to addiction-resistant animals. The study employed an intravenous self-administration (IVSA) addiction-phenotyping paradigm.

Male Sprague-Dawley rats (n = 30) were scored on four addictive behaviours, cue-induced METH-seeking, motivation to take-METH, habitual METH-seeking and resistance-to-extinction to characterise rats as either addiction-vulnerable (AVul) or addiction-resistant (ARes). AVul, ARes and control (n = 5) rats then had their brains stained for calmodulin-kinase-II-alpha (CaMKIIa), glial-fibrillary acidic-protein (GFAP), and synapsin-I. Glutamate activity, astrocyte quantity and morphology, and relationship between astrocyte-synapse connections and glutamate activity, at each level of each region investigated, were then measured.

Results revealed decreased glutamate activity in the nucleus accumbens core (NAcc), central amygdala (CeA) and basolateral amygdala (BLA) in AVul rats, compared to controls. There was no difference in astrocyte proliferation in AVul or ARes rats compared to controls, except for a decrease in the CeA of AVul rats. There was a widespread increase in astrocyte hypertrophy in AVul compared to ARes and control rats, with METH-induced hypertrophy, independent of phenotype. Correlational analyses suggested changes in glutamate homeostasis throughout addiction neurocircuitry.

Findings from this study suggested dysregulation of glutamate homeostasis in the rostral NAcc and rostral-central BLA in AVul rats, regions involved in cue-induced relapse in humans and animals. Likewise, widespread astrocyte hypertrophy was found to be generally more severe in AVul, compared to ARes and control, rats. Therefore, it was posited that suppressed glial-glutamate release and increased neuroinflammatory mechanisms may be a factor in METH-addiction behaviours. These findings therefore highlight the potential of glutamatergic and astrocytic targets for relapse-prevention.

Table of Contents

Table of Figures

Table of Tables

List of Abbreviations

5-HT	Serotonin
ACC	Anterior cingulate cortex
AMPAR	α-amino-3-hydroxy-5-methyl-4-isoxazolepropionic acid receptors
ANOVA	Analysis of variance
ARes	Addiction resistant
AVul	Addiction vulnerable
BBB	Blood brain barrier
BLA	Basolateral amygdala
BNST	Bed nucleus of the stria terminalis
BP	Breakpoint
Ca^{+2}	Calcium ion
CaMKIIa	Calmodulin-kinase-II alpha
CeA	Central amygdala
CNS	Central nervous system
CPP	Conditioned place preference
D1R	Dopamine D1 receptor
DA	Dopamine

DLS	Dorsolateral striatum
DMS	Dorsomedial striatum
DS	Dorsal striatum
DSM-5	Diagnostic and statistical manual-5
FR	Fixed ratio
GABA	γ-amino butyric acid
GDNF	Glial-derived neurotrophic factor
GFAP	Glial fibrillary acidic protein
GFAP+	Glial fibrillary acidic protein positive
GFP	Green fluorescent protein
GLT-1	Glutamate transporter-1
GP	Globus pallidus
HDS	Habitual drug seeking
HSD	Honest significant difference
iGluR	Ionotropic glutamate receptor
IL	Infralimbic cortex
ILe	Interleukin
lCeA	Lateral central amygdala
LOFC	Lateral orbitofrontal cortex
mCeA	Medial central amygdala

MDT	Medial dorsal thalamus
METH	Methamphetamine
mGluR2/3	Metabotropic glutamate receptor 2 and 3
mGluR5	Metabotropic glutamate receptor 5
MSN	Medium spiny neuron
mPFC	Medial prefrontal cortex
NA	Noradrenaline
NAc	Nucleus accumbens
NAcc	Nucleus accumbens core
NAcs	Nucleus accumbens shell
NHS	Normal horse serum
NO	Nitric oxide
nNOS	Neuronal nitric oxide synthase
PAP	Perisynaptic astrocytic process
PBS	Phosphate-buffered saline
PFA	Paraformaldehyde
PFC	Prefrontal cortex
PR	Progressive ratio
PrL	Prelimbic cortex
ROI	Region of interest

ROS	Reactive oxygen species
SC	Subcutaneous
Sev-1	Severe diffuse (astrogliosis)
Sev-2	Severe with scar tissue (astrogliosis)
SN	Substantia nigra
STN	Subthalamic nucleus
TPBS	Tris + phosphate-buffered-saline
TPBSm	Tris + phosphate-bufered-saline with merthiolate
VMAT-2	Vesicular monoamine transporter-2
vmPFC	Ventromedial prefrontal cortex
VP	Ventral pallidum
VTA	Ventral tegmental area
Xc-	Cystine-glutamate antiporter

Statement of Originality and Ethical Approval

I, Timothy Justin Hill, hereby confirm that all material contained in this project are my original authorship and ideas, except where the work of others has been acknowledged or referenced. I also confirm that the work has not been submitted for a higher degree to any other university or institution.

The research project was approved by the Macquarie University Animal Ethics Committee.

Animal Research Authority: 2019/006

Mr Hill was supported by the Research Training Pathway Scholarship Scheme for the latter half of the Master of Research Year 2. Research studies were funded by internal funding from Macquarie University and NHMRC grants awarded to JLC.

_____

Timothy Justin Hill

Date: 12/12/19

Co-Author Contribution

Cornish, J.L **5%**

Contributed to research design, provided assistance with surgeries, perfusions, and manuscript editing.

Baracz, S.J **4%**

Contributed to research design, provided assistance with surgeries, perfusions, self-administration and brain analysis.

Turner, A.J **2%**

Provided assistance with surgeries, self-administration, and perfusions.

Katherine, R.J **2%**

Provided guidance on brain analysis tools and techniques.

Everitt, N.A **2%**

Contributed to research design and assisted with coding.

Acknowledgements

After a big year full of learning, sacrifice and plenty of lab time I would like to thank the following people. First and foremost, I would like to thank my two mentors Jen and Sarah. Jen, your passion for neuroscience and dedication to my research training have been instrumental in my growth as a researcher over the past two years. Sarah, thank you for your guidance in and out of the lab and for introducing me to the world of immunohistochemistry. Thank you both for always making time for me and my project even when you were both as busy as ever, and for being patient with me as challenges arose throughout my project.

I would also like to thank my colleagues Nick and Katie for helping me brainstorm solutions to many problems and providing me additional support throughout my project. Also, to the Cornish lab honours students, thank you for sharing likely the hardest year of university with me. It has been fantastic getting to know you all and I'm excited to see you all accomplish so much.

Thank you to my family who are a constant source of support and love for me when I need it the most. You have always told me to just keep going and believed in me even when I couldn't see the light at the end of the tunnel and that means more than you can know. I'd also like to thank my friends who provided a much-needed escape when necessary and were exceptionally understanding and supportive.

Finally, thank you to my beautiful partner Zeyad. Despite our hopes, we were both put through the ringer again this year and came out the end better for it. You always make me feel like I can accomplish whatever I set my mind to and provide me with unconditional love and support. May the next few years be a little bit less stressful and a little more enjoyable as we both move on from our current research degrees and into a new chapter.

1. Introduction

Drug addiction is a neuropsychiatric disease affecting approximately 31 million individuals worldwide (United Nations Office on Drugs and Crime, 2018). In the Diagnostic Statistical Manual-5 (DSM-5), "Substance Use Disorder", including drug addiction, is defined as a habitual, compulsive drug-use disorder characterised by chronic relapse to drug-seeking despite significant adverse consequences (American Psychiatric Association, 2013). This cycle of chronic drug relapse is maintained by aversive withdrawal symptoms and powerful cravings (Koob & Volkow, 2016; Robinson & Berridge, 1993) persisting for months to years despite protracted abstinence from drug exposure (Hyman, Malenka, & Nestler, 2006; Koob & Volkow, 2010).

Illicit drug-use is common, with approximately 275 million consumers worldwide in 2016 (United Nations Office on Drugs and Crime, 2016). However, drug addiction only occurs in a subset of drug abusers (Volkow & Morales, 2015; Wagner, 2002). Acutely, drugs of abuse often induce a hedonic state, which may reinforce drug-taking behaviours (Volkow & Morales, 2015). Although, a transition from impulsive drug-use to compulsive drug-abuse is required for the development of an addiction disorder (Piazza & Deroche-Gamonet, 2013). Following this transition, drug-use becomes uncontrollable, driven less by hedonism and more by cravings and withdrawal symptoms. Ultimately, this compulsion results in a chronic relapsing syndrome that holds addicts in a cycle of addiction (Koob & Volkow, 2016). The transition to chronic compulsive use is reflected in pathological dysregulation of the neurocircuitry typically involved in drug reward (Koob & Volkow, 2016; Volkow & Morales, 2015). Therefore, it is imperative that research investigates changes to the

neurocircuitry involved in this vicious relapse cycle to enable the development of effective treatments for this severely undertreated disorder (United Nations Office on Drugs and Crime, 2018).

1.1 Methamphetamine.

In Australia and overseas, amphetamine-based stimulants, including methamphetamine (METH), are the second most commonly abused illicit drug, after cannabis (Australian Institute of Health and Welfare, 2016; United Nations Office on Drugs and Crime, 2018). Approximately 1.4% of Australians have consumed METH within the last twelve months, with 57% of METH-users consuming the drug in its most potent form, "ice" or crystalline-METH. Recently, a sudden increase in METH-related fatalities and harms has been attributed to an increase in the use of "ice" and the intravenous administration method (Darke, Kaye, & Duflou, 2017; Degenhardt et al., 2017). Due to its potency and delivery route, crystalline-METH rapidly accesses the brain, resulting in an intense "high", contributing to the development of addiction (Rose & Grant, 2008; Volkow & Morales, 2015) and enhancing acute neurotoxicity, the leading cause of METH-associated deaths in Australia (Darke et al., 2017). Currently, there are no approved efficacious pharmacotherapies for METH-addiction (Morley, Cornish, Faingold, Wood, & Haber, 2017).

1.1.1 Pharmacology of METH. Methamphetamine (N-methyl-1-phenylpropane-2-amine) is a potent psychostimulant and a synthetic derivative of another commonly abused drug, amphetamine, or "base" (Courtney & Ray, 2014). When compared, METH and amphetamine are structurally similar compounds, however METH is highly lipophilic and more easily penetrates the blood brain barrier (BBB), increasing the abuse potential of METH compared to amphetamine (Cruickshank & Dyer, 2009). METH induces the swift and efficient release of the monoamine neurotransmitters noradrenaline (NA), dopamine (DA) and serotonin (5-HT), listed in order of release efficacy (Rothman et al., 2001), via three

mechanisms (Courtney & Ray, 2014). The primary mechanism is the reversal of vesicular monoamine transporter-2 (VMAT-2), expressed on presynaptic terminals, leading to vesicular monoamine release into the cytosol. The second mechanism is the reversal of NA, DA and 5-HT transporters, funnelling monoamines from the cytosol into the synaptic cleft. The final mechanism is the suppression of monoamine oxidase, hindering the metabolism of these monoamines. These processes complement one another to encourage a spike of monoamine levels in the synapse, facilitating the activation of monoamine receptors, promoting the euphoria that is often associated with acute METH-use, in tandem with a suite of additional acute effects (Courtney & Ray, 2014; Elkashef et al., 2008).

1.1.2 Acute psychological and physiological effects of METH-use. Subsequent to use, METH-users report feeling euphoria with spikes in energy, heightened confidence, suppressed fatigue and hyper-sexuality (Elkashef et al., 2008). The euphoria experienced is believed to be onset by the amplified DA neurotransmission in the brain, rendering METH both rewarding and therefore highly reinforcing (Courtney & Ray, 2014). Enhancements in sustained and divided attention are frequently reported, in addition to improved reaction time, when METH is used for this intention (Cruickshank & Dyer, 2009). Aversive acute psychological effects of METH include irritability, depressive states, negative affect, paranoia, hallucinations and anxiety (Courtney & Ray, 2014; Darke, Kaye, McKetin, & Duflou, 2008), often related to withdrawal. Undesirable physiological symptoms include hypertension, hyperthermia, excessive sweating, dehydration, tachycardia and hasty breathing (Darke et al., 2008; Zorick, Rad, Rim, & Tsuang, 2008). At high doses, METH can also induce neurotoxicity, psychosis and occasionally even death (Cruickshank & Dyer, 2009; Mash, 2016).

1.1.3 Chronic psychological and physiological effects of METH-use. Certain acute psychological consequences of METH-use persist with chronic consumption, such as

depression and anxiety. Additionally, other symptoms arise after considerable, enduring METH-abuse, such as protracted fatigue, reduced psychomotor activity, dysregulated sleep patterns, psychosis and anhedonia (Darke et al., 2008; McKetin, Lubman, Baker, Dawe, & Ali, 2013). The more severe symptoms often fade after seven to ten days, however the more insidious symptoms, such as anhedonia, can endure for months to a year (McKetin et al., 2013; Rose & Grant, 2008). Chronic METH-consumption may also result in the development of mild to severe neuropsychological impairments, such as diminished executive functions, poor impulse control, and a deficit in working memory (Darke et al., 2008; Panenka et al., 2013). Following chronic METH-use, drug tolerance can often develop, leading to a required escalation of dose and potency to experience the same rewarding effects (Courtney & Ray, 2014). A need for higher dosing is usually accompanied by a shift from less potent routes of administration, such as oral dosing, to more direct routes, such as intravenous injection. This transition quite often exacerbates the psychological and physiological consequences of acute and chronic METH use, predominantly those related to withdrawal, neurotoxicity and addiction (Cruickshank & Dyer, 2009).

1.1.4 Lack of treatments for METH-addiction.

Despite the significant psychological and neuropsychiatric impacts of METH-addiction, and the burden it has on the world's health systems and economy (Australian Institute of Health and Welfare, 2016; Degenhardt et al., 2017; United Nations Office on Drugs and Crime, 2018), no effective treatments exist (Courtney & Ray, 2014; Morley et al., 2017). Behavioural therapies show poor treatment efficacy at preventing METH-relapse (Morley et al., 2017) and effective neuropsychological programs have yet to be implemented. Some promising pharmacotherapies for treatment of this disease have surfaced, including methylphenidate (Rezaei et al., 2015), mirtazapine (Colfax et al., 2011) and topiramate (Rezaei, Ghaderi, Mardani, Hamidi, & Hassanzadeh, 2016). Unfortunately, none of these candidates have

demonstrated consistent efficacy to warrant use, and none have been approved for clinical applications (Morley et al., 2017). Due to the lack of effective treatment options available to METH-addicts, it is vital that novel targets for treatment are uncovered. For this to occur, understanding of the neurobiological consequences and mechanisms of METH-addiction needs to be advanced.

1.2 Neurobiology of reward.

The common neural pathway that is affected by the administration of drugs of abuse is intrinsic to most motivated behaviours; the DA reward pathway (Kalivas & Volkow, 2005; Volkow & Morales, 2015). Reward is an event that results in a pleasurable or emotionally positive psychological experience (Kalivas & Volkow, 2005). Importantly, experience of this reward leads to positive reinforcement which encourages the repetition of actions that lead to the reward (Koob, 2005). This process maintains drug-use in the initial stages of addiction (Hyman et al., 2006; Kalivas & Volkow, 2005), but is also essential to survival due to the reinforcement of adaptive rewarding behaviours, such as feeding and sex (Cannon & Bseikri, 2004). Reward processes are orchestrated by the release of monoamines, such as DA, within the mesocorticolimbic system (Hyman et al., 2006; Koob & Volkow, 2010). The mesocorticolimbic pathway, originating in the ventral tegmental area (VTA) innervates several key brain regions of the addiction circuit, notably the nucleus accumbens (NAc), prefrontal cortex (PFC) and amygdala (Hyman et al., 2006; Koob & Volkow, 2010) (Figure 1). Stimulation of DA-containing VTA projections induces DA release into the NAc which is known to draw an organism's attention to the appearance of novel, salient stimuli (Fiorillo, Tobler, & Schultz, 2003; Ungless, 2004), and facilitate encoding of stimuli associations (Abler, Walter, Erk, Kammerer, & Spitzer, 2006; Jay, 2003).

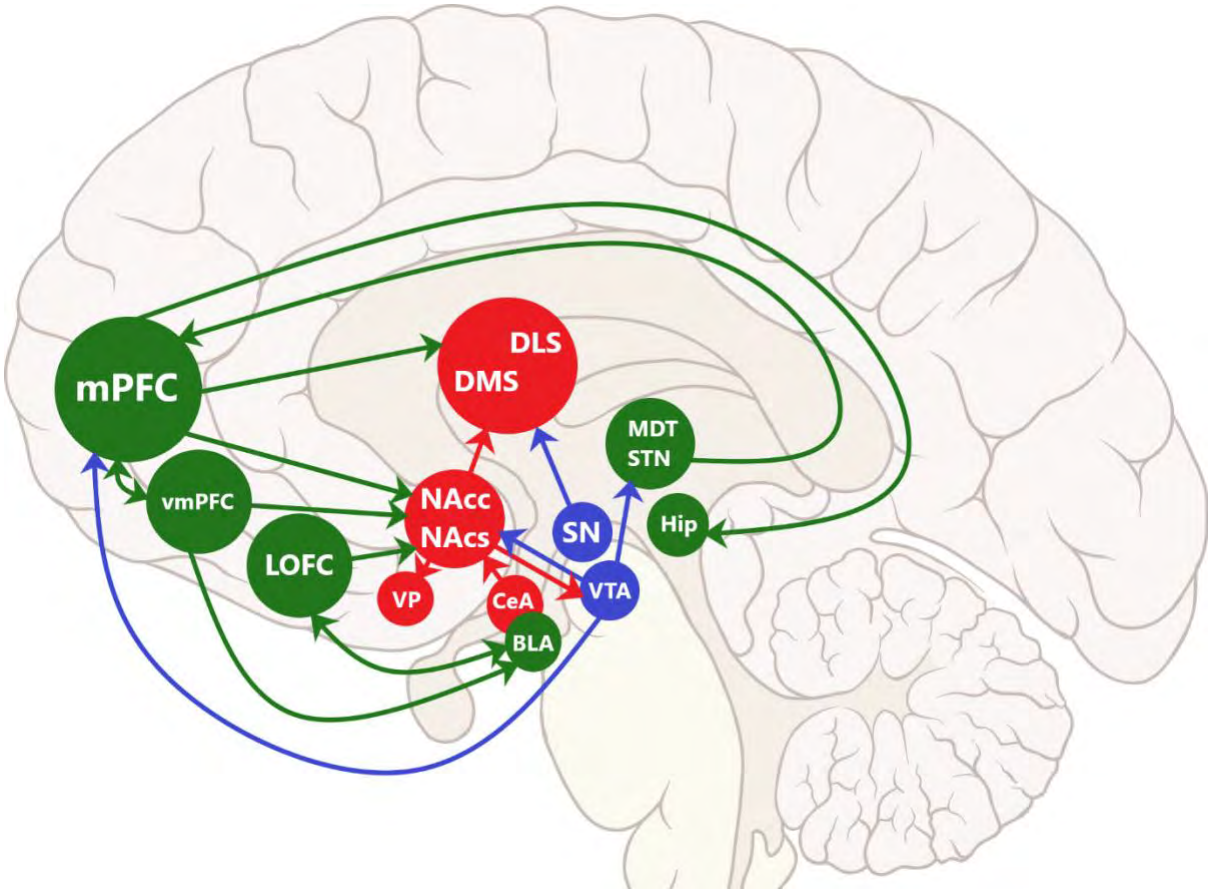

Figure 1. Neurocircuitry of addiction.The neurocircuitry involved in the processing of methamphetamine (METH)-reward, relapse to METH-seeking, habitual drug-seeking, motivation to take-METH and incubation of METH-craving. This includes the mesocorticolimbic dopamine pathway involved in reward, as well as the frontostriatal circuitry involved in inhibiting drug-seeking behaviours. Purple circles indicate functionally distinct brain regions. Green arrows indicate glutamatergic projections, blue arrows indicate dopaminergic projections and red arrows indicate γ-amino butyric acid (GABA)-ergic projections. Dorsal striatum (DS), thalamus (Th), hippocampus (Hip), substantia nigra (SN), ventral tegmental area (VTA), amygdala (Am), ventral pallidum (VP), nucleus accumbens (NAc), dorsal striatum (DS), medial prefrontal cortex (mPFC), ventromedial prefrontal cortex (vmPFC), lateral orbitofrontal cortex (LOFC). Note not all connections have been included for clarity.

1.2.1 Acute drug-mediated neurotransmission in reward circuits. Acutely, drug-administration activates reward circuitry that normally enhances the salience of natural rewards necessary for survival and procreation (Di Chiara et al., 2004). They induce rapid and supraphysiological DA release in the NAc, which stimulates DA-D1 receptors (D1Rs), the process believed to be responsible for the “high” associated with drug-reward (Volkow, Fowler, & Wang, 2003). METH-administration induces potent release of monoamines within the mesocorticolimbic pathway which in turn activates DAergic, 5-HTergic and NAergic systems within reward circuitry (Cruickshank & Dyer, 2009; Panenka et al., 2013). The

resulting intense hedonic state can promote METH-use over natural rewards, which are unable to induce such high levels of DA release when compared to METH's pharmacological effects (Carelli & West, 2014; Courtney & Ray, 2014; Koob & Volkow, 2016; Volkow & Morales, 2015). These potent rewarding outcomes reinforce METH-seeking and METH-use, resulting in potentiated motivation to seek- and take-drugs (Edwards & Koob, 2010; Lominac et al., 2014).

1.2.2 Chronic drug-mediated plasticity in reward circuitry. Studies suggest widespread structural and metabolic modifications in the brain following chronic METH-abuse (Chye et al., 2019; Mackey et al., 2019; Thompson et al., 2004). Vesicular stores of monoamines can be severely depleted after repeated METH-exposure, resulting in dysfunction of the mesocorticolimbic system (Courtney & Ray, 2014; Panenka et al., 2013). METH-induced neurotoxicity can include the degeneration of DA and 5-HT axons and terminals, and the suppression of DA and 5-HT transporter expression (Halpin, Collins, & Yamamoto, 2014; London, Kohno, Morales, & Ballard, 2015). Grey and white matter abnormalities have also been demonstrated in abstinent METH-users (Daumann et al., 2011; Tobias et al., 2010). As a potential mechanism for this process, METH elicits the upregulation of reactive oxygen species (ROS) and nitric oxide (NO) leading to oxidative stress within DAergic neurons which results in neuronal degradation and eventually apoptosis (Asanuma, Miyazaki, Higashi, Tsuji, & Ogawa, 2004; Thomas & Kuhn, 2005). Typically, antioxidant enzymes, such as monoamine oxidase, metabolise ROS in the central nervous system (CNS), however METH suppresses function of this oxidase, permitting a potentiation in the activity of these neurotoxic agents (Krasnova & Cadet, 2009). It is these neurotoxic consequences that are believed to underlie the neuropsychological deficits associated with chronic METH-consumption (Darke et al., 2008).

1.2.2.1 Incentive sensitisation and reward circuitry pathology. METH-induced mesocorticolimbic system pathology are likely responsible for the development of neurological METH-sensitisation and heightened attentional-bias towards METH-related stimuli (Robinson & Berridge, 2008; Robinson & Berridge, 1993). The incentive-sensitisation theory, by Robinson and Berridge (1993), stipulates that chronic mesocorticolimbic pathway activation results in compulsive attentional-bias towards drug-cues. Repeated pairings of stimuli with drug-reward results in the classical conditioning of drug-cues to predict drug-reward (Robbins, 1976). When experiencing cravings, drug-cues act as a potent secondary reinforcer to motivate drug-seeking. On a neurochemical level, presentation of drug-cues induces DA and glutamate neurotransmission in the NAc (Kalivas, 2000; Schultz, 1998). This suppresses inhibitory control over drug-seeking behaviours via stimulation of γ-amino butyric acid (GABA) projections to behavioural output regions (Baracz & Cornish, 2016; Koob & Volkow, 2016). Engagement of PFC-derived glutamatergic fibres synapsing on medium spiny neurons (MSNs) in the NAcc, likewise instigates METH-seeking (Parsegian & See, 2013; Rocha & Kalivas, 2010). This circuitry underlies cue-induced drug-relapse, however other equally important circuits are involved in METH-addiction.

1.3 Key brain regions involved in drug addiction.

1.3.1 Role of the nucleus accumbens in addiction. Arguably at the epicentre of drug-reward circuitry, the NAc lies within the ventral striatum (Hyman et al., 2006), and contains predominantly (~90%) GABAergic MSNs (Smith, Lobo, Spencer, & Kalivas, 2013). Intra-striatal inhibitory tone is sustained by GABAergic interneurons which are impacted by DAergic, glutamatergic and cholinergic inputs from cortical and limbic regions (Yager, Garcia, Wunsch, & Ferguson, 2015). Functionally, projections from the NAc to the ventral pallidum (VP) modulate maladaptive or inappropriate behavioural outputs (Baracz &

Cornish, 2016; Hamani, SaintCyr, Fraser, Kaplitt, & Lozano, 2004), and, via connections with the motor system, information from limbic regions impacts on NAc-driven motivational processes (Koob & Weiss, 1992).

The NAc is considered the major input area of the basal ganglia (Salgado & Kaplitt, 2015b) as it receives direct innervation from the amygdala (McDonald, 1991), hippocampus (Yang & Mogenson, 1984), thalamus, ACC (Brog, Salyapongse, Deutch, & Zahm, 1993), PFC (Beckstead, 1979), VTA (Van Bockstaele & Pickel, 1995) and SN (Fallon & Moore, 1978). In return, the NAc has major efferent projections to several regions in various circuits, including the VTA (Rahman & McBride, 2002), SN (Montaron, Deniau, Menetrey, Glowinski, & Thierry, 1996) and other brainstem regions, as well as the thalamus (Williams, Crossman, & Slater, 1977), globus pallidus (GP)(Yang & Mogenson, 1989), VP (Groenewegen & Russchen, 1984), lateral hypothalamus (Zahm & Heimer, 1993), amygdala (Russchen, Bakst, Amaral, & Price, 1985) and septum (Groenewegen & Russchen, 1984). The NAc receives the majority of its glutamatergic, cortical input from the medial PFC (mPFC), lateral orbitofrontal cortex (LOFC) and the ACC, and DAergic input from the VTA and SN (Haber & Knutson, 2010).

In the context of drug-reward, acute drug-administration activates the mesocorticolimbic pathway by stimulating DAergic projections from the VTA to the NAc resulting in an influx of DA into the NAc (Di Chiara, 2002). In response, the NAc sends GABAergic projections to two major addiction circuits. The first involves inhibitory projections to the VP, impacting on maladaptive behavioural outputs via the subthalamic nucleus (STN) and GP (Hamani et al., 2004). The second involves inhibitory projections to the VTA and SN, which result in glutamatergic innervation of the PFC via DAergic projections to the mediodorsal thalamus (MDT)(Figure 1). This second feedback circuit

regulates the activity of the first circuit via glutamatergic modulation of NAc DAergic stimulation (Kalivas, 2000)

Functionally, the primary role of the NAc is to respond to motivationally significant stimuli, such as food (Carelli, 2002), supraphysiological reinforcers such as drugs of abuse (Di Chiara et al., 2004), or aversive stimuli, such as non-appetitive food (Roitman, Wheeler, Wightman, & Carelli, 2008; Young, 2004), and emotional stimuli (Barrot et al., 2002). In the mesocorticolimbic pathway, the NAc serves two vital functions: to compel an organism to attend to salient, novel stimuli and encourage learning-induced neuroplasticity (Keitz, Martin-Soelch, & Leenders, 2003) and to predict the presentation of a learnt, motivational event via associations forged between the event and environmental stimuli (cues) predicting said event (Schultz, 1998).

The NAc can be divided into two subregions, the dorsolateral core (NAcc) and the ventromedial shell (NAcs), based on distinct differences in functionality and circuitry (Di Chiara, 2002; Salgado & Kaplitt, 2015a). For example, the NAcs is involved in the initial stages of addiction as it is responsible for the rewarding sensation associated with reinforcing stimuli (Di Chiara, 2002) whereas the NAcc is involved in attending to learnt drug-cue associations as presentation of drug-associated cues stimulates the NAcc (Sellings & Clarke, 2003). With many glutamatergic efferents projecting to the NAc from the mPFC (Kalivas & Volkow, 2005; Scofield et al., 2016b), the NAc and the PFC are highly interconnected leading to close functional relationships between the two regions. An increase in DA release in the NAc can result in potentiated glutamatergic activity within the PFC, hippocampus and VTA, which, under optimal conditions, works to attenuate stimulation of inhibitory GABAergic projections from the NAc to motor output regions (Baracz & Cornish, 2016; Koob & Volkow, 2010). However, following chronic METH-exposure, the mPFC to NAcc pathway has been found to be responsible for cue-induced drug-seeking (Rocha & Kalivas,

2010; Siemsen et al., 2019). This positions the NAc as a crucial element in the addiction neurocircuitry.

1.3.2 Role of the prefrontal cortex in addiction. The PFC is a functionally heterogenous region involved in various executive functions, such as impulse control and decision-making (Goldstein & Volkow, 2011b). These functions are all impacted by drug addiction which has led to interest in its study. At a cellular level, the PFC is made up of predominantly glutamatergic pyramidal neurons, with roughly 20-30% GABAergic interneurons (Garcia, Nakata, & Ferguson, 2018; Koella, 1981) which maintain an important balance of excitatory and inhibitory activity. The pyramidal neurons project to various downstream brain regions such as the NAc, hippocampus, VTA, dorsal striatum (DS), STN and autonomic regions (Ding, Gabbott, & Totterdell, 2001; Garcia et al., 2018; Koob & Volkow, 2010; Maurice, Deniau, Glowinski, & Thierry, 1998a).

Hyper-responsiveness of the PFC to drug-cues has been linked to behavioural drug-cue reactivity (Childress et al., 1993; Droungas, Ehrman, Childress, & O'Brien, 1995; Franklin et al., 2007; Garavan et al., 2000). Cocaine addicts that viewed cocaine-related videos demonstrated greater PFC activation to cocaine-cues over and above novel cues compared to controls (Garavan et al., 2000). Interestingly, measures of activity in the PFC following cue exposure in addicts is likely a more sensitive method of detecting group differences in conditioned responses to drug-cues, as alcoholics demonstrate no difference in valence, arousal ratings or autonomic reactivity (Grusser et al., 2004) compared to controls, despite a difference in PFC activation. In addition, PFC reactivity is correlated with drug-craving (Brody et al., 2002) and lifetime drug-intake (Yalachkov, Kaiser, & Naumer, 2009), and predicts performance on primed emotion recognition tasks (Artiges et al., 2009) and later drug-use (Grusser et al., 2004), highlighting the clinical relevance of PFC activity in addiction.

Debate exists surrounding the validity of translating findings in the PFC of rodents to those in humans, however there is a general consensus in neuroscience that there is significant overlap between analogous brain regions in the rodent PFC and human PFC (Ongur & Price, 2000). In the realm of addiction, similarities are also seen in the functional role of the PFC in addiction behaviours (Goldstein & Volkow, 2011a; Volkow & Morales, 2015). Two particular mPFC subregions demonstrate pronounced control over drug-seeking behaviours.

1.3.2.1 The medial prefrontal cortex in addiction. The mPFC is located in the medial portion of PFC. Its major input regions are the hippocampus, basolateral amygdala (BLA), various thalamic subregions and the VTA (Hoover & Vertes, 2007; Hyman et al., 2006). Primary efferent projections from the dorsal mPFC, the prelimbic cortex (PrL), are the ventral-dorsomedial striatum (DMS) and the NAcc. The ventral mPFC (vmPFC), or infralimbic cortex (IL), projects primarily to the NAcs and BLA (Heidbreder & Groenewegen, 2003; McDonald, Mascagni, & Guo, 1996). The dense NAc projections are predominantly glutamatergic, innervating GABAergic MSNs which modulate motivational and reward behaviours (Di Chiara et al., 2004; Kalivas & Volkow, 2005)(see 1.3.1). The mPFC regulates the rewarding effects of administered drugs learnt associations between drugs and neutral environmental stimuli (Konova et al., 2019), and context and cue-induced relapse to drug-seeking (Bossert et al., 2011; Rocha & Kalivas, 2010).

The rodent-equivalent of the mPFC, the PrL, has been implicated in compulsive drug-seeking behaviours, which signal the switch to addiction (American Psychiatric Association, 2013). Interestingly, pharmacological inactivation of the PrL reduced suppression of conditioned aversion to cocaine-seeking (Limpens, Damsteegt, Broekhoven, Voorn, & Vanderschuren, 2015). Concurrently, researchers found that pharmacological PrL inactivation prevented cue-induced and METH-primed METH-seeking (Rocha & Kalivas,

2010). Intriguingly, the PrL was the only brain region commonly activated by cue-induced relapse to cocaine-seeking and heroin-seeking, in a poly-drug intravenous self-administration (IVSA) model (Rubio et al., 2019). Therefore, these studies imply that the PrL plays a common major role in drug-seeking behaviours between different drug classes. Due to the potential universality of PrL activity to drug-seeking behaviours (Kalivas, 2009; Rocha & Kalivas, 2010; Rubio et al., 2019), it is essential to understand how the PrL, and the mPFC more broadly, fits into the neurocircuitry of these addiction behaviours.

The vmPFC, or IL in rodents, is implicated in the neuropathology of addiction. Traditionally, activation of the IL is believed to suppress drug-seeking behaviours, whereas PrL activity has been associated with driving drug-seeking behaviours (Gourley & Taylor, 2016), however this dichotomy has recently been challenged with growing evidence suggesting a more complex functional conceptualisation for the two regions (Moorman, James, McGlinchey, & Aston-Jones, 2015; Rocha & Kalivas, 2010). Importantly, there appears to be a functional disparity between the role of the IL in relapse to cocaine-seeking and METH-seeking (Rocha & Kalivas, 2010). Activation of the IL has been repeatedly shown as vital to the suppression of cocaine-seeking behaviours (Cameron, Murugan, Choi, Engel, & Witten, 2019; Peters, LaLumiere, & Kalivas, 2008). Due to its important role in extinguishing conditioned fear responses (Milad et al., 2007; Quirk & Mueller, 2007), it has been hypothesised that this suppression occurs via the enhancement of learning-associated plasticity. In contrast, inactivation of the IL has shown no effect on METH-primed reinstatement to drug-seeking, yet attenuated cue-induced METH-seeking (Rocha & Kalivas, 2010). This demonstrates potentially divergent roles of the IL cocaine compared to METH-relapse triggers, warranting further inquiry into the role of the IL in METH-addiction circuitry.

1.3.2.2 The lateral orbitofrontal cortex in addiction. The LOFC is located in the ventrolateral PFC. It receives major afferent projections from olfactory, gustatory, visual, parietal, somatosensory and perirhinal cortices, the BLA, and MDT (Ongur & Price, 2000; Reep, Corwin, & King, 1996). Major efferents from the LOFC project to the BLA, NAcc, MDT and hypothalamus (Carmichael & Price, 1995; Haber, Kunishio, Mizobuchi, & Lynd-Balta, 1995; Ongur, An, & Price, 1998). Importantly, the OFC is the only PFC sub-region to receive all modalities of sensory information (Wallis, 2011) which, along with its connections to the basal ganglia and limbic system, allows it to appraise affective stimuli based on a multitude of sensory information.

The LOFC is believed to be vital to cue-induced drug-seeking (Schoenbaum, Roesch, & Stalnaker, 2006). Cocaine-addicts demonstrate increased blood flow to the OFC, as well as the BLA, following exposure to representations of drug-associated cues (Goldstein & Volkow, 2002). In rats, GABA-A/B receptor-mediated pharmacological inhibition of the LOFC attenuated cue-induced relapse to cocaine-seeking (Fuchs, Evans, Parker, & See, 2004). Importantly, optogenetic inhibition of LOFC neurons expressing a Cre-dependant viral-vector that project to Cre-recombinase expressing neurons in the BLA, but not projections in the opposite direction, inhibited cue-induced relapse to cocaine seeking (Arguello et al., 2017). This would suggest that the LOFC-BLA circuit is vital to cue-induced drug-relapse, however no study has of yet investigated this effect in METH nor whether addiction-phenotype mediates functioning of this circuit, warranting investigation of the LOFC and amygdala.

1.3.3 Role of the amygdala in addiction. The amygdala is situated in the medial temporal lobe. It is comprised of predominantly glutamatergic principal projection neurons with some inhibitory GABAergic interneurons to maintain inhibitory-excitatory balance

(Duvarci & Pare, 2014). Importantly, two highly interconnected subregions, the BLA and central amygdala (CeA) have both been implicated in distinct addictive behaviours.

1.3.3.1 The basolateral amygdala in addiction. The BLA-complex includes the lateral, basal and basomedial nuclei, and receives strong, input from the thalamus, mPFC, OFC and VTA (Albanese & Minciacchi, 1983; Janak & Tye, 2015). It has reciprocal projections to the thalamus and PFC as well as largely unidirectional projections to the hippocampus, NAc, and hypothalamus (Cardinal, Parkinson, Hall, & Everitt, 2002; McDonald, 1991; Pitkänen, Pikkarainen, Nurminen, & Ylinen, 2000). The BLA has been characterised as an integrator of the value, consequences and past experiences of reward (Wassum & Izquierdo, 2015). This means that the BLA codes for distinct and temporally flexible outcome representations which are modified following prolonged drug-abuse.

As mentioned above (see 1.3.2.2), the LOFC and BLA form a circuit that is crucial to the expression of cue-induced drug-seeking (Arguello et al., 2017; Everitt et al., 1999). Indeed, bilateral lesioning of the BLA blocks cue-induced relapse to cocaine-seeking in rats (Meil & See, 1997) which is likely due to the BLA gating the Pavlovian stimulus-response (S-R) mechanism to gain influence over volitional behaviour (Burns, Robbins, & Everitt, 1993; Everitt & Robbins, 2000). Not only this, the BLA is involved in learning drug-cue associations, as lesions to the BLA block the acquisition and maintenance of cue-induced drug-seeking (Everitt, Cardinal, Parkinson, & Robbins, 2003; Whitelaw, Markou, Robbins, & Everitt, 1996). Interestingly, just as DA activity in the NAc of drug-users corresponds with cue-presentation (Schultz, 1998), not drug-reward, DA release in the BLA is necessary for cue-induced drug-seeking behaviours (Di Ciano & Everitt, 2004; See, Kruzich, & Grimm, 2001). This may implicate the BLA-NAc projections in the development of drug-cue associations and motivating behavioural responses to these behaviours (Everitt et al., 2003).

1.3.3.2 The central amygdala in addiction. The CeA is a subregion of the extended amygdala and shares many local circuit connections with the BLA (LeDoux, 2007). Within the CeA, there are two subdivisions, the medial CeA (mCeA) and the lateral CeA (lCeA), with the lCeA receiving input from the amygdaloid complex (Pitkänen et al., 1995; Savander, Go, Ledoux, & Pitkänen, 1995). The mCeA sends information to the lCeA via unidirectional GABAergic projections (Pitkänen et al., 2000) with the lCeA also receiving direct glutamatergic, and indirect GABAergic, innervation from the BLA (Krettek & Price, 1978; Royer, Martina, & Paré, 1999). The lCeA is the major output area of the CeA sending GABAergic projections to the VTA and extended amygdala to affect behavioural and physiological responses to emotionally salient events (Pape & Pare, 2010; Pitkänen et al., 2000).

The role of the CeA in METH-addiction is not as well characterised as many other regions in the addiction circuitry, however it seems to be involved in the incubation of METH-craving and other psychostimulants (Funk et al., 2016; Li, Zeric, Kambhampati, Bossert, & Shaham, 2015). Two weeks after a 12 day period of 2-hour METH IVSA sessions, rats demonstrated a significant increase in Fos expression, a marker of neuronal activity (Chung, 2015), in the CeA, as well as the DS, OFC and NAc (Funk et al., 2016). Importantly, pharmacological inactivation of the CeA blocked METH-craving in rats that underwent ten 9-hour METH IVSA sessions before 1-month of extinction (Li et al., 2015). Additionally, no association with vmPFC activation and incubation of METH-craving was found, contradicting previous findings implicating this region in incubation of cocaine-craving (Koya et al., 2009). This indicates the mechanisms for drug-craving may be different between cocaine and METH, warranting further investigation into the role of the CeA in METH-craving.

1.3.4 Role of the dorsal striatum in addiction. The DS is a major processing hub of the basal ganglia, responsible for executing motor movements (Malvaez & Wassum, 2018). It comprises the dorsomedial striatum (DMS) and the dorsolateral striatum (DLS) based on functional and neurocircuit differences. The DMS receives major afferent projections from the PrL, ACC, OFC, and motor cortices (McGeorge & Faull, 1989; Wall, De La Parra, Callaway, & Kreitzer, 2013). The DLS receives major afferent projections from motor and somatosensory cortices (Alloway, Lou, Nwabueze-Ogbo, & Chakrabarti, 2006; Haber & Knutson, 2010). Both subregions have major efferent projections to the GP and SN (Haber, 2014; Perez-Costas, Melendez-Ferro, & Roberts, 2010).

The DMS, or associative striatum, is necessary for goal-directed behaviour and action-outcome motivated behaviours (Everitt & Robbins, 2013b). As such, the DMS has been implicated in the initial stages of drug addiction as drug-seeking (action) is motivated by drug-reward (outcome)(Koob & Volkow, 2016; Smith & Laiks, 2018; Volkow & Morales, 2015). In contrast, the DLS, or sensorimotor striatum, is responsible for executing habitual behaviours (McNamee, Liljeholm, Zika, & Doherty, 2015; Tricomi, Balleine, & O'Doherty, 2009). As such, the DLS is responsible for S-R motivated behaviours (Tricomi et al., 2009; Vanderschuren, Di Ciano, & Everitt, 2005), implicating this brain region in the automated, habitual drug-seeking (HDS) characteristics of the later stages of addiction (American Psychiatric Association, 2013). Indeed, following 28 days of chronic METH-exposure, researchers found decreased glutamate transporter and receptor expression in the rodent DMS, which correlated with habitual food-seeking (Furlong, Corbit, Brown, & Balleine, 2018). Likewise, similar METH-exposure in rats induced structural plasticity in the DMS which also correlated with habitual food-seeking (Jedynak, Uslaner, Esteban, & Robinson, 2007). These studies suggest that prolonged METH-exposure may decrease glutamatergic activity in the DMS, which could be responsible for the suppression of goal-directed

behaviour. Of importance to this understanding of potentially pathological glutamatergic activity within the METH-addiction circuitry, is the role of astrocytes in METH-addiction.

1.4 Astrocytes.

Astrocytes are star-shaped glial cells that are crucial to many neurological processes, notably synaptic functioning (Allen & Barres, 2009; Frank, 2013; Parpura et al., 2012). Astrocytic processes create tripartite synapses, releasing neuroactive molecules to regulate neurotransmission (Araque et al., 2014; Perea, Navarrete, & Araque, 2009). Modulation of these neuroactive molecules has demonstrated impacts on circuit-level functions and behavioural outcomes (Oliveira, Sardinha, Guerra-Gomes, Araque, & Sousa, 2015). Astrocyte morphology is vital to synaptic regulation as greater astrocytic process proliferation and branching form more tripartite synapses and provide more support for neurotransmission compared to smaller, simpler astrocytes (Medvedev et al., 2014; Oberheim, Goldman, & Nedergaard, 2012).

Astrocyte morphology is dramatically altered under pathological states, where processes become thicker and ramify further into the interstitial space with greater structural complexity, termed astrocyte hypertrophy. Astrocytes also migrate to and proliferate at the site of injury (Hol & Pekny, 2015; Nash et al., 2011; Oberheim et al., 2012). These processes fall under what is known as astrogliosis, which is a mechanism that is designed to compensate for neuronal injury and varies with severity (Sofroniew, 2015). Mild-moderate astrogliosis results in minimal astrocyte hypertrophy whereas severe astrogliosis results in pronounced astrocyte hypertrophy (Sofroniew, 2015). Importantly, chronic METH-abuse is linked to neuronal cell damage and can induce astrogliosis (Krasnova et al., 2010a; Zhang, Gong, Feng, Zhang, & Li, 2017)

1.4.1 Astrogliosis, neuroinflammation, neurotoxicity and METH.

Studies have demonstrated that reactive astrogliosis is linked to METH-associated neuroinflammation and

neurotoxic apoptosis (Krasnova, Justinova, & Cadet, 2016). Astrogliosis has been defined here as any process that results from CNS injury or disease (Sofroniew, 2015). Following astrogliosis, astrocytes release pro-inflammatory cytokines and chemokines (Ramesh, MacLean, & Philipp, 2013; Ransohoff & Brown, 2012) which bind to receptors in microglia, increasing the release of neurotoxic agents, including reactive oxygen species (ROS)(Rocha, Cristovão, Campos, Fonseca, & Baltazar, 2012), and the further release of pro-inflammatory cytokines (Asanuma et al., 2004; Ramesh et al., 2013), which induce glial and neuronal apoptosis (Greenlund, Deckwerth, & Johnson, 1995; Shah, Kumar, Simon, Singh, & Kumar, 2013). Additionally, hyper-reactive astrogliosis, indicated by overexpression of S100β, a marker of astrocytic activation, increased neuronal apoptosis via astrocytic release of nitric oxide (Hu, Ferreira, & Van Eldik, 1997). These neurotoxic and neuroinflammatory processes have been linked to the chronic relapse and socio-emotional symptoms associated with METH-addiction, even after protracted abstinence (Yang et al., 2018). These studies highlight the remediation of these processes as a potential-treatments for METH-induced psychological symptoms and warrants better understanding of the relationship between METH-addiction and reactive astrogliosis.

The relationship between METH-addiction and astrogliosis has recently begun to emerge. Following experimenter-driven METH-exposure in rats, astrocyte proliferation occurs within addiction-related brain regions, such as the cortex and striatum (Granado et al., 2011; Robson et al., 2014). Measured 7 days after forced abstinence, Krasnova et al. (2010b) found extended access to METH (15-hours/day) resulted in an increase in the DS and cortex of glial-fibrillary acidic-protein (GFAP)-expression, a marker of reactive astrogliosis (Oberheim et al., 2012; Yang & Wang, 2015). Crucially, more research is needed in this area as understanding of the role of astrogliosis in METH-addiction remains poorly understood and may provide important targets for future therapies. One aspect of astrocyte-synapse

interactions that has become of interest to the field of addiction, particularly psychostimulant addiction, is glutamate homeostasis of astrocytes.

1.5 Glutamate homeostasis hypothesis of addiction.

It has become apparent that the traditional focus on DAergic activity in the mesocorticolimbic pathway in the field of addiction, despite its central role in instigating and maintaining drug-use, is likely insufficient to understand addiction neurocircuitry and associated behavioural outputs. Indeed, over the past two decades an emerging theory attempting to delineate the neural substrates of drug-relapse has suggested that glutamatergic pathways from the mPFC to the striatum are essential for cue-induced drug-relapse (Kalivas, 2000, 2009; Spencer, Scofield, & Kalivas, 2016). This is a potentially crucial mechanism to leverage with pharmacotherapies, as clinicians site drug-relapse as the most vital component of addiction for remediation of the addiction disorder (Morley et al., 2017).

1.5.1 Glutamate and astrocytes in the nucleus accumbens during drug-relapse.

As previously mentioned (see 1.3.1, 1.3.2), glutamatergic pyramidal neurons in the PrL and IL contain dense projections to the NAcc and NAcs, respectively (Ding et al., 2001; Maurice, Deniau, Glowinski, & Thierry, 1998b) and synapse onto GABA MSNs that express various glutamate receptors (Blaha, Yang, Floresco, Barr, & Phillips, 1997; Maldonado-Irizarry, Swanson, & Kelley, 1995). Chronic exposure to cocaine reduces glutamatergic tone in the NAc (McFarland, Lapish, & Kalivas, 2003), and chronic METH attenuates basal extracellular glutamatergic activity in the NAc (Parsegian & See, 2013). Following drug-primed and cue-induced relapse, researchers have demonstrated a marked influx of glutamate into the NAcc, which when pharmacologically blocked prevents cue- and drug-induced relapse to METH-seeking (Parsegian & See, 2013). Likewise, GABAergic inhibition of the PrL prevented

relapse to METH or cocaine-seeking (Cannella et al., 2013; Rocha & Kalivas, 2010). This suggests that this PFC-NAc glutamatergic pathway is vital to drug-relapse.

Important to this process is the regulation of glutamate uptake by glutamate transporters and other molecular structures located on astrocytes. Substantial evidence indicates that glutamate release from the presynaptic bouton is regulated by astrocyte reuptake of glutamate (Cassé et al., 2012; Parpura & Zorec, 2010; Verkhratsky & Parpura, 2016), 90% of which occurs via the glutamate transporter-1 (GLT-1) which is highly expressed in astrocytes (Danbolt, 2001; Williams et al., 2005)(Figure 2). Glutamate is then converted into glutamine and released into the synapse for uptake into presynaptic boutons to be synthesised into glutamate and packaged into vesicles for synaptic release (Albrecht, Sidoryk-Wegrzynowicz, Zielinska, & Aschner, 2010). Likewise, astrocytes also release glutamate via multiple alternative mechanisms, such as hemichannels, anion-channels, ionotropic purinergic receptors, calcium-ion (Ca^{2+})-dependent vesicular release, cystine-glutamate antiporter (Xc-)-mediated glutamate exchange, and GLT-1 reversal (Kalivas, 2009; Malarkey & Parpura, 2008; Warr, Takahashi, & Attwell, 1999). This glutamate regulation occurs in the extrasynaptic space surrounding the synapse with the concentration of extrasynaptic glutamate modulating activity at inhibitory metabotropic glutamate receptor-2 and 3 (mGluR2/3)(Moussawi & Kalivas, 2010; Schwendt, Reichel, & See, 2012). Crucially, binding to these receptors inhibits synaptic glutamate release, prevents long-term-potentiation and reduces subsequent binding to excitatory ionotropic glutamate receptors (iGluRs), an effect which has been pharmacologically manipulated with mGluR2/3 agonists to prevent cue- and drug-induced relapse to METH-seeking (Schwendt et al., 2012).

Perisynaptic astrocytic processes (PAP)s are fine, highly-plastic process tips that are the primary source of astrocyte-synapse contact in the CNS (Scofield, 2018), and arguably are responsible for the greatest amount of glutamate reuptake across the astrocyte. The close

proximity of PAPs also allows for synaptic-sheathing, which prevents glutamate spill-over into the extracellular space (Rusakov, 2001). These astrocyte-synapse connections are also important for glial glutamate release as they are generally the closest access point for glutamate to bind with inhibitory presynaptic mGluR2/3s which regulate neuronal glutamate neurotransmission (Lavialle et al., 2011; Xi, Baker, Shen, Carson, & Kalivas, 2002).

Under ideal conditions, glutamate homeostasis is maintained by astrocytic glutamate regulation, however following acute and chronic drug-use, the integrity of these regulatory mechanisms fails (Kalivas, 2009)(Figure 2). Acute drug-exposure, across drug-classes, demonstrates a marked reduction in the expression of GLT-1 (Gipson et al., 2013; Sari & Sreemantula, 2012) as does chronic cocaine exposure (Fischer-Smith, Houston, & Rebec, 2012). Chronic cocaine and nicotine have shown a reduction in the expression of the catalytic subunit of the Xc- (Kau et al., 2008; Knackstedt et al., 2009). As the Xc- is responsible for more than 50% of glial glutamate release, this effect is a possible mechanism through which low basal levels of extracellular glutamate are seen after chronic drug-exposure (Baker et al., 2003; McFarland et al., 2003; Parsegian & See, 2013).

During drug relapse, there is an influx of mPFC-derived glutamate into the NAcc which cannot be regulated by the impaired astrocytic regulatory system (Parsegian & See, 2013; Scofield et al., 2016b; Siemsen et al., 2019). As well, due to lack of synaptic glutamate clearance, there may be glutamate spill-over into the extrasynaptic space that could activate mGluR5s and GluN2B containing NMDA receptors (Pomierny-Chamiolo et al., 2015; Shen, Scofield, Boger, Hensley, & Kalivas, 2014). Activation of these receptors increases the intracellular concentration of Ca^{2+} leading to synaptic potentiation (Yashiro & Philpot, 2008) and drug-seeking behaviour (Kalivas, 2009). Coupled with reduced mGluR2/3 mediated inhibition of synaptic glutamate release (Hao, Martin-Fardon, & Weiss, 2010; Lu, Uejima, Gray, Bossert, & Shaham, 2007; Moussawi & Kalivas, 2010), these conditions facilitate an

increase in glutamate neurotransmission in the NAcc, thought to drive relapse to drug-seeking behaviours (Cornish & Kalivas, 2000).

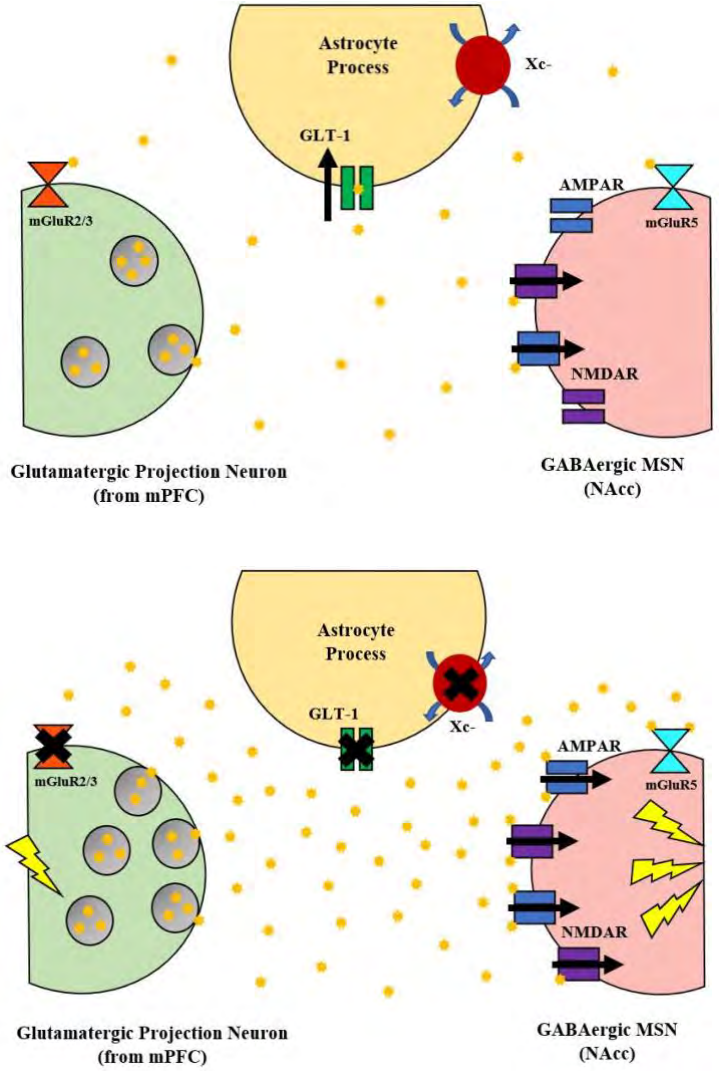

Figure 2. Glutamate homeostasis: the tripartite synapse. Depiction of a tripartite synapse in the nucleus accumbens core (NAcc) of a drug-addicted animal during cue induced relapse to drug-seeking. Here, the terminal of a pre-synaptic glutamatergic medial prefrontal cortex (mPFC) projection neuron is synapsing with a post-synaptic dendrite of a γ-amino butyric-acid (GABA)ergic medium spiny neuron (MSN) and an astrocyte process. Hourglass figures represent metabotropic glutamate receptors (mGluRs). Yellow stars signify glutamate and black arrows indicate direction of glutamate travel at glutamate transporter-1 (GLT-1) and of Ca^{2+} influx at AMPAR and NMDARs. Black crosses indicate lack of function or downregulation due to chronic drug-exposure. Yellow lightning bolts represent activity as a result of excitatory post-synaptic potentials at the pre- and post-synaptic terminals. Xc- = cystine-glutamate exchanger/antiporter. (a) During a healthy state, astrocyte processes regulate glutamate transmission via GLT-1 mediated glutamate reuptake, Xc-mediated glutamate reuptake and release. Glial-derived glutamate also binds to mGluR2/3s and mGluR5s to inhibit and potentiate glutamate activity, respectively. Following chronic drug-exposure, GLT-1, Xc- and mGluR2/3 expression is reduced, reducing the efficacy of glutamate regulation. (b) During exposure to drug-paired cues, glutamate neurotransmission is potentiated due to chronic METH-use reducing expression of GLT-1, Xc- and mGluR2/3s, resulting in failure of glutamate homeostasis regulatory mechanisms. Adapted from Scofield et al. 2014.

Despite concurrence between the findings in METH and cocaine, in regard to the glutamate homeostasis hypothesis, this hypothesis has never been examined in the context of addiction-phenotyping. It is therefore still unknown if there is a difference in glutamatergic activity within the METH-addiction neurocircuitry in METH addiction-vulnerable, compared to addiction-resistant animals and humans. Importantly, drug-addicts, in humans and rats, represent only 10-20% of those that use drugs (Australian Institute of Health and Welfare, 2016; Deroche-Gamonet, Belin, & Piazza, 2004b; Wagner, 2002). Therefore, it is likely that certain aspects of brain function that are specific to this subset of drug-users may explain the development of addiction in these individuals. As astrocytes regulate synaptic and extrasynaptic glutamate as well as release glutamate in a brain-region specific manner (Malarkey & Parpura, 2008), it is vital to understand the interaction between METH-addiction and astrocytes to understand the complex relationships between glutamate activity, astrocyte morphology and METH-addiction within the frontostriatal circuitry and beyond. In order for researchers to probe and expand on the nature of these mechanisms, preclinical models of addiction play an important role.

1.6 Preclinical models of addiction.

Currently, the only way to investigate the causal relationship between neurocircuitry and drug addiction is through the use of animal models of addiction. With control over environmental factors impacting on the animal, causal inferences can be drawn by the researcher, whereas human drug addicts each have unique experiences, and therefore the aetiology of the neural-behavioural relationship remains unknown. One of the most common species used in addiction models is the rat (Panlilio & Goldberg, 2007). Rats and humans both have very similar physiology (Dolenšek, Rupnik, & Stožer, 2015; Mestas & Hughes, 2004; Papadimitriou, Xanthos, Dontas, Lelovas, & Perrea, 2008) and importantly, there is considerable structural and neurobiological overlap in the brain (Everitt, Giuliano, & Belin,

2018; Hoover & Vertes, 2007; Moorman et al., 2015). Given these apparent similarities and the experimental advantages over human subjects, rats are commonly employed in animal models of addiction to investigate neurobiological correlates with addictive behaviours.

1.6.1 The self-administration paradigm. Preclinical addiction models can encompass a wide range of paradigms (Belin-Rauscent, Fouyssac, Bonci, & Belin, 2016; Everitt et al., 2018). Some models, such as conditioned place preference (CPP) and locomotor sensitisation, assay the effects of acute or short chronic periods of drug-exposure on behaviours associated with the initial stages of drug-use. However, for many years the drug self-administration paradigm has been considered the gold standard for preclinical models of addiction (Everitt et al., 2018) as it demonstrates better ecological and face validity compared to models such as CPP and locomotor sensitisation (Cox et al., 2017). In the self-administration model, rats are trained to press a lever for drug-delivery (Everitt et al., 2018; Weeks, 1961). The underlying assumptions of this paradigm stem from the principles of both operant and classical conditioning (Everitt et al., 2018). In terms of operant conditioning, drug-contingent operant responding results in delivery of a drug-reward, which reinforces these drug-taking behaviours. In terms of classical conditioning, neutral stimuli are presented preceding, simultaneous to, or following drug-delivery to endow these conditioned stimuli with certain properties. In terms of the drug-paired conditioned stimulus, this is normally a prominent light or sound that is presented concurrent with drug-delivery. Importantly, in humans, only a subset of those that chronically take drugs become addicted to them (Australian Institute of Health and Welfare, 2016; United Nations Office on Drugs and Crime, 2018; Wagner, 2002) which reduces the ecological validity of most self-administration studies as all rats that acquire METH self-administration are generally considered METH-addicted. Consideration of this phenomenon led to the incorporation of addiction-phenotyping into the self-administration model (Belin, Mar, Dalley, Robbins, &

Everitt, 2008; Brown, Flynn, Smith, & Dayas, 2011; Deroche-Gamonet et al., 2004b; Jadhav et al., 2018).

1.7 Addiction-phenotyping.

In rats and mice, the ratio of human users transitioning to addiction has been mirrored in preclinical paradigms that assay addictive behaviours aligning with the DSM-5 criteria for drug dependence (Belin & Deroche-Gamonet, 2012; Brown et al., 2011). In the first report of this procedure, Deroche-Gamonet et al. (2004b) assessed the propensity for a rat to respond on a drug-paired lever in three contexts designed to distinguish distinct addictive behaviours. Rats responding above the 66th percentile for all three behaviours were then considered to be addicted. They confirmed that these behaviours predicted and correlated with cue-induced relapse to drug-seeking, a critical addictive behaviour predictive of treatment efficacy (DeJong, 1994), and demonstrated via factor analysis that together all three behaviours loaded onto a single latent variable.

A variety of permutations of the phenotyping model have since arisen, with one notable example being that of Brown et al. (2011). These researchers incorporated cue-induced relapse to drug-seeking as one of their criterion for the addiction-vulnerable phenotype, preserving two of the criterion previously employed by Deroche-Gamonet et al. (2004b). The three context-specific addictive behaviours employed in this study reflect distinct criteria described in the DSM-5 (American Psychiatric Association, 2013), which is important as meeting a predetermined number of criteria is the current clinical method for diagnosis of addiction. As such, adoption of the criterion-based approach known as addiction-phenotyping provides even greater face validity than a simpler drug self-administration paradigm that assumes that chronic drug-taking is sufficient for the development of addiction. The criteria employed by Brown et al. (2011), high motivation to take drugs, cue-induced

relapse to drug-seeking, and habitual drug-seeking (HDS), are vital characteristics of the addiction disorder (American Psychiatric Association, 2013).

1.7.1 Modelling motivation for drug-taking. To model motivation to take drugs in an IVSA paradigm, the schedule of reinforcement is incrementally increased gradually across self-administration sessions (Panlilio & Goldberg, 2007). The schedule of reinforcement refers to the pattern of responding necessary for drug-delivery (Everitt et al., 2018). Once rats acquire the drug-lever associations, rats are introduced to the progressive ratio (PR) schedule where, within a session, the number of responses after each subsequent infusion increases according to a function (Richardson & Roberts, 1996). A PR schedule is employed so that the economic value of consecutive infusions rises until drug-seeking is forsaken. This point of cessation is known as the breakpoint and is the operationalised measure of the effort the animal is prepared to expend to obtain a given dose of a rewarding drug (Panlilio & Goldberg, 2007). The breakpoint as a measure of motivation is independent of the rate of responding, which is modulated by reinforcing drugs themselves which confounds the interpretation of motivation (Panlilio & Goldberg, 2007). Therefore, using the breakpoint is a methodological strength of the PR schedule. This paradigm permits the addicted animal to replicate the high motivation to take rewarding drugs seen in the addiction-phenotype in humans (American Psychiatric Association, 2013). Humans that suffer from an addiction disorder are highly motivated to seek out drugs of abuse and are willing to spend considerable time and effort in their procurement and preparation. As such, the PR schedule most frequently used in preclinical models may require rats that are highly motivated to take drugs to lever press hundreds, if not thousands, of times to receive a single drug reward. These rats that expend such extraordinary amounts of effort for a small drug-reward are likely

to also demonstrate other addictive behaviours (Belin et al., 2008; Deroche-Gamonet, Belin, & Piazza, 2004a).

1.7.2 Modelling cue-induced relapse to drug-seeking. Arguably the most ecologically valid measure of the addictive phenotype is relapse to drug-seeking induced by drug-cues (Everitt et al., 2018; Kalivas & Volkow, 2005). Relapse maintains and reinforces the addictive cycle and has been identified as the crucial addiction behaviour for remediation of drug addiction (Kalivas & Volkow, 2005; Koob & Le Moal, 2001; Koob & Weiss, 1992). Generally, during drug self-administration, simultaneous to delivery of the drug-reward, one or more salient cues are presented, such that over time these stimuli gain reinforcing properties independent of drug-availability (Panlilio & Goldberg, 2007). Once rats have been given sufficient time to become addicted to the rewarding drug, rats are then trained to extinguish the drug-lever association over a given period. Here, the drug-paired cues would not be presented and lever pressing results in no consequence. Despite a decrease in lever pressing in the absence of drug-reward signalling and availability, the drug-cue association persists. Following the extinction period, rats are then exposed to the drug-paired cue and lever responding is recorded, typically with each lever press resulting in drug-cue presentation and no additional consequence. Importantly, this paradigm assesses the reinforcing efficacy of the drug-paired cue itself, which is an indirect measure of the drug-cue's effect on drug-seeking behaviours. Drug-cues are well-documented triggers of relapse to drug-seeking and taking in humans (Kalivas & Volkow, 2005), therefore using cue-induced relapse has strong ecological validity and high potential for translatability (Everitt et al., 2018). Another key component of the addiction-phenotype is that of HDS.

1.7.3 Modelling habitual drug-seeking. Drug addiction can be characterised as a habitual drug-taking disorder, and this is especially true for the later stages of addiction (Koob & Volkow, 2016; Volkow & Morales, 2015). Habitual drug-seeking behaviours

therefore indicate the transition from reward to addiction (American Psychiatric Association, 2013; Koob & Volkow, 2010). One model of HDS, requires that rats that have already acquired self-administration undertake training in a cyclic drug-available/drug-free paradigm (Brown et al., 2011; Deroche-Gamonet et al., 2004a; Fuchs, Higginbotham, & Hansen, 2019). These periods are purposefully signalled by drug-availability cues and as such, rats recognise that responding during this period will not yield a drug-reward. The measure of HDS is lever pressing during the non-drug available (NDAv) periods throughout the session as rats with strong habit formation are more likely to continue responding during this period, despite learnt drug unavailability (Deroche-Gamonet et al., 2004b). HDS is a vital component of the addiction-phenotype as following the transition to addiction, drug-seeking becomes automated and driven by habit (American Psychiatric Association, 2013; Volkow & Morales, 2015). This habit formation is related to the loss of control over drug-seeking, where addicts are unable to prevent themselves from partaking in drug-seeking behaviours due to the formation of a robust and powerful habit (Clemens & Holmes, 2018; Everitt & Robbins, 2013a) that is unable to be inhibited by a dysfunctional PFC (Lominac et al., 2016).

This model has not yet been employed in a METH self-administration paradigm and therefore it is unknown whether rats will demonstrate this type of HDS and if this correlates with other addictive behaviours. Interestingly, Torres et al. (2017) found that rats that demonstrated greater foot-shock-mediated compulsive drug-seeking, defined as drug-taking that is maintained despite adverse consequences, also showed greater cue-induced relapse scores after incubation of drug-craving. Currently, no other studies investigating METH-addiction have employed an addiction-phenotyping paradigm in a preclinical self-administration model.

1.8 Aims and research question.

To date, no studies have employed a METH-addiction-phenotyping procedure, similar to that developed for cocaine by Deroche-Gamonet et al. (2004a), that investigate neural correlates across separate phenotypes. Therefore, the neural circuitry associated with the METH addiction-phenotype, above and beyond substantial METH-exposure, are currently unknown. This study aims to uncover which brain regions demonstrate an association with glutamatergic activity, reactive astrogliosis and astrocyte proliferation, and METH-addiction vulnerable rats. It also aims to reveal which regions, if any, demonstrate a relationship between astrocyte-synapse interactions and glutamate activity, and METH addiction-vulnerable rats. Due to the lack of research investigating the neural substrates of the METH addiction-vulnerable rats, many brain regions within the characterised addiction circuitry will be assayed. These are chosen based on their involvement in circuits relevant to the addiction behaviours assessed, notably motivation to take drugs (mPFC, NAc, BLA), cue-induced drug-relapse (mPFC, NAc, BLA, LOFC, CeA) and HDS (DS, mPFC).

1.8.1 Hypotheses.

1. It was hypothesised that baseline glutamatergic activity will be reduced in the PrL, IL, LOFC, BLA, CeA, NAcc, NAcs, DLS, aDMS and pDMS demonstrated by less CaMKIIa fluorescence, in addiction-vulnerable, compared to addiction-resistant rats.

2. It was hypothesised that astrocyte proliferation will be increased in the PrL, IL, LOFC, aDMS, pDMS, DLS, NAcc, NAcs, BLA and CeA, measured by a greater number of GFAP-stained nuclei, in addiction-vulnerable, compared to addiction resistant rats.

3. It was hypothesised that astrogliosis will be increased in the PrL, IL, LOFC, NAcc, NAcs, aDMS, pDMS, DLS, BLA and CeA, measured as increased ring intersections, number of processes, and longer primary processes, in addiction-vulnerable, compared to addiction-resistant rats.

4. It was hypothesised that baseline glutamate activity, measured by intensity of CaMKIIa fluorescence, in the PrL, LOFC, BLA, NAcc and NAcs, will positively and significantly correlate with astrocyte-synapse interactions, measured by the GFAP-synapsin-I colocalisation coefficient, in addiction-vulnerable rats, and that this correlation will be stronger and opposite in valence when compared to addiction-resistant rats.

5. It was hypothesised that baseline glutamate activity, measured by intensity of CaMKIIa fluorescence, in the IL and CeA will negatively and significantly correlate with astrocyte-synapse interactions, measured by the GFAP-synapsin-I colocalisation coefficient, in addiction-vulnerable rats, and that this correlation will be stronger and opposite in valence when compared to addiction-resistant rats.

2. Methods

2.1 Animals

Male Sprague-Dawley rats (n = 40) were born at the PC2-Certified Central Animal Facility at Macquarie University (North Ryde, NSW) from six dams purchased from the Animal Resource Centre (Perth, WA). Their holding room remained on a 12h light-dark cycle (lights on at 0400h or 0600h) at a constant temperature (21±ºC) and 40-65% humidity. Subsequent to weaning, rats were pair-housed in wire-covered plastic cages (629x400x310mm) lined with bedding, except following surgery where they were single-housed (see 2.2). Rats were supplied wooden blocks, straws, sunflower seeds, and shredded paper for environmental enrichment. During the early postnatal period, they were left largely undisturbed with minimal handling until 8-9 weeks postnatal. Subsequently, rats were handled by the primary researcher daily for one week. Rats' tails were tagged with permanent marker. Food was available *ad libitum* until 8-9 weeks of age, following then a minimum of 20g of chow per rat was administered to each cage daily to restrict excessive weight gain across the length of the experiment (Carroll, France, & Meisch, 1981; Osborne & Olive, 2008). Water was available *ad libitum* throughout, except during experimental sessions. All experiments were conducted during the light cycle.

2.2 Surgery

Following handling, rats underwent jugular-vein catheter implantation surgery to allow chronic drug-delivery. The surgical procedures used have been previously described (Baracz, Everett, McGregor, & Cornish, 2016) and involved insertion of a catheter into the righthand jugular vein, externalised at the back and sealed with a plastic and brass cap. For catheter assembly see Appendix A. Each rat was monitored closely throughout surgical

procedures (see Appendix B). Rats were anaesthetised with 2.5% isoflurane (2-chlor-2-1, 1, 1-trifluoroethyl difluoroethane) in oxygen (2L/min). Once anaesthetised, they were given Carprofen (5mg/kg/mL, subcutaneous) analgesia. Following surgery, catheters were flushed with 0.2mL of cephazolin solution (100mg/mL). The antiseptic betadine was applied to wounds, and 0.9% saline (2ml, subcutaneous) was injected into the left flank for hydration. Rats were then placed in individual cages inside a heating chamber (27ºC) and monitored for 45-minutes with access to water, then single-housed with restored access to food and water.

2.2.1 Post-operative care. For 5-7 days following surgery, rats were weighed daily and received betadine treatment. For the first 2 days after surgery, rats also received Carprofen (5mg/kg, subcutaneous) analgesia and catheters were flushed with 0.2mL of cephazolin solution (100mg/mL). Subsequently, rats were pair-housed with their original cage mates, dependent on recovery. Throughout the remainder of the experiment, catheters were flushed daily with 0.2mL of heparinised (60IU) cephazolin solution to prevent catheter occlusion.

2.3 Drugs

Methamphetamine hydrochloride (99.8±1.3% pure, METH) was obtained from the Australian Government Analytical Laboratories (Pymble, NSW). For intravenous self-administration (IVSA), METH was dissolved in 0.9% saline at a concentration of 0.1mg//kg/0.05mLinfusion, based on average rat weight, then passed through a Millipore syringe filter (0.22μm). METH solutions for IVSA were made on a weekly basis.

2.4 Intravenous self-administration of METH

2.4.1 Self-administration apparatus. Behavioural experiments were undertaken in 20 standard operant chambers (32x25x34cm; Med Associates, VT, USA) within sound-attenuating boxes. Each chamber had a right and left lever with a bright cue-light above and house-light. A 10mL syringe of METH set in an infusion pump was connected to PE

infusion-line tubing, which ran through a swivel and spring connector to connect to the catheter back mount. Active and inactive lever location was counterbalanced across the chamber side to control for location preference. A tone generator was situated over a perforated slat on the chamber exterior.

2.4.2 Self-administration procedure. Prior to each IVSA session, infusion lines were disinfected with ethanol (70%) before loading with METH. Catheters were flushed with 0.1mL heparin solution (10IU) before sessions. IVSA sessions were completed at the same time every day for 3 hours. Rats began on a fixed ratio-1 (FR1) schedule of reinforcement, where presses on the active-lever resulted in a 3-second infusion of METH (0.1mg/kg/infusion). Drug-delivery was paired with a compound-cue, consisting of a 3-second cue-light illumination, a distinct 5-second tone (70dB, 2900hZ, rise-fall duration 10ms) and the mechanical infusion-pump sound. Subsequently, there was a 17-second timeout before drug and compound-cue availability were restored. This prevented excessive binge consumption and METH-induced toxic overdose. Rats were limited to 120 infusions, upon which the session would end.

2.4.3 Acquisition of METH self-administration. Rats ac quired METH IVSA for 14 days on an FR1 schedule of reinforcement. Acquisition criteria were met when active-lever presses had escalated and were significantly greater than inactive-lever presses by the end of FR1 acquisition.

2.4.4 Habitual Drug-Seeking. Following acquisition on a FR1 schedule, rats acquired 3-hour habitual drug-seeking (HDS) sessions. During HDS sessions, each hour was divided into 2 distinct periods based on previously reported methods (Brown et al., 2011). During the first 40 minutes, METH was available via active-lever depression. During the preceding twenty minutes, all lever presses had no consequence. Therefore, each HDS session consisted of three drug-available (DAv) and three non-drug-available (NDAv)

periods. Each period was signalled by distinctive cues. During the DAv period, a white-noise was played (except during compound-cue presentation and the timeout period, whereas during the NDAv period a house-light was illuminated. Rats acquired FR1 HDS sessions for 3 days, then FR3 sessions for 2 days, then FR5 for 3-5 days. This schedule-escalation is a standard procedure used to facilitate transition to harder schedules of reinforcement, such as a progressive-ratio (PR) schedule. A FR5 schedule in HDS sessions is also standard for addiction-phenotyping paradigms (Brown et al., 2011; Deroche-Gamonet et al., 2004b) as it increases inter-animal response variability, facilitating the assessment of addiction-resistant (ARes) and addiction-vulnerable (AVul) phenotypes.

Following completion of the HDS acquisition protocol, rats were tested for HDS over 5 identical test-sessions (Figure 3). HDS scores were calculated from the number of active-lever presses during NDAv periods, averaged across sessions.

2.4.5 Motivation to take-METH. Following the 5-day HDS test period, rats acquired the PR schedule over 2 sessions. They were then tested for motivation to take-METH over a further 3 sessions. PR is the same as FR, however rewards are received contingent on an ever increasing number of responses, according to this function: Response ratio (nearest integer) = $5e^{(\text{injection number} X 0.2) - 5}$ (Richardson & Roberts, 1996). From this, a 3-hour breakpoint (BP) for each animal can be calculated. A BP is defined as the point at which a subject is unwilling to expend further effort to seek a discrete reward (Panlilio & Goldberg, 2007). In the current study, this is operationalised as the amount of active-lever presses the animal is willing to make to obtain the last drug-infusion, in 3-hours. Rats' average BP was calculated from the BP values over the 3 PR test-sessions; this value constituted their motivation to take-METH score. Aft the final PR session, rats undertook one FR5 HDS session. This final session

ensured that rats' final METH-session was on a FR schedule to facilitate extinction training (Brown et al., 2011; Nevin, 2012).

2.4.6 Relapse to drug-cues. Following the final day of METH IVSA, active-lever responding was extinguished over 31-32 days during 1-hour extinction (Ext) sessions, except on Ext day-1 (3-hours) and Ext day-2 (2-hours). During Ext sessions, responding on either lever had no consequence. Additionally, the compound-cue was withheld, and the house-light remained off. Rats were considered to have extinguished when their active-lever presses were 20 or less over 3 consecutive sessions. Once extinguished, rats were exposed to the compound-cue during one session with no METH-access. Rats had one non-contingent cue presentation, 30-seconds after lever protraction (pump on for 3-seconds, compound-cue on for 5-seconds). Subsequently, rats could press for compound-cue presentation over the remainder of the 60-minutes, with no timeout, following the preceding compound-cue presentation. A normalised cued-relapse score was calculated from the total active-lever presses during the relapse session minus the active-lever presses during the final Ext session (Atkins, Mashhoon, & Kantak, 2008; Kim et al., 2015) and was used to phenotype rats as either relapse-vulnerable or relapse-resistant.

2.5 Forced abstinence and sacrifice

Following the IVSA protocol, rats remained in home-cages for one week, to minimise any cue-relapse effects before sacrifice. For cull day, rats were given a lethal intraperitoneal injection of the barbiturate pentobarbital sodium (200mg/kg at 46.25mg/mL). Animals' consciousness was assessed with a firm tail or toe pinch. Upon no response after at least 3 pinch-tests and once breathing ceased, rats underwent perfusion fixation via intracardiac puncture.

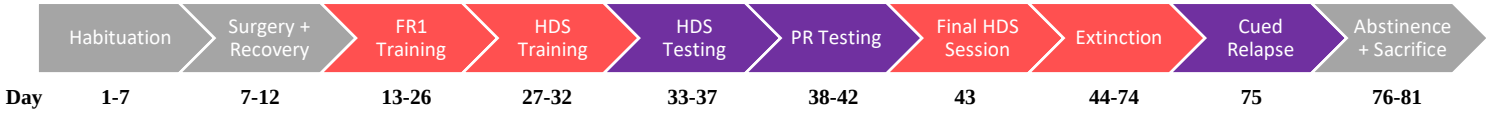

Figure 3. A timeline of the intravenous self-administration (IVSA) paradigm.Preparation and post-IVSA period (grey), acquisition, stabilisation and extinction sessions (red) and the test sessions assessing addictive behaviours (purple).

2.5.1 Perfusion. Rats' chest cavities were opened with surgical scissors and the heart was exposed. An incision was then made from the opening down to the urethra to facilitate removal of the colon for analyses outside of this study. Either end of the colon was clamped before surgical removal. A blunt 18G needle was inserted into the aorta and 1mL of heparin solution (1000IU) was then injected intracardially. Finally, a small incision was made at the left atrium, then the rat was perfused with ice-cold heparinised saline (10IU/200mL) over 6-minutes followed by 200-250mL of 4% paraformaldehyde (PFA) for a further 6-8 minutes.

2.6 Immunohistochemical procedure

2.6.1 Histology Preparation. Brains were then removed and post-fixed in 4% PFA overnight at 4°C. They were then transferred to a graded protocol of sucrose phosphate-buffered saline (PBS; 24-hours 10% sucrose, 24-hours 20% sucrose, and 48-hours 30% sucrose). Subsequently, brains were preserved in cryoprotectant solution (30% ethylene glycol, 30% sucrose and 2% polyvinylpyrrolidone dissolved in 0.1M PBS) and kept at -20°C until sectioning. Using a 1mm graticule, brains were coronally sectioned rostral to the cerebellum and mounted rostral-side up. Brains were then sectioned coronally (50μm thick, 1:4 serial slices) with a vibrating microtome (VTS1200S; Leica) then placed in pots of cryoprotectant solution.

2.6.2 Immunohistochemistry. Immunohistochemistry was employed to visualise astrocytes (glial-fibrillary acidic protein [GFAP])(Lu et al., 2019), synapses (synapsin-1) (Scofield et al., 2016b) and glutamate activity at α-amino-3-hydroxy-5-methyl-4-

isoxazolepropionic-acid receptors (AMPARs)(calmodulin-kinase-II-alpha [CaMKIIa])(Larsson, 2017). It was employed for analysis the six AVul, six ARes, and five yoked-saline rat brains (one Yoked excluded due inadequate perfusion). GFAP is widely used to visualise astrocytes (Sampedro-Piquero et al., 2014; Siemsen et al., 2019), therefore it was used here. CaMKIIa regulates AMPAR activity and was used to chemogenetically modulate glutamate activity (Zhang et al., 2019), and was therefore used here.

Firstly, tissue slices were washed thrice for 30-minutes in Tris phosphate-buffered-saline (TPBS; Tris-HCl 10mM + sodium phosphate buffer 0.1M + 0.9% NaCl), followed by a 30-minute wash in Tris (10mM, pH 10) and Tween 20 (0.01%) at 80°C to enhance antigen retrieval. Samples were then cooled at room temperature for 1-hour before a further three 5-minute washes in TPBS. The slices were then pre-incubated with TPBS and 0.05% merthiolate (TPBSm) and 10% normal-horse-serum (NHS) for 1.5 hours. Subsequently, tissue sections were incubated with primary antibodies for 8-hours at room temperature and 40 hours at 4°C. The primary antibodies used for detecting astrocytes was goat anti-GFAP (1:1000 dilution, Abcam, ab53554), glutamate activity was mouse anti-CaMKIIa (1:1000, Thermo-Fischer, pa519128), and synapses was rabbit-anti synapsin-I (1:500, Abcam, ab8). Following three 30-minute washes post-incubation, slices were pre-incubated in TPBSm and 10% NHS for 1.5 hours before incubation with secondary antibodies (dilutions 1:500 for all, Cy™3 donkey anti-goat, Alexa Fluor 647 donkey anti-mouse and Alexa Fluor 488 donkey anti-rabbit, Jackson Immunoresearch) for 24 hours at 4°C. Slices were washed with TPBS thrice then mounted on glass slides and cover-slipped with Dako-fluorescence mounting-media with DAPI (Agilent Technologies).

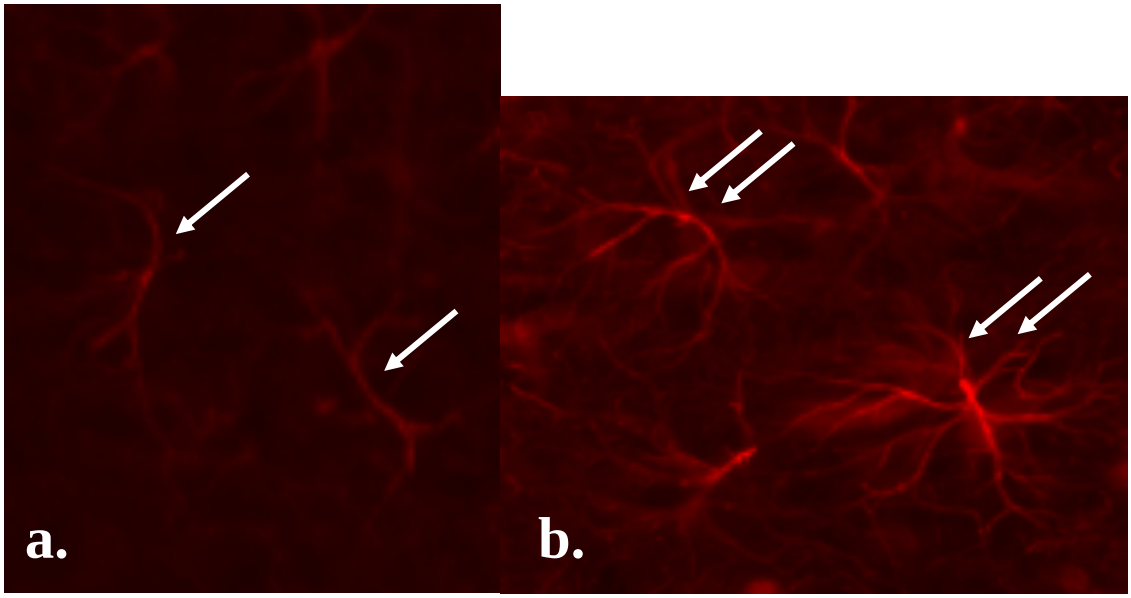

Figure 4. Non-reactive vs. hypertrophied astrocytes. Glial-fibrillary acidic protein (GFAP)-stained astrocytes in the prelimbic cortex of a (a) yoked and (b) addiction-vulnerable sample. White arrows indicate an astrocyte. (a) As can be visualised, in astrocytes of yoked rats there are minimal nodes with fewer long processes. (b) Addiction-vulnerable astrocytes had greater hypertrophy with more, longer processes.

2.6.3 Microscopy and image analysis. Ten brain slices (ranging from AP +3.72 to -3.48mm from Bregma; Figure 6) were imaged using epifluorescence with a Zeiss Axioimager Z2 microscope (Carl Zeiss Microscopy) via Zen 2.0 2011 imaging software (Zeiss). Tiled images of sections were acquired at 20x magnification at a constant exposure time for each channel, then stitched. Brightness and contrast were modified consistently across images. The total number of GFAP positive (GFAP+) astrocytes was quantified whilst the experimenter was blind to treatment employing ImageJ software (Beauquis et al., 2013). The mean intensity of CaMKIIa fluorescence was quantified for each region using the same software Hartig (2013). A co-localisation coefficient for GFAP+ astrocytes and synapsin-1 was quantified using the Coloc-2 ImageJ plugin (Pompey, Michaely, & Luby-Phelps, 2013).

A modified Sholl analysis (Dall'Oglio, Gehlen, Achaval, & Rasia-Filho, 2008; Sampedro-Piquero et al., 2014; Saur et al., 2014) was performed on 6 randomly-selected astrocytes per region per image using the Sholl Analysis ImageJ plugin for 6 rats (2 random controls, ARes, and AVul each). The morphology of n = 864 astrocytes within a total of 24

ROIs (Figure 6) across 10 sections per animal was analysed. Briefly, the number of astrocyte process-ring intersections was quantified manually following overlay of a maximum 25 concentric-rings at 3.91µm intervals (Saur et al., 2014)(Figure 5). The longest-process length was measured for each astrocyte and the total node-number was quantified by summing points from which processes arose (Sampedro-Piquero et al., 2014). Only randomly selected GFAP+ astrocytes that were uniformly stained, relatively isolated and located completely within the ROI were analysed.

Figure 5. Sholl analysis image. Sholl rings overlaid on an astrocyte for analysis of hypertrophy. Intersections are highlighted with dots automatically by the ImageJ plugin Sholl Analysis, then confirmed by experimenter during data collection. The number of nodes are then manually quantified and the length of the longest process is measured with a tracing tool.

2.7 Statistical analyses

Lever presses and infusions were recorded using MED-PC-V software (Med-PC, VT, USA), then statistically analysed using SPSS v20. Significance level was set at $\alpha = 0.05$. Whenever the assumption of sphericity was not met, the Greenhouse-Geiser correction was used. Whenever the assumption of homoscedasticity was not met for a one-way ANOVA, the non-parametric Kruskal-Wallis test was used followed by the use of non-parametric planned contrasts.

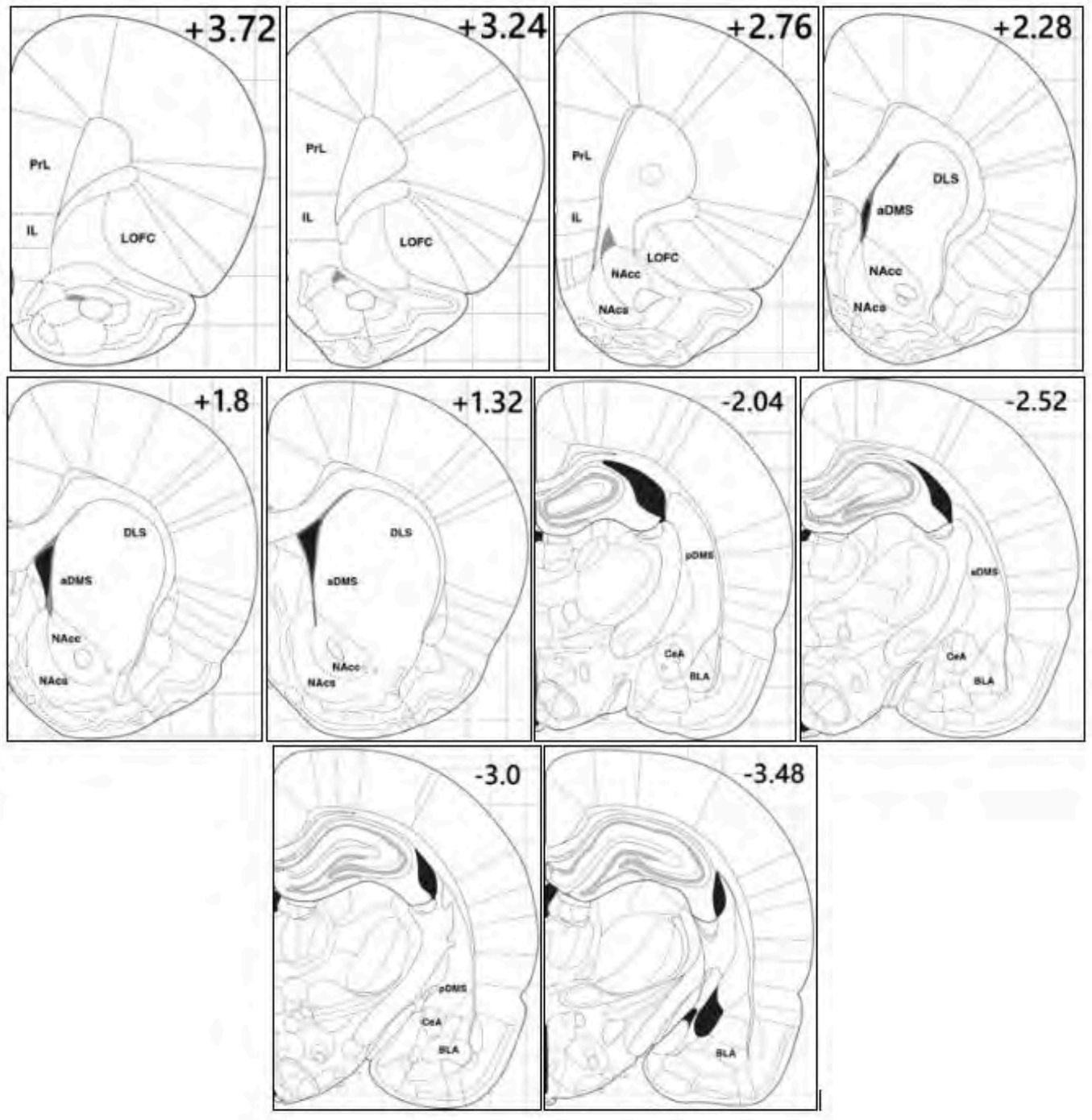

Figure 6. Regions of interest used for all brain regions at 10 bregma levels. Map of sections used (measured as mm from Bregma) with labels of all regions examined. PrL = prelimbic cortex; IL = infralimbic cortex; LOFC = lateral orbitofrontal cortex; NAcc = nucleus accumbens core; NAcs = nucleus accumbens shell; aDMS = anterior dorsomedial striatum; DLS = dorsolateral striatum; pDMS = posterior dorsolateral striatum; CeA = central amygdala; BLA = basolateral amygdala.

2.7.1 Exclusions. Two rats were excluded from analyses (one died from a stroke of unknown origin; one did not acquire on FR1 IVSA). A further 3 rats were not included in the phenotyping analyses as two did not acquire the HDS paradigm and the third's brain was inoperable. Therefore $n = 35$ rats were included for analyses.

2.7.2 Acquisition of self-administration. The assumptions of the IVSA model were first tested. Escalation of METH-intake and METH-seeking behaviour were assessed with a repeated-measures analysis of variance (ANOVA) with a planned contrast comparing day 1 and 14 of the FR1 acquisition period. Acquisition of an operant lever-drug association was assessed with a paired-samples t-test, comparing active and inactive lever presses on the final FR1 acquisition session. To ensure this association persisted following acquisition of the HDS paradigm, a paired-samples t-test was conducted, comparing the active and inactive lever presses on the final day of the HDS acquisition period. Additionally, to assess learning. of period-specific cues, the white-noise and house-light, a paired-samples t-test was used to compare the DAv period active-lever presses to the NDAv active-lever presses on the final HDS acquisition session. Finally, to confirm the lever-drug association persisted into PR sessions, a paired-samples t-test was used to compare the active to inactive-lever presses during the second and final PR acquisition session.

2.7.3 Phenotyping analysis. To be considered for the AVul phenotype, rats needed to have a normalised cued-relapse score equal to or above the 60th percentile and an HDS score or motivation score equal to or above the 66th percentile. In other words, they needed to meet the relapse criterion for addiction, as well as either the motivation or HDS criterion. Their motivation and HDS scores had to also be above the 33rd percentile, with one exception. If a rats' relapse score and motivation score met AVul criteria, however their HDS score was below the 33rd percentile, their resistance to extinction score was considered (Chesworth & Corbit, 2017; Dell et al., 2007). This was calculated as the number of days taken to meet

extinction criteria. Of these rats, those scoring equal to or above the 66th percentile for resistance to extinction were considered to be AVul. This procedure was adopted as it was difficult to interpret the lack of responding during NDAv periods, as psychostimulants facilitate the development of strong drug-cue associations (see 4.3.1). This is evidenced here by strong cue-induced relapse to METH-seeking amongst rats considered for the AVul phenotype (see Figure 7). This resulted in n = 6 rats in the AVul phenotype.

Criteria for the ARes phenotype was set at: a relapse score equal to or below the 40th percentile and a motivation or HDS score equal to or below the 33rd percentile. This resulted in n = 6 rats in the ARes phenotype.

2.7.4 Analysis of addiction behaviours and neural markers. For each bregma level, per region, the average CaMKIIa intensity, total number of immunoreactive GFAP+ astrocytes, ring-intersections, nodes, and longest-process length were analysed using five one-way ANOVAs with three levels to test the main effect of phenotype on the number of astrocytes, CaMKIIa expression, and degree of astrocyte hypertrophy in AVul, ARes and yoked rats. Two planned *a priori* contrasts were then employed. To test the mean difference per bregma level, per region, per marker, between AVul rats, and ARes and Yoked rats, separately, two *a priori* contrasts were used, whereas for comparing ARes to Yoked rats, parametric Tukey HSD and non-parametric Games Howell post-hoc tests were used. The colocalisation coefficient for GFAP+ astrocyte-synapsin-I colocalisation was correlated with average CaMKIIa intensity to assess the relationship between astrocyte-synapse connections and glutamate activity.

3. Results

3.1 Acquisition of METH IVSA

Rats successfully acquired METH IVSA on a FR1 schedule of reinforcement, demonstrated by escalation of intake over the FR1 acquisition period, $F(3.12,93.5) = 11.49$, $p < 0.001$ (Figure 7a). Planned contrasts revealed a significant increase in active lever presses when comparing FR1 acquisition day 1 and 14, $F(1,30) = 8.76$, $p = 0.006$. Rats learnt the lever-drug association, demonstrated by significantly greater active compared to inactive lever presses on day 14 of FR1 acquisition, $t(29) = 17.53$, $p < 0.001$. This association persisted following training on a FR5 schedule during HDS sessions, $t(29) = 11.7$, $p < 0.001$ (Figure 7b). Rats were also able to distinguish between the DAv and NDAv periods of the HDS paradigm, demonstrated by significantly greater active presses during the DAv period on the last day of HDS acquisition, $t(29) = 11.34$, $p < 0.001$ (Figure 7b/c), compared to the NDAv period. The drug-lever association persisted into the PR phase, demonstrated by significantly greater active ($M = 725.4$, $SEM = 187.68$) compared to inactive presses ($M = 45.33$, $SEM = 82.77$) on the final day of PR acquisition, , $t(29) = 3.62$, $p = 0.001$.

3.2 Addiction-phenotype and addiction behaviours

Addiction-vulnerable (AVul) rats ($n = 6$) demonstrated significantly greater active presses during the cued relapse session, $t(10) = 4.48$, $p = 0.001$ (Figure 8a), a significantly greater average breakpoint across the last 3 motivation test sessions, $t(10) = 5.37$, $p < 0.0005$ (Figure 8c), and a significantly greater number of days taken to reach extinction criteria, $t(10) = 2.33$, $p = 0.042$ (Figure 8d), compared to ARes rats ($n = 6$). Excluding the two AVul rats that demonstrated a lack of HDS, AVul HDS-positive rats ($n = 4$) were found to have significantly greater NDAv active presses averaged across the 5 HDS test sessions compared

to ARes rats, $t(8) = 1.97$, $p = 0.033$ (Figure 8b). No significant difference in lifetime METH-intake, measured as mg/kg, was found when comparing AVul ($M = 125.05$, $SEM = 14.88$) to ARes ($M = 132.65$, $SEM = 14.2$) rats, $t(10) = 0.37$, $p = 0.719$.

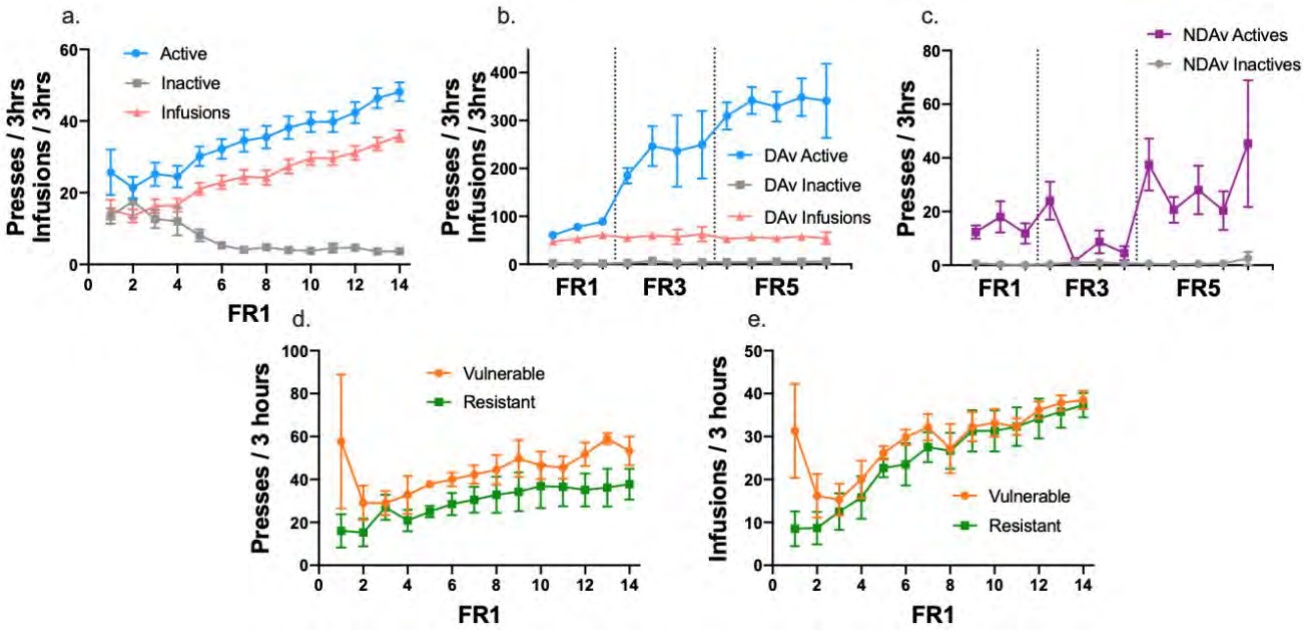

Figure 7. Acquisition of methamphetamine (METH) intravenous self-administration. (a) Acquisition on a fixed-ratio (FR)-1 schedule of reinforcement, measured by active and inactive lever presses, and infusions per session. (b) Acquisition on the habitual drug-seeking paradigm, transitioning from a FR-1 to FR-3 to FR-5, measured by active and inactive lever presses, and infusions per session. (c) Demonstration of continued distinction between the active and inactive lever during non-drug available periods by the end of acquisition. (d) and (e) Demonstration of the similarities in acquisition of METH self-administration between the vulnerable and resistant groups. Marks/numbers on the x-axis indicate the session number.

3.3 METH IVSA reduced the number of GFAP-positive astrocytes in the central CeA

There was no main effect of phenotype on the number of GFAP+ astrocytes in the PrL, IL, LOFC, aDMS, DLS, pDMS, NAcc, NAcs, BLA or CeA, at any of the bregma levels assayed (see Appendix X). As a priori contrasts were planned, they were examined. Contrasts performed on the number of astrocytes between groups in the PrL, IL, LOFC, aDMS, DLS, pDMS, NAcc, NAcs and BLA demonstrated no significant differences between groups (see Appendix X). In the CeA however, it was found that at -2.52mm bregma, AVul rats had fewer astrocytes compared to Yoked rats, $t(13) = 2.544$, $p = .024$, however no significant difference was found when comparing to ARes rats, $t(13) = 1.815$, $p = .093$ (Figure 7c), suggesting that METH-exposure affected AVul and ARes groups equally.

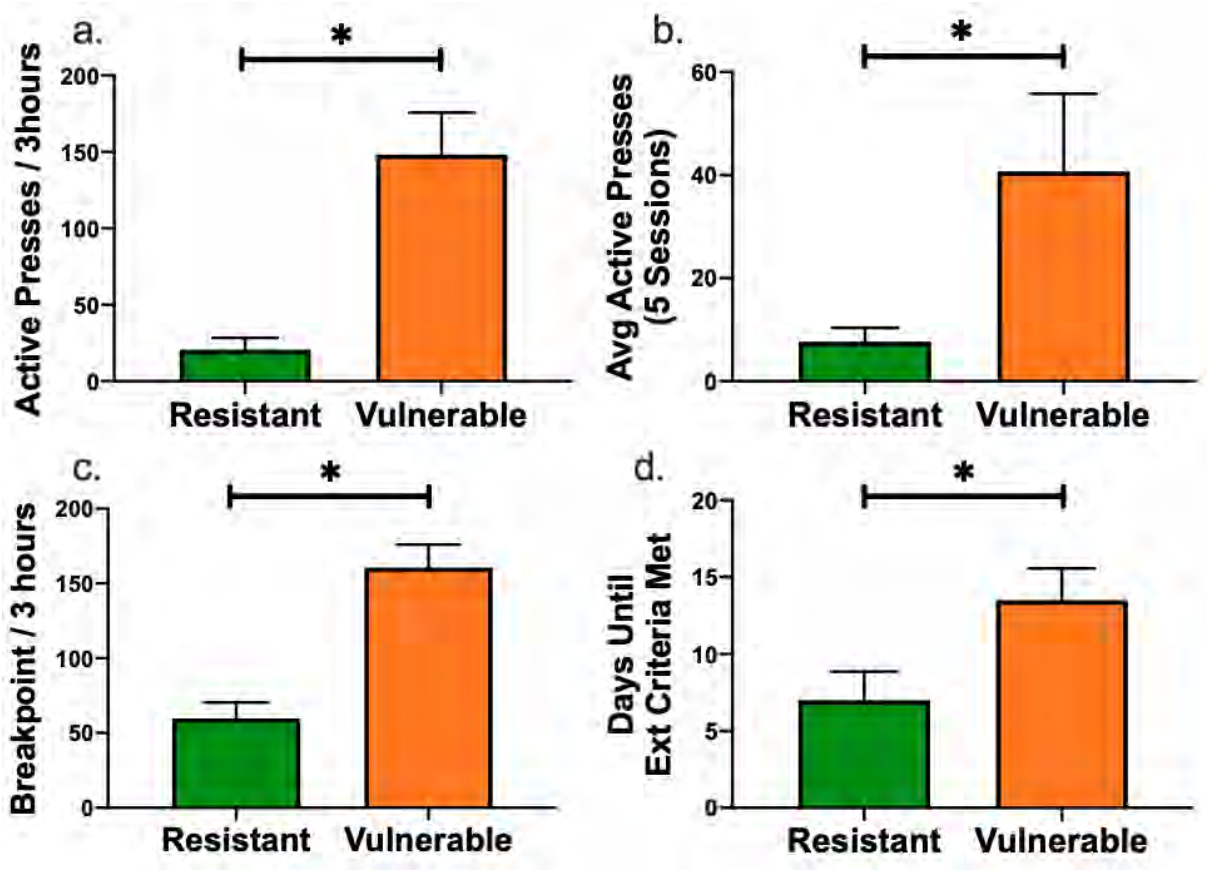

Figure 8. Addiction behaviours in addiction-vulnerable and addiction-resistant rats. (a) Active lever presses during cue-induced relapse to methamphetamine-seeking behaviours, (b) active lever presses during the non-drug available periods of the habitual drug-seeking paradigm in subset of AVul (n = 4) compared to ARes rats, (c) three-hour breakpoint averaged across three progressive-ratio test sessions, and (d) the number of days needed to meet extinction criteria were used as criteria for addiction-phenotyping. * Significance level is set at $p < .05$.

3.4 METH IVSA reduced glutamatergic activity in the NAcc, BLA, and CeA

There was no main effect of phenotype on CaMKIIa fluorescence as an index of glutamate activity in the PrL, IL, LOFC, aDMS, DLS, pDMS, NAcc, NAcs, BLA or CeA (see Appendix X) at any of the bregma levels assayed. However, since contrasts were planned, a priori contrasts were examined.

Contrasts performed on the amount of CaMKIIa fluorescence between groups in the PrL, IL, LOFC, aDMS, DLS, pDMS and NAcs found no significant difference between Yoked, ARes and AVul groups. However, it was found that AVul rats had less CaMKIIa fluorescence compared to Yoked rats in the NAcc at +2.72mm bregma, $t(13) = 2.243$, $p = .043$ (Figure 9b), BLA at -2.52mm bregma, $t(14) = 2.519$, $p = .025$ (Figure 9c), and CeA at

-2.52mm bregma, $t(14) = 2.398$, $p = .031$ (Figure 9d). There was no significant difference in CaMKIIa fluorescence between AVul and ARes rats, nor ARes and AVul rats in the NAcc, BLA and CeA (see Appendix X).

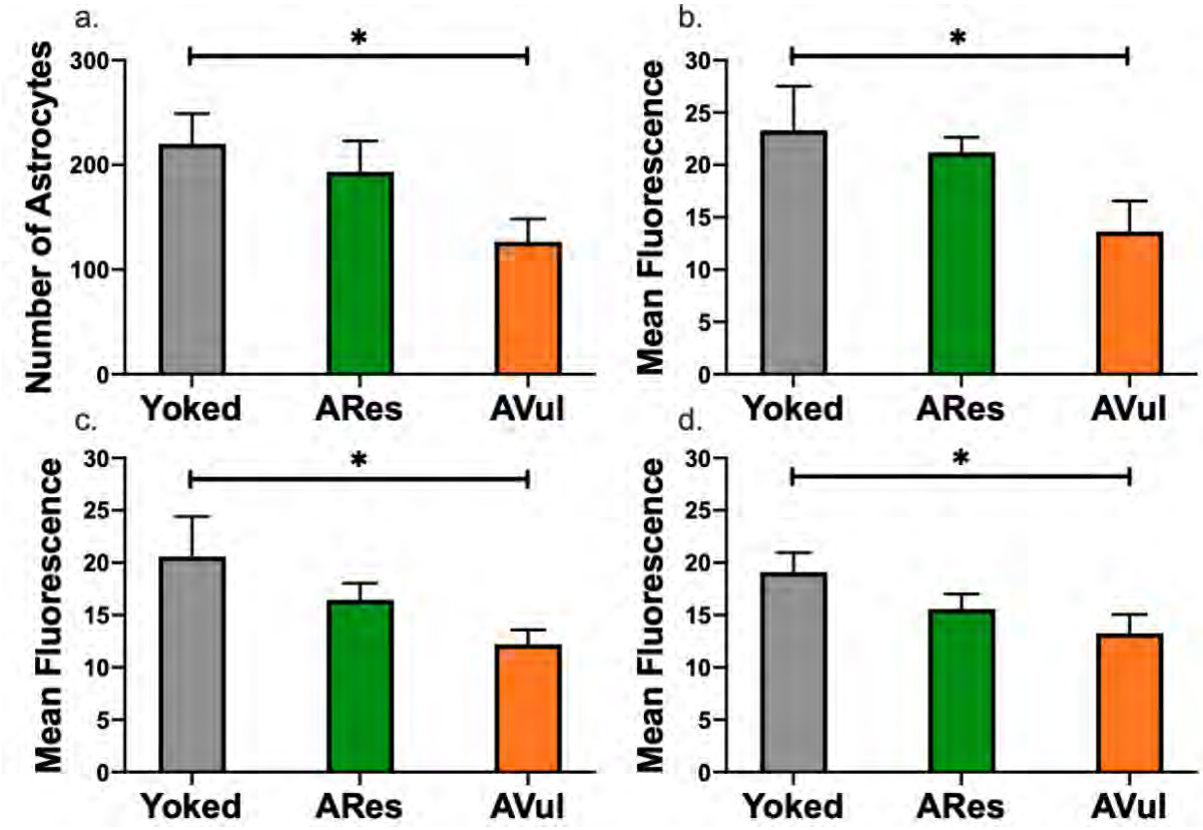

Figure 9. Astrocyte proliferation and baseline glutamate activity in AVul, ARes and yoked rats. The number of glial fibrillary acidic protein (GFAP)-positive astrocytes and mean calmodulin kinase-II alpha (CaMKIIa) expression at bregma levels of regions demonstrating a significant main effect of phenotype. (a) Number of astrocytes at -2.52mm bregma in the central amygdala, and the mean CaMKIIa expression in the (b) nucleus accumbens core at +2.72mm bregma, (c) basolateral amygdala at -2.52mm bregma, and (d) central amygdala at -2.52mm bregma. * Significance level is set at $p < .05$

3.5 Addiction-phenotype and METH IVSA mediated astrocyte hypertrophy in various brain regions

Each index of morphology, astrocytic branching, astrocyte node-number and longest process length, will be described in turn, starting with main effects, followed by the effect of METH IVSA on astrocyte morphology, finishing with changes in astrocyte morphology specific to groups.

3.5.1 Main effect of phenotype on astrocyte branching. There was a significant main effect of phenotype on the number of astrocyte process-ring intersections as a measure

of astrocyte branching in the PrL at +3.72mm, +3.24mm, and +2.76mm bregma, IL at +3.72mm, +3.24mm, and +2.76mm bregma, LOFC at +3.72mm and +3.24mm bregma, NAcc at +2.28mm bregma, NAcs at +2.28mm bregma, BLA at -2.04mm, -3mm, and -3.48mm bregma, and CeA at -2.52mm bregma (Table 1). There was no significant main effect of phenotype in the LOFC at +2.76mm bregma, NAcc at +2.76mm, +1.8mm, and +1.32mm bregma, NAcs at +2.76mm, +1.8mm, and +1.32mm bregma, BLA at -2.52mm bregma, and CeA at -2.04mm and -3mm bregma (Table 1). Planned contrasts were performed on all bregma levels of each brain region, however post-hoc tests were only performed on those that found significant main effects.

Table 1. Analyses of astrocyte branching between groups

Region & Bregma Level	AVul M ± SEM	ARes M ± SEM	Yoked M ± SEM	Statistic (F, t, chi)	df	p-value
IL +3.72	50.75 ± 6.32	29.33 ± 3.01	18.5 ± 1.06	15.628	2,30	< .0005*
	•	•		3.058	15.754	.008*
	•		•	5.032	11.603	< .0005*
		•	•	-	-	.012*
IL +3.24	37.17 ± 1.62	38.17 ± 3.1	20.75 ± 1.49	29.421	2,27	< .0005*
	•	•		-0.341	27	.736
	•		•	6.856	27	< .0005*
		•	•	-	-	.003*
IL +2.76	40.75 ± 7.16	33.75 ± 2.39	20.83 ± 2.33	8.052	2,30	.018*
	•	•		0.927	13.413	.370
	•		•	2.644	13.127	.020*
		•	•	-	-	.005*
PrL +3.72	66.5 ± 6.51	41.42 ± 2.83	23.17 ± 2.1	18.974	2,30	< .0005*
	•	•		3.531	15.014	.003*
	•		•	6.329	13.101	< .0005*
		•	•	-	-	< .0005*
PrL +3.24	49.25 ± 2.76	40.17 ± 2.06	23.58 ± 1.75	35.288	2,27	< .0005*
	•	•		2.407	27	.023*
	•		•	8.33	27	< .0005*
		•	•	-	-	< .0005*
PrL +2.76	53.33 ± 8.63	34.17 ± 3.88	17 ± 1.29	21.103	2,30	.005*
	•	•		2.026	15.273	.061
	•		•	4.164	11.485	.001*
		•	•	-	-	.003*
LOFC +3.72	52.58 ± 8.46	37.5 ± 4.5	22.83 ± 4.59	7.524	2,30	.023*
	•	•		1.574	16.772	.134
	•		•	3.092	15.475	.007*
		•	•	-	-	.093
LOFC +3.24	45.92 ± 4.41	30.5 ± 3.84	31.92 ± 2.58	8.417	2,30	.015*
	•	•		2.639	15.016	.019*
	•		•	2.742	17.751	.014*
		•	•	-	-	.950
LOFC +2.76	49.42 ± 7.4	34.33 ± 2.39	27 ± 2.1	5.107	2,30	.078
	•	•		1.939	13.272	.074
	•		•	2.914	12.659	.012*

Region & Bregma Level	AVul M ± SEM	ARes M ± SEM	Yoked M ± SEM	Statistic (F, t, chi)	df	p-value
NAcc +2.76	43.75 ± 5.78	37.5 ± 6.1	28.83 ± 3.81	1.248	2,27	.303
	•	•		0.805	27	.428
	•		•	1.569	27	.128
NAcc +2.28	43.25 ± 6.48	31.83 ± 4.37	23.5 ± 2.08	8.478	2,36	.014*
	•	•		1.461	19.274	.160
	•		•	2.901	13.233	.012*
		•	•	-	-	.227
NAcc +1.8	43.25 ± 6.48	33.17 ± 2.32	35.75 ± 3.74	0.787	2,27	.465
	•	•		1.25	27	.458
	•		•	0.753	27	.548
NAcc +1.32	48.92 ± 4.22	45.75 ± 6.34	41.75 ± 3.17	0.569	2,27	.572
	•	•		0.47	27	.295
	•		•	1.064	27	.557
NAcs +2.76	45.92 ± 11.38	49.92 ± 10.3	22.67 ± 4.45	1.345	2,27	.278
	•	•		-0.286	27	.186
	•		•	1.357	27	.123
NAcs +2.28	52.75 ± 6.2	35.5 ± 1.93	28.17 ± 3.21	9.71	2,36	.008*
	•	•		2.652	13.099	.020*
	•		•	3.508	16.649	.003*
		•	•	-	-	.158
NAcs +1.8	34.5 ± 5.15	33.33 ± 3.31	33.67 ± 3.39	0.02	2,27	.981
	•	•		0.198	27	.889
	•		•	0.141	27	.945
NAcs +1.32	43.25 ± 4.88	45.42 ± 4.04	32 ± 3.57	2.946	2,33	0.66
	•	•		-0.365	33	.717
	•		•	1.896	33	.067
BLA -2.04	57.33 ± 6.11	42.92 ± 4.59	28.17 ± 5.44	7.251	2,33	.002*
	•	•		1.882	33	.069
	•		•	3.808	33	.001*
		•	•	-	-	.147
BLA -2.52	41.92 ± 5.34	41.5 ± 4.02	29.5 ± 2.7	2.871	2,33	.071
	•	•		.071	33	.944
	•		•	2.11	33	.043*
BLA -3	38.67 ± 3.45	44.33 ± 2.4	31.25 ± 3.04	4.803	2,33	.015*
	•	•		-1.338	33	.190
	•		•	1.752	33	.089
		•	•	-	-	.011*
BLA -3.48	37.92 ± 3.77	28.42 ± 2.44	54 ± 6.2	9.296	2,27	.001*
	•	•		1.958	27	.061
	•		•	-2.707	27	.012*
		•	•	-	-	.001*
CeA -2.04	49.5 ± 4.26	43.25 ± 3.56	31.67 ± 8.27	3.725	2,36	.155
	•	•		1.125	21.321	.273
	•		•	1.916	16.459	.073
CeA -2.52	43.17 ± 4.66	39.75 ± 2.98	23.25 ± 2.78	12.371	2,33	.002*
	•	•		0.618	18.694	.544
	•		•	3.673	17.945	.002*
		•	•	-	-	.001*
CeA -3	40.75 ± 4.64	43.83 ± 6.23	32.25 ± 3.82	1.44	2,33	.252
	•	•		1.202	33	.238
	•		•	-0.436	33	.666

Note: AVul = addiction-vulnerable; ARes = addiction-resistant; IL = infralimbic cortex; PrL = prelimbic cortex; LOFC = lateral orbitofrontal cortex; NAcc = nucleus accumbens core; NAcs = nucleus accumbens shell; BLA = basolateral amygdala; CeA = central amygdala. • denotes the groups that were included in a contrast or post-hoc test. Pale yellow cells highlight a significant main effect. Red cells with white writing highlight a significant difference between AVul and ARes astrocytes. Orange cells highlight a significant difference between AVul and Yoked astrocytes. Green cells highlight a significant difference between ARes and Yoked astrocytes. * p > .05

3.5.2 METH IVSA increased astrocytic branching in the IL, LOFC, NAcs, BLA and CeA. Planned contrasts demonstrated AVul, compared to Yoked, astrocytes had significantly more process-ring intersections in the IL at +3.24mm and +2.76 bregma, LOFC at +3.72mm and +2.76mm bregma, NAcc at +2.28mm bregma, BLA at -2.52mm bregma, and CeA at -2.52mm bregma (Table 1). A similar trending increase was found in the BLA at -3mm bregma (Table 1). Post-hoc tests indicated ARes, compared to Yoked, astrocytes had significantly more process-ring intersections in the IL at +3.24mm and +2.76mm bregma, BLA at -3mm bregma, and CeA at -2.52mm bregma (Table 1). Neither AVul nor ARes, compared to Yoked, astrocytes showed a significant difference in process-ring intersections in the LOFC at +3.72mm bregma and NAcc at +2.28mm bregma (Table 1). In the LOFC at +2.76mm bregma, and BLA at -2.52mm bregma, there was no main effect hence post-hoc tests were not performed.

AVul, compared to ARes, astrocytes had no significant difference in process-ring intersections the IL at +3.24mm and +2.76mm bregma, LOFC at +3.72mm and +2.76mm bregma, NAcc at +2.28mm bregma, NAcs at +1.32mm bregma, BLA at -3mm bregma, and CeA at -2.52mm bregma (Table 1). Planned contrasts revealed no significant difference between AVul, ARes and Yoked astrocytes, in the NAcc at +2.76mm, +1.8mm, and +1.32mm bregma, NAcs at +2.76mm, +1.8mm and +1.32mm bregma, and CeA at -2.04mm bregma (Table 1).

3.5.2.1 Addiction vulnerability resulted in increased astrocytic branching in the LOFC, NAcs, and BLA. Planned contrasts revealed AVul, compared to ARes, astrocytes had significantly more astrocyte process-ring intersections in the LOFC at +3.24mm bregma and NAcs at +2.28mm bregma, and a trend for an increase in the BLA at -2.04mm bregma (Table 1). AVul, compared to Yoked, astrocytes had significantly more process-ring intersections in the LOFC at +3.24mm bregma, NAcs at +2.28mm bregma, and BLA at -2.04mm bregma

(Table 1). Post-hoc tests revealed no significant difference in process-ring intersections between Yoked and ARes astrocyte in in the LOFC at +3.24mm bregma, NAcs at +2.28mm bregma, and BLA at -2.04mm bregma.

3.5.2.2 Addiction vulnerability resulted in exacerbated astrocytic branching in the PrL and IL. Contrast tests revealed AVul, compared to ARes, astrocytes had significantly more process-ring intersections in the PrL at +3.72mm and +3.24mm bregma, and IL at +3.72mm bregma (Table 1). AVul, compared to ARes, astrocytes had a close non-significant increase in process-ring intersections in the PrL at +2.76mm bregma (Table 1). Additionally, AVul, compared to Yoked, astrocytes had significantly more process-ring intersections in the PrL at +3.72mm, +3.24mm, and +2.76mm bregma, and IL at +3.72mm bregma (Table 1). Post-hoc tests revealed ARes, compared to Yoked, astrocytes had significantly more process-ring intersections in the PrL at +3.72mm, +3.24mm, and +2.76mm bregma, and IL at +3.72mm bregma (Table 1).

3.5.2.3 METH IVSA reduced astrocytic branching in the BLA. Planned contrasts revealed AVul, compared to Yoked, astrocytes had significant less process-ring intersections the BLA at -3.48mm bregma (Table 1). Tukey HSD post-hoc tests revealed a significant decrease in process-ring intersections in ARes, compared to Yoked, astrocytes in the BLA at -3.48mm bregma (Table 1). There was a non-significant trending increase in process-ring intersections between AVul and ARes astrocytes (Table 1).

3.5.3 Effect of phenotype on astrocyte node-number. There was a significant main effect of addiction-phenotype on node-number in the PrL at +3.72mm, +3.24mm, and +2.76mm bregma, IL at +3.72mm, +3.24mm, and +2.76mm bregma, LOFC at +3.72mm, +3.24mm, and +2.76mm bregma, NAcc at +2.28mm bregma, NAcs at +1.32mm bregma, BLA at -2.04mm, -3mm, and -3.48mm bregma, and CeA at -2.04mm bregma (Table 2). There was no significant main effect of addiction-phenotype on node-number in the NAcc

+2.76mm, +1.8mm and +1.32mm bregma, NAcs at +2.76mm, +2.28mm, and +1.8mm bregma, BLA at -2.52mm bregma, and CeA at -2.52mm, and -3mm bregma (Table 2). Planned contrasts were performed on all bregma levels of each brain region, however post-hoc tests were only performed on those that demonstrated significant main effects.

3.5.3.1 METH IVSA increased the astrocyte node-number in the PrL, IL, LOFC, NAcs, BLA and CeA. Planned contrasts revealed a significant increase in node-number in AVul-group, compared to Yoked-group, astrocytes, in the PrL at +3.72mm and +2.76mm bregma, IL at +3.24mm and +2.76mm bregma, LOFC at +3.72mm and +2.76mm bregma, NAcs at +1.32mm bregma, BLA at -2.04mm bregma, and CeA at -2.04mm bregma (Table 2). Post-hoc tests revealed in ARes astrocytes, a significant increase in node-number, compared to Yoked-group astrocytes, in the PrL at +3.72mm and +2.76mm bregma, IL at +3.24mm and +2.76mm bregma, and LOFC at +3.72mm and +2.76mm bregma (Table 2). There was a non-significant trending increase in node-number in ARes, compared to Yoked, astrocytes in the BLA at -2.04mm bregma (Table 2). There was no significant difference in node-number between ARes and Yoked astrocytes in the NAcs at +1.32mm bregma and CeA at -2.04mm bregma (Table 2).

Table 2. Analyses of the node-number between groups.

Region & Bregma Level	AVul M ± SEM	ARes M ± SEM	Yoked M ± SEM	Statistic (F, t, chi)	df	p-value
IL +3.72	16.33 ± 2.01	10.67 ± 1.35	6.67 ± 0.21	8.506	2,30	.014*
	•	•		2.344	19.209	.030*
	•		•	4.786	11.241	.001*
		•	•	-	-	.032*
IL +3.24	11.42 ± 0.53	13 ± 0.93	7.17 ± 0.51	24.375	2,27	< .0005*
	•	•		-1.674	27	.106
	•		•	5.504	27	< .0005*
		•	•	-	-	< .0005*
IL +2.76	12.83 ± 1.89	11.58 ± 0.45	7 ± 0.93	10.447	2,30	.005*
	•	•		.643	12.251	.532
	•		•	2.768	15.037	.014*
		•	•	-		.006*
PrL +3.72	23.42 ± 3.29	17 ± 0.85	7.17 ± 0.65	14.414	2,30	.001*
	•	•		1.889	12.473	.082
	•		•	4.847	11.847	< .0005*
		•	•	-	-	< .0005*

Region & Bregma Level	AVul M ± SEM	ARes M ± SEM	Yoked M ± SEM	Statistic (F, t, chi)	df	p-value
PrL +3.24	15.17 ± 0.65	12.33 ± 1.48	8.42 ± 0.69	20.17	2,27	< .0005*
	•	•		2.171	27	.039*
	•		•	6.335	27	< .0005*
		•	•	-	-	.015*
PrL +2.76	16.25 ± 2.31	12.67 ± 1.55	6.5 ± 0.89	10.427	2,30	.005*
	•	•		1.288	19.278	.213
	•		•	3.947	13.819	.001*
		•	•	-	-	.009*
LOFC 3.72	16.75 ± 2.9	12.83 ± 1.01	6.83 ± 0.98	9.326	2,30	.009*
	•	•		1.276	13.611	.223
	•		•	3.239	13.276	.006*
		•	•	-	-	.002*
LOFC 3.24	12.92 ± 1.21	8.33 ± 0.88	8.33 ± 0.5	8.203	2,27	.002*
	•	•		3.109	27	.005*
	•		•	3.698	27	.001*
		•	•	-	-	1.000
LOFC 2.76	14.5 ± 1.97	11 ± 0.67	7.83 ± 0.31	7.922	2,30	.019*
	•	•		1.683	13.548	.115
	•		•	3.348	11.528	.006*
		•	•	-	-	.002*
NAcc 2.76	13.92 ± 2.07	9.25 ± 1.05	8.83 ± 1.37	2.927	2,27	.071
	•	•		2.141	27	.041*
	•		•	1.904	27	.068
NAcc 2.28	11.42 ± 1.36	7.67 ± 0.81	6.75 ± 0.75	5.995	2,33	.006*
	•	•		2.626	33	.013*
	•		•	3.268	33	.003*
		•	•	-	-	.798
NAcc 1.8	10.67 ± 1.09	11.5 ± 9.75	9.75 ± 0.76	1.275	2,27	.296
	•	•		-.620	27	.540
	•		•	.683	27	.500
NAcc 1.32	14 ± 1.17	15.17 ± 10.68	12.83 ± 0.87	0.412	2,36	.814
	•	•		-.496	17.565	.626
	•		•	.799	20.268	.434
NAcs 2.76	13.83 ± 2.9	12.25 ± 2.64	6.33 ± 1.02	1.515	2,27	.238
	•	•		0.444	27	.661
	•		•	1.718	27	.097
NAcs 2.28	13.58 ± 1.43	10.83 ± 0.37	9.83 ± 1.09	3.244	2,36	.198
	•	•		1.866	12.439	.086
	•		•	2.091	20.539	.049*
NAcs 1.8	10.5 ± 0.72	8.5 ± 0.67	9.42 ± 0.96	1.125	2,33	.339
	•	•		1.479	27	.151
	•		•	0.801	27	.430
NAcs 1.32	13.58 ± 1.32	12.17 ± 1.08	9.17 ± 0.89	4.125	2,33	.025*
	•	•		0.902	33	.374
	•		•	2.813	33	.008*
		•	•	-	-	.152
BLA -2.04	17.08 ± 1.94	13.33 ± 1.17	8.5 ± 1.49	7.539	2,33	.002*
	•	•		1.692	33	.100
	•		•	3.873	33	< .0005*
		•	•	-	-	.089
BLA -2.52	12.42 ± 1.29	13.08 ± 1.53	8.92 ± 1	2.993	2,33	.064
	•	•		-.364	33	.718
	•		•	1.913	33	.064
BLA -3	11.58 ± 1.18	14.33 ± 1.04	10.08 ± 0.78	4.526	2,33	.018*
	•	•		-1.919	33	.064
	•		•	1.047	33	.303
		•	•	-	-	.015*

Region & Bregma Level	AVul M ± SEM	ARes M ± SEM	Yoked M ± SEM	Statistic (F, t, chi)	df	p-value
BLA -3.48	13.25 ± 1.36	9.83 ± 0.69	18 ± 1.57	9.553	2,27	.001*
	•	•		2.225	27	.035*
	•		•	-2.526	27	.018*
		•	•	-	-	.001*
CeA -2.04	14.08 ± 0.83	12.5 ± 0.91	8.67 ± 2.05	6.913	2,36	.032*
	•	•		1.287	21.821	.212
	•		•	2.453	14.524	.027*
		•	•	-	-	.233
CeA -2.52	8.5 ± 1.49	11.42 ± 0.98	7.5 ± 0.81	5.784	2,36	.055
	•	•		-1.635	19.024	.118
	•		•	.589	17.033	.563
CeA -3	13.08 ± 1.61	14.5 ± 1.58	11.33 ± 1.07	1.208	2,33	.312
	•	•		-.694	33	.492
	•		•	.858	33	.397

Note: AVul = addiction-vulnerable; ARes = addiction-resistant; IL = infralimbic cortex; PrL = prelimbic cortex; LOFC = lateral orbitofrontal cortex; NAcc = nucleus accumbens core; NAcs = nucleus accumbens shell; BLA = basolateral amygdala; CeA = central amygdala. • denotes the groups that were included in a contrast or post-hoc test. Pale yellow cells highlight a significant main effect. Red cells with white writing highlight a significant difference between AVul and ARes astrocytes. Orange cells highlight a significant difference between AVul and Yoked astrocytes. Green cells highlight a significant difference between ARes and Yoked astrocytes. * p > .05

Planned contrasts revealed no significant difference in the node-number between AVul and ARes astrocytes in the PrL at +3.72mm and +2.76mm bregma, IL at +3.24mm and +2.76mm bregma, LOFC at +3.72mm and +2.76mm bregma, NAcs at +1.32mm bregma, BLA at -2.04mm bregma, and CeA at -2.04mm bregma (Table 2). Interestingly, post-hoc tests revealed a significant increase in the node-number in ARes compared to Yoked astrocytes in the BLA at -3mm bregma (Table 2). In contrast, planned comparisons revealed a non-significant trend for a decrease in nodes in AVul compared to Yoked astrocytes in the BLA at -3mm bregma (Table 2). There was no significant difference in node-number in AVul compared to ARes astrocytes in the BLA at -3mm bregma (Table 2). Along with no main effect of phenotype, planned contrasts revealed there was no significant difference in node-number between AVul-group, ARes-group and Yoked-group astrocytes, in the NAcc at +1.8mm and +1.32mm bregma, NAcs at +2.76mm and +1.8mm bregma, BLA at -2.52mm bregma, and CeA at -2.52mm and -3mm bregma (Table 2).

3.5.3.2 Addiction vulnerability resulted in an increase astrocyte node-number in the LOFC, NAcc, and NAcs. Planned contrasts revealed a significantly greater node-number in AVul, compared to ARes, astrocytes in the LOFC at +3.24mm bregma, NAcc at +2.76mm

and +2.28mm bregma (Table 2). A non-significant trending increase between AVul and ARes astrocytes in node-number was found in the NAcs +2.28mm bregma (Table 2). When comparing AVul with Yoked astrocytes, planned contrasts revealed a significant increase in node-number in the LOFC at +3.24mm bregma, NAcc at +2.28mm bregma, and NAcs at +2.28mm bregma (Table 2). There was a non-significant trend for an increase in node-number in AVul, compared to Yoked, astrocytes in the NAcc at +2.76mm bregma (Table 2). Post-hoc tests revealed that there was no significant difference between ARes and Yoked astrocytes in node-number in the LOFC at +3.24mm bregma and NAcc at +2.28mm bregma (Table 2). No post-hoc tests were performed on node-number in the NAcc at +2.76mm bregma, and NAcs at +2.28mm bregma due to no main effect of phenotype.

3.5.3.3 Addiction vulnerability resulted in exacerbation of astrocyte node number in the PrL and IL. When comparing AVul, to ARes astrocytes, planned contrasts revealed a significant increase in node-number in the PrL at +3.24mm bregma and IL at +3.72mm bregma (Table 2). There was a significant increase in node-number in AVul, compared to Yoked, astrocytes in the PrL at +3.24mm bregma, and IL +3.72mm bregma (Table 2). Post-hoc analyses revealed a significant increase in node-number in ARes, compared to Yoked, astrocytes, in the PrL at +3.24mm bregma and IL at +3.72mm bregma (Table 2).

3.5.3.4 METH IVSA reduced astrocyte node-number in the BLA. In AVul astrocytes, compared to Yoked, planned contrasts revealed a significant decrease in node-number in the BLA at -3.48mm bregma (Table 2). Post-hoc tests revealed a significant decrease in nodes in ARes, compared to Yoked, astrocytes in the BLA at -3.48mm bregma (Table 2). Interestingly, planned contrasts demonstrated a significant increase in node-number in AVul compared to ARes astrocytes (Table 2).

3.5.4 Main effect of phenotype on longest-process length. There was a significant main effect of addiction-phenotype on longest-process length in the PrL at +3.72mm,

+3.24mm, and +2.76mm bregma, IL at +2.76mm bregma, LOFC at +3.72mm bregma, NAcc at +2.28mm bregma, NAcs at +2.28mm bregma, BLA at -2.04mm bregma, and CeA at -2.04mm, -2.52mm, and -3mm bregma (Table 3). There was no significant main effect of addiction-phenotype on longest-process length in the IL at +3.72mm and +3.24mm bregma, and LOFC at +3.24mm and +2.76mm bregma, NAcc at +2.76mm, +1.8mm and +1.32mm bregma, NAcs at +2.76mm, +1.8mm and +1.32mm bregma, and BLA at -2.52, -3mm, and -3.48mm bregma (Table 3). Planned contrasts were performed on all bregma levels of each brain region, however post-hoc tests were only performed on those that demonstrated significant main effects.

3.5.4.1 Addiction vulnerability results in increased longest-process length in the IL and BLA. Planned contrasts demonstrated a significant increase in longest-process length in AVul, compared to ARes, astrocytes in the IL at +3.24mm bregma and BLA at -2.04mm bregma (Table 3). Likewise, there was a significant increase in longest-process length when comparing AVul to Yoked astrocytes in the BLA at -2.04mm bregma (Table 3). There was no significant difference between AVul and Yoked astrocytes in the IL at +3.24mm (Table 3). Post-hoc analyses revealed no significant difference in longest-process length between ARes and Yoked astrocytes in the BLA at -2.04mm bregma (Table 3). Due to non-significant main effects, post-hoc analyses, comparing longest-process length in ARes and Yoked astrocytes in the IL at +3.2mm bregma, were not performed.

Table 3. Analyses of the longest-process length between groups.

Region & Bregma Level	AVul M ± SEM	ARes M ± SEM	Yoked M ± SEM	Statistic (F, t, chi)	df	p-value
IL +3.72	33.53 ± 2.01	29 ± 2.86	25.74 ± 1.34	2.201	2,27	.130
	•	•		1.421	27	.167
	•		•	1.989	27	.057
IL +3.24	35.51 ± 2.1	30.95 ± 3.26	28.67 ± 2.51	2.242	2,27	.126
	•	•		1.14	27	.264
	•		•	2.095	27	.046*
IL +2.76	31.93 ± 3.1	31.6 ± 1.8	56.37 ± 2.61	13.582	2,30	.001*
	•	•		0.95	17.669	.929
	•		•	-6.035	15.263	< .0005*
		•	•	-	-	< .0005*

Region & Bregma Level	AVul M ± SEM	ARes M ± SEM	Yoked M ± SEM	Statistic (F, t, chi)	df	p-value
PrL +3.72	39.42 ± 1.98	36.82 ± 3.17	27.04 ± 2.93	4.045	2,27	.029*
	•	•		0.724	27	.476
	•		•	2.806	27	.009*
		•	•	-	-	.087
PrL +3.24	35.84 ± 2.33	34.86 ± 2.35	26.72 ± 1.45	6.519	2,27	.005*
	•	•		0.298	27	.768
	•		•	3.407	27	.002*
		•	•	-	-	.050
PrL +2.76	42.36 ± 4.77	36.82 ± 3.64	57.02 ± 1.34	7.477	2,30	.024*
	•	•		0.923	20.583	.367
	•		•	-2.961	12.623	.011*
		•	•	-	-	< .0005*
LOFC +3.72	41.05 ± 2.57	34.21 ± 2.12	25.09 ± 2.4	8.559	2,27	.001*
	•	•		2.154	27	.040*
	•		•	4.104	27	< .0005*
		•	•	-	-	0.66
LOFC 3.24	37.79 ± 2.01	33.56 ± 1.67	34.21 ± 3.86	1.716	2,30	.424
	•	•		1.619	15.331	.126
	•		•	0.823	16.561	.422
LOFC 2.76	34.21 ± 2.37	35.51 ± 34.21	30.95 ± 3.411	0.713	2,27	.499
	•	•		-0.417	27	.680
	•		•	0.851	27	.402
NAcc 2.76	31.6 ± 2.21	29.65 ± 3.06	36.82 ± 2.18	1.381	2,27	.269
	•	•		0.553	27	.585
	•		•	-1.205	27	.239
NAcc 2.28	40.4 ± 2.97	35.51 ± 2.04	26.39 ± 2.06	8.796	2,33	.001*
	•	•		1.441	33	.159
	•		•	4.132	33	< .0005*
		•	•	-	-	.029*
NAcc 1.8	40.07 ± 6.5	41.38 ± 2.87	36.49 ± 2.69	0.611	2,27	.550
	•	•		-0.236	27	.815
	•		•	0.648	27	.522
NAcc 1.32	36.16 ± 2.72	39.42 ± 4.03	36.49 ± 1.87	0.357	2,33	.703
	•	•		-0.767	33	.449
	•		•	-0.077	33	.939
NAcs 2.76	32.91 ± 3.92	38.12 ± 4.34	33.56 ± 6.52	0.423	2,27	.659
	•	•		-0.872	27	.391
	•		•	-0.089	27	.930
NAcs 2.28	44.63 ± 3.31	39.42 ± 2.04	30.95 ± 3.56	5.141	2,33	.011*
	•	•		1.21	33	.235
	•		•	3.177	33	.003*
		•	•	-	-	.136
NAcs 1.8	32.91 ± 4.91	32.25 ± 1.43	31.93 ± 1.02	0.320	2,30	.852
	•	•		0.127	5.865	.903
	•		•	0.195	5.433	.853
NAcs 1.32	34.86 ± 1.97	38.77 ± 1.85	44.07 ± 4.64	2.3	2,36	.317
	•	•		-1.444	21.913	.163
	•		•	-1.826	14.861	.088
BLA -2.04	40.40 ± 3.05	29.65 ± 1.40	25.09 ± 2.47	10.682	2,33	< .0005*
	•	•		3.16	33	.003*
	•		•	4.501	33	< .0005*
		•	•	-	-	.383
BLA -2.52	41.7 ± 6.64	34.54 ± 2.41	29.32 ± 2.33	2.4	2,36	.301
	•	•		1.014	13.853	.328
	•		•	1.759	13.669	.101
BLA -3	32.25 ± 2.2	31.93 ± 1.83	28.34 ± 1.92	1.192	2,33	.316
	•	•		0.116	33	.908
	•		•	1.392	33	.173

Region & Bregma Level	AVul M ± SEM	ARes M ± SEM	Yoked M ± SEM	Statistic (F, t, chi)	df	p-value
BLA -3.48	31.93 ± 2.23	28.02 ± 1.63	32.91 ± 2.97	1.412	2,27	.261
	•	•		1.396	27	.172
	•		•	-0.285	27	.778
CeA -2.04	43.98 ± 4.59	37.47 ± 7.55	27.04 ± 4.71	4.566	2,33	.018*
	•	•		1.152	33	.258
	•		•	2.996	33	.005*
		•	•	-	-	.171
CeA -2.52	39.1 ± 3.49	34.54 ± 2.55	25.74 ± 3.02	4.973	2,33	.013*
	•	•		1.059	33	.297
	•		•	3.102	33	.004*
		•	•	-	-	.118
CeA -3	34.21 ± 2.06	32.58 ± 1.37	25.41 ± 1.77	7.108	2,33	.003*
	•	•		0.656	33	.516
	•		•	3.543	33	.001*
		•	•	-		.018*

Note: AVul = addiction-vulnerable; ARes = addiction-resistant; IL = infralimbic cortex; PrL = prelimbic cortex; LOFC = lateral orbitofrontal cortex; NAcc = nucleus accumbens core; NAcs = nucleus accumbens shell; BLA = basolateral amygdala; CeA = central amygdala. • denotes the groups that were included in a contrast or post-hoc test. Pale yellow cells highlight a significant main effect. Red cells with white writing highlight a significant difference between AVul and ARes astrocytes. Orange cells highlight a significant difference between AVul and Yoked astrocytes. Green cells highlight a significant difference between ARes and Yoked astrocytes. * p > .05

3.5.4.2 Addiction-vulnerability exacerbates METH-induced increase in longest-process length in the LOFC. Planned contrasts revealed a significant increase in longest-process length in AVul, compared to ARes, astrocytes in the LOFC at +3.72mm bregma, and compared to Yoked astrocytes (Table 3). Post-hoc tests revealed a non-significant increase in longest-process length between ARes-group, compared to Yoked-group, astrocytes in the LOFC at +3.72mm bregma (Table 3).

3.5.4.3 METH IVSA increased the longest process length in the PrL, NAcc, NAcs, and CeA. In AVul, compared to Yoked, astrocytes there was a significant increase in longest-process length in the PrL at +3.72mm and +3.24mm bregma, NAcc at +2.28mm bregma, NAcs at +2.28mm bregma, and CeA at -2.04mm, -2.52mm, and -3mm bregma (Table 3). There was likewise an increase in longest-process length in ARes, compared to Yoked, astrocytes in the NAcc at +2.28mm bregma (Table 3). There was a non-significant trend for an increase in longest-process length in ARes, compared to Yoked, astrocytes in the PrL at +3.72mm and +3.24mm bregma, NAcs at +2.28mm bregma, and CeA at -2.04mm bregma (Table 3). Furthermore, there was no significant difference in the CeA at -2.52mm or -3mm

bregma (Table 3). Planned contrasts revealed no significant difference between longest-process length in AVul and ARes astrocytes in the PrL at +3.72mm and +3.24mm bregma, NAcc at +2.28mm bregma, NAcs at +2.28mm bregma, and CeA at -2.04mm, -2.52mm, and -3mm bregma (Table 3).

Planned contrasts demonstrated no significant difference in longest-process length between AVul, ARes and Yoked astrocytes in the IL at +3.72mm bregma, LOFC at +3.24mm and +2.76mm bregma, NAcc at +2.76mm, +1.8mm, and +1.32mm bregma, NAcs at +2.76mm, +1.8mm, and +1.32mm bregma, and BLA at -2.52mm, -3mm, and -3.48mm bregma (Table 3).

3.5.4.4 METH IVSA reduced astrocyte longest-process length in the PrL and IL. Planned contrasts showed a significant decrease in longest-process length in AVul, compared to Yoked, astrocytes in the PrL at +2.76mm bregma and IL at +2.76mm bregma (Table 3). Likewise, post-hoc tests revealed a significant reduction in longest-process length in ARes, compared to Yoked, astrocytes in the PrL at +2.76mm bregma and IL at +2,76mm bregma (Table 3). There was no significant difference in longest-process length between AVul and ARes astrocytes in the PrL at +2.76mm bregma and IL at +2.76mm bregma (Table 3).

3.6 Glutamate homeostasis varies between addiction-phenotypes.

In AVul rats there was a significant, very strong negative correlation between CaMKIIa fluorescence and GFAP-synapsin-I colocalisation in the BLA at -2.04mm bregma, r = -.961, p = .009 (Figure 10d) suggesting decreased synaptic contact between glutamatergic synapses and astrocytes. In the ARes group, there was a significant, very strong positive correlation between CaMKIIa fluorescence and GFAP-synapsin-I colocalisation in the IL at +3.72mm bregma, r = .935, p = .020 (Figure 11a) suggesting increased synaptic contact between glutamatergic synapses and astrocytes. In the Yoked group, there was a significant, very strong positive correlation between CaMKIIa fluorescence and GFAP-synapsin-I

colocalisation in the LOFC at +3.72mm bregma, $r = .971$, $p = .029$ (Figure 12b), and a very strong negative correlation in the BLA at -2.52mm bregma, $r = -.969$, $p = .007$ (Figure 12g), suggesting increased glutamatergic synapse-astrocyte contact in the LOFC and decreased contact in the BLA.

There were no other significant correlations between CaMKIIa fluorescence and GFAP-synapsin-I colocalisation in regions measured in AVul rats. Some notable non-significant positive correlations above $r = .600$ were found in the IL at +2.76 bregma, $r = .619$, $p = .190$, NAcc at +2.28mm bregma, $r = .735$, $p = .096$, BLA at -2.52mm, $r = .761$, $p = .061$, and -3.48mm bregma, $r = .645$, $p = .167$ (Figure 10). A notable non-significant negative correlation was found in the IL at +3.72mm bregma, $r = -.619$, $p = .190$ (Figure 10a). In the ARes group, all other regions had no significant correlations between CaMKIIa fluorescence and GFAP-synapsin I colocalization. Some notable non-significant negative correlations below $r = -.600$ were found in the NAcs at +2.76mm bregma, $r = -.800$, $p = .056$, BLA at -2.52mm, $r = -.714$, $p = .111$, and -3.48mm bregma, $r = -.725$, $p = .103$ (Figure 11). A notable non-significant positive correlation was found in the LOFC at +3.72mm bregma, $r = .641$, $p = .170$ (Figure 11b). In the Yoked group, all other regions had no significant correlations between CaMKIIa fluorescence and GFAP-synapsin I colocalization. Some notable non-significant positive correlations above $r = .600$ were found in the NAcc at +2.28mm bregma, $r = .639$, $p = .361$, and NAcs at +2.28mm bregma, $r = .819$, $p = .181$ (Figure 12). A notable non-significant negative correlation was found in the IL at +3.24mm bregma, $r = -.673$, $p = .213$, LOFC at +2.76mm bregma, $r = -.802$, $p = .198$, BLA at -2.04mm, $r = -.863$, $p = .059$, and CeA at -2.52mm bregma, $r = -.663$, $p = .223$ (Figure 12).

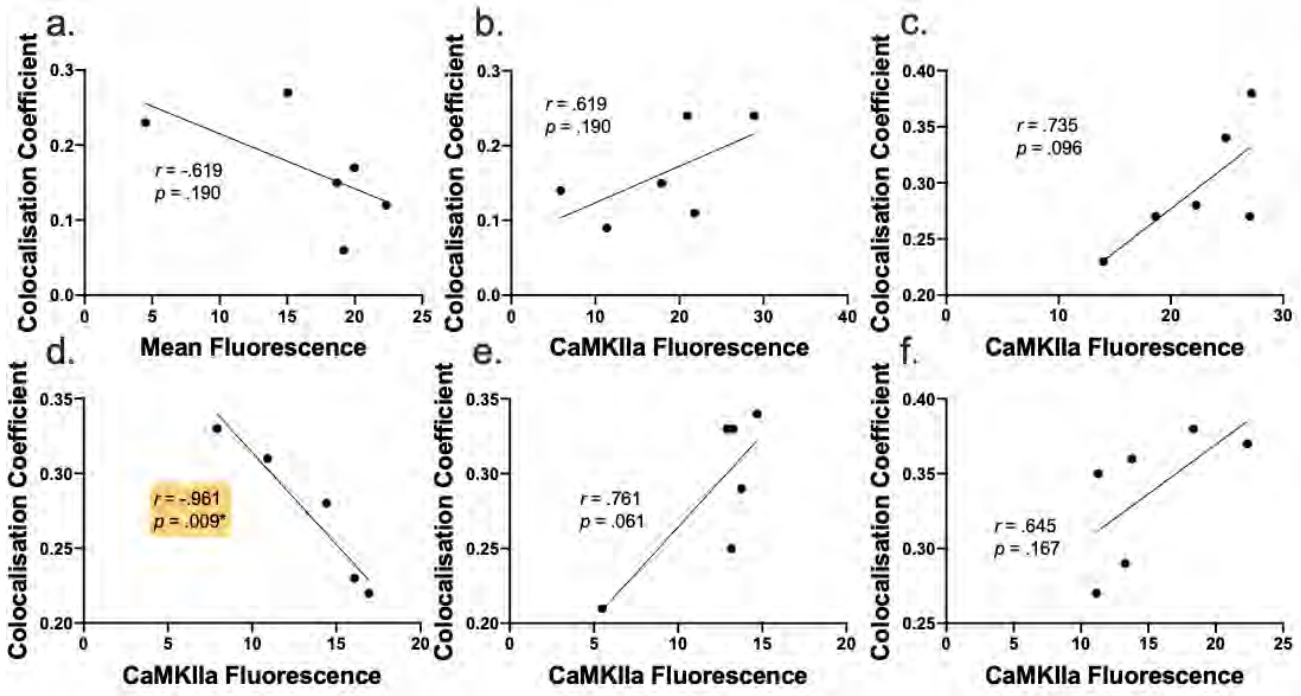

Figure 10. Correlational analyses: addiction-vulnerable. Strong to very strong correlations between calmodulin-kinase-II alpha (CaMKIIa) fluorescence and glial fibrillary acidic protein (GFAP)-synapsin I colocalization in distinct levels of various brain regions in the addiction vulnerable group. (a) Infralimbic cortex at +3.72mm, and (b) +2,76mm bregma. (c) Nucleus accumbens core at +2.28mm bregma. (d) Basolateral amygdala at -2.04mm, (e) -2.52mm, and (f) -3.48mm bregma. Yellow highlights significant correlations.

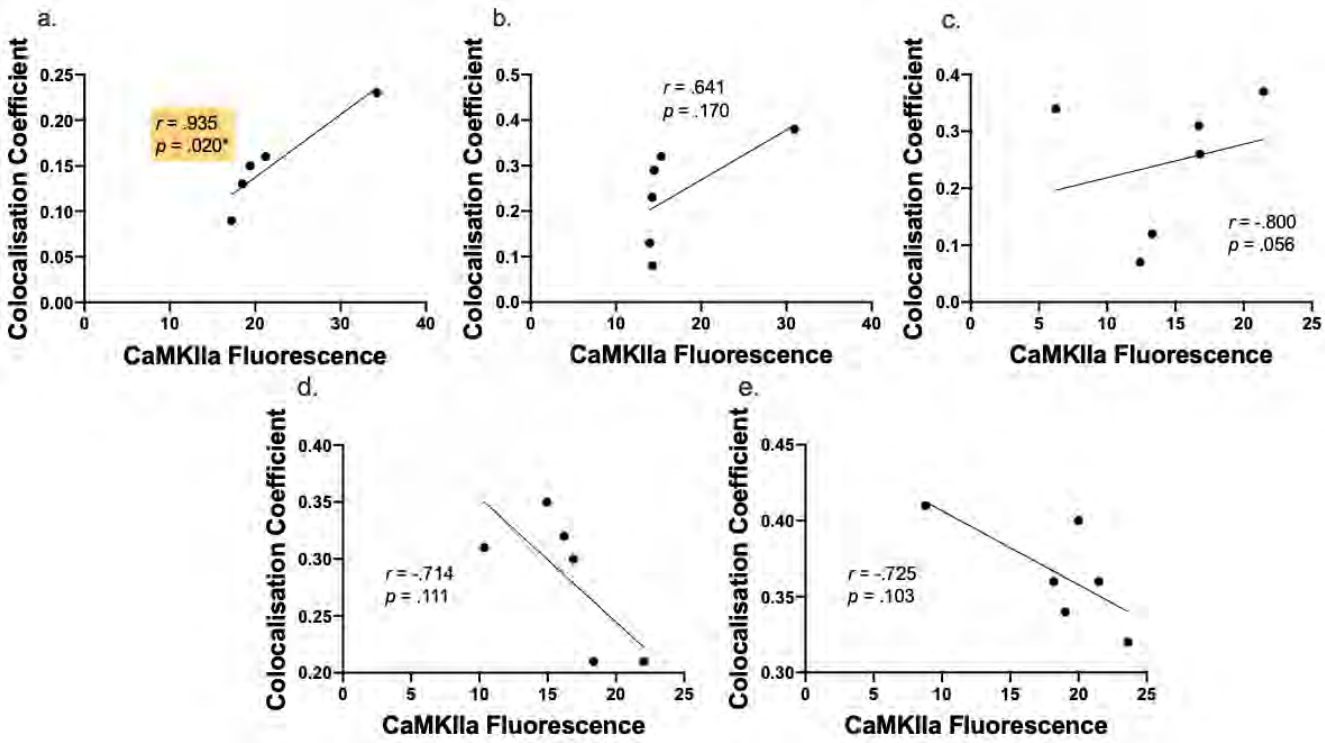

Figure 11. Correlational analyses: addiction-resistant. Strong to very-strong correlations between calmodulin-kinase-II alpha (CaMKIIa) fluorescence and glial fibrillary acidic protein (GFAP)-synapsin I colocalization in distinct levels of various brain regions in the addiction resistant group. (a) Infralimbic cortex at +3.72mm bregma. (b) Lateral orbitofrontal cortex at +3.72mm bregma. (c) Nucleus accumbens shell at +2.76mm bregma. (d) Basolateral amygdala at -2.52mm, and (e) -3.48mm bregma. Yellow highlights significant correlations.

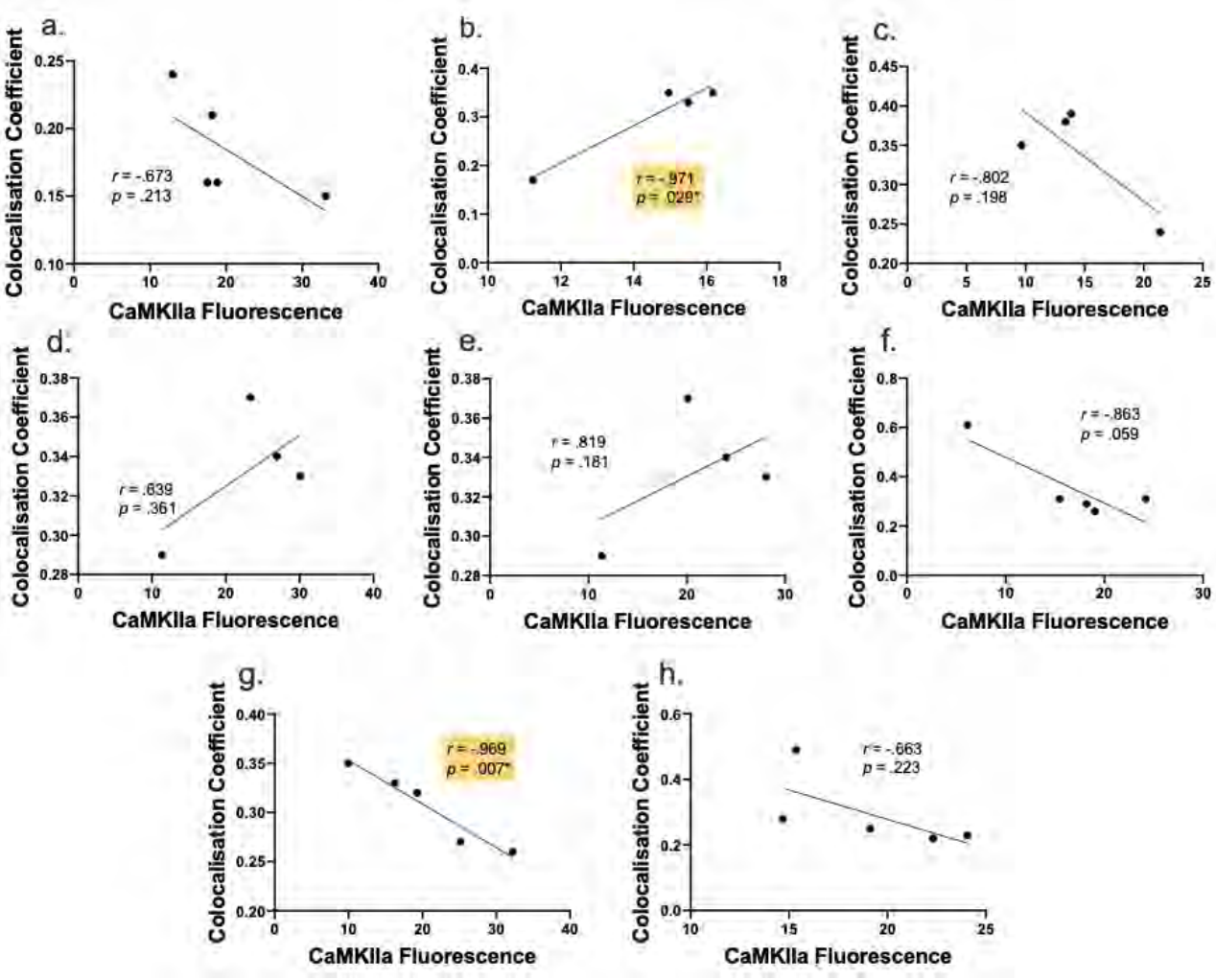

Figure 12. Correlational analyses: yoked. Strong to very-strong correlations between calmodulin-kinase-II alpha (CaMKIIa) fluorescence and glial fibrillary acidic protein (GFAP)-synapsin-I colocalization in distinct levels of various brain regions in the yoked group. (a) Infralimbic cortex at +3.24mm bregma. (b) Lateral orbitofrontal cortex at +3.72mm, and (c) +2.76mm bregma. (d) Nucleus accumbens (NAc) core at +2.28mm bregma, and (e) NAc shell at +2.28mm bregma. (f) Basolateral amygdala at -2.04mm, and (g) -2.52mm bregma. (h) Central amygdala at -2.52mm bregma. Yellow highlights significant correlations.

4. Discussion

4.1 Summary and hypotheses

The aim of this study was to investigate whether METH addiction-phenotype had an effect on glutamate activity, and astrocyte proliferation and hypertrophy within addiction neurocircuitry. This study also aimed to reveal associations between astrocyte-synapse connections and glutamate activity in METH addiction-vulnerable rats within addiction neurocircuitry. Glutamate activity was found to be reduced in the NAcc, CeA and BLA of AVul rats, whereas only the CeA of AVul rats demonstrated a *significant decrease* in astrocyte proliferation, when compared to yoked controls. Astrocyte hypertrophy was potentiated in all measured brain regions in AVul rats when compared to yoked rats. Interestingly, there was also a general increase in astrocyte hypertrophy in ARes, compared to yoked, rats suggesting that commonalities between these groups, such as METH-exposure or a protracted extinction, may explain this effect. Intriguingly, astrocytes in the mPFC, LOFC, rostral NAcc and BLA showed a particularly high level of hypertrophy in AVul rats, compared to ARes and control rats, with most sections demonstrating either increased or exacerbated hypertrophy. Finally, correlational analyses suggested a dysregulation of glutamate homeostasis in the NAcc and BLA.

4.1.1 Addiction-phenotyping in a METH IVSA model. An assumption of the addiction-phenotyping model is that in a given population of animals a subset of these are vulnerable to addiction (Deroche-Gamonet et al., 2004b; Wagner, 2002). In this study, roughly 18% of METH-exposed rats met criteria for the addiction-vulnerable phenotype, with the same proportion meeting criteria for addiction-resistant. Surprisingly, upon initial examination, only two ARes rats and one AVul rat met criteria for all three addiction

behaviours, therefore amended phenotyping criteria were utilised, similar to Jadhav et al. (2018). Here, rats demonstrated significant differences in the addictive behaviours of cue-induced relapse, motivation to take-METH, and resistance to extinction training. A subset of $n = 4$ HDS AVul rats also demonstrated significantly greater HDS compared to ARes rats. Crucially, there was no significant difference in the amount of mean lifetime METH-intake between AVul (132.65mg/kg) and ARes rats (125.05mg/kg). These groups therefore represented an AVul phenotype and an ARes phenotype that was independent of the amount of lifetime METH-consumption.

4.1.2 Astrocyte proliferation in METH addiction-vulnerable rats. It was hypothesised that astrocytes would proliferate in the PrL, IL, LOFC, DS, NAc, BLA and CeA in AVul, compared to ARes and Yoked, rats. In contrast, the CeA, at -2.52mm bregma, contained *significantly less* astrocytes in AVul rats, compared to controls, indicating an AVul-specific effect. However, as no significant differences in astrocyte populations were measured between AVul, ARes and control rats in the PrL, IL, LOFC, DS, NAc and BLA, this may be an artefact, with abnormally high astrocyte numbers at this level in controls. Nevertheless, it is still possible that in METH-exposed rats, astrocytes experienced apoptosis in the CeA, as this has been observed in METH-affected animals previously (Shah et al., 2013). Globally however, results indicated that neither addiction-phenotype, nor METH IVSA, altered the number of astrocytes within the addiction neurocircuitry. These data suggest that astrogliosis previously reported in METH-affected rodents (Granado et al., 2011; Krasnova et al., 2010b; Raineri et al., 2012) is likely the result of upregulated GFAP-expression, measured using fluorescence intensity, rather than astrocyte proliferation, measured by quantifying GFAP+ nuclei.

Most studies employ experimenter METH-delivery, which may explain these differing results. Two exceptions to this are Krasnova et al. (2010b), where rats undertook 10

extended-access IVSA sessions and 7-days of forced abstinence (average ~96mg/kg/rat) and Friend and Keefe (2013), who employed a neurotoxic METH-regimen and 30-days of forced abstinence (40mg/kg/rat). They found increased GFAP-expression in the striatum and cortex, and striatum, respectively. Rats in this study experienced longer abstinence and greater METH-intake compared to both studies; therefore, it is possible that astrocytes proliferate in the shorter term with less METH. Although, as GFAP-expression remained elevated at 30 days after an acute 40mg/kg METH-dose (Friend & Keefe, 2013), this is unlikely. Importantly, Sofroniew (2015) have categorised astrogliosis into mild-moderate, severe diffuse (Sev-1) and severe with scar tissue (Sev-2), with astrocyte proliferation a permanent feature, characteristic of Sev-2. Therefore, the results of this study suggest that astrogliosis as a result of METH-toxicity is unlikely to reach Sev-2, which is associated with severe neuroinflammation and apoptosis (Voskuhl et al., 2009; Wanner et al., 2013).

4.1.3 Baseline glutamate activity in METH-addicted rats. It was hypothesised that glutamatergic activity will be potentiated in the PrL, LOFC, NAc, DLS, pDMS, BLA and CeA, and attenuated in the IL and aDMS, in AVul, compared to ARes, rats. However, it was found that AVul and ARes rats had a significant reduction in CaMKIIa fluorescence at one level of each of the NAcc, BLA and CeA, compared to controls, which indicates a METH-induced reduction in baseline glutamate activity at the respective levels of these regions. No significant differences in CaMKIIa expression between AVul, ARes and control rats in all other regions were found, indicating no effect of addiction-phenotype, nor METH-IVSA, on baseline glutamate activity in the PrL, IL, LOFC, NAcs and DS.

Previously, there have been few studies that have investigated the baseline glutamate levels of METH-affected animals (Parsegian & See, 2013), with none in rats phenotyped as METH-addicted. Using microdialysis, one study reported that rats who had undergone short-access METH IVSA sessions for two weeks, followed by 10 days of extinction, had reduced

glutamate levels in the NAc and PrL at baseline (Parsegian & See, 2013). METH-addicts are highly likely to relapse to METH-seeking even after protracted abstinence (DeJong, 1994; Wang et al., 2013), therefore it is likely that there are permanent alterations to their neurobiology that explain persistent craving to relapse. Hyperreactivity of the PFC to cue-exposure is a well-documented phenomenon in humans (Goldstein & Volkow, 2011a; Konova et al., 2019) and a similar effect is seen in rats exposed to drug-cues with a simultaneous METH-prime (Parsegian & See, 2013). Therefore, the current study has demonstrated, in rats that are highly reactive to cues have decreased glutamate activity in the NAcc, BLA and CeA of AVul rats. While a reduction in glutamate levels may seem counterintuitive to PFC hyperactivity in AVul rats, the current measures were taken at baseline and not following a relapse event.

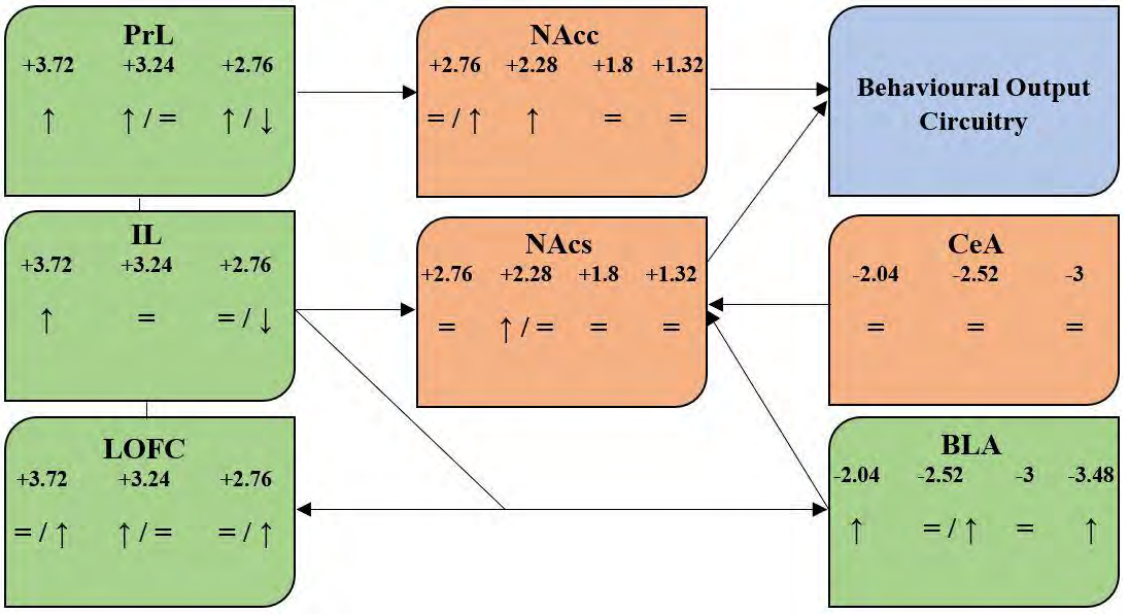

Figure 13. Neurocircuitry of AVul vs ARes rats. Diagram depicts the astrocyte morphology results organised into their relevant brains regions for AVul compared to ARes rats. Boxes represent regions, with green regions containing predominantly glutamatergic afferents, and orange containing γ-amino butyric-acid (GABA)ergic afferents. Arrows within boxes indicate the direction of any difference in astrocyte hypertrophy or glutamate activity. Arrows represent regional connections. An equal sign indicates no significant difference. Symbols following backslashes indicate an effect that was only found in one index of astrocyte hypertrophy, whereas those in front of backslashes were found in two indices. Lone symbols indicate the same effect was found in all three indices. Numbers indicate the bregma level (mm) at which the effect below was discovered.

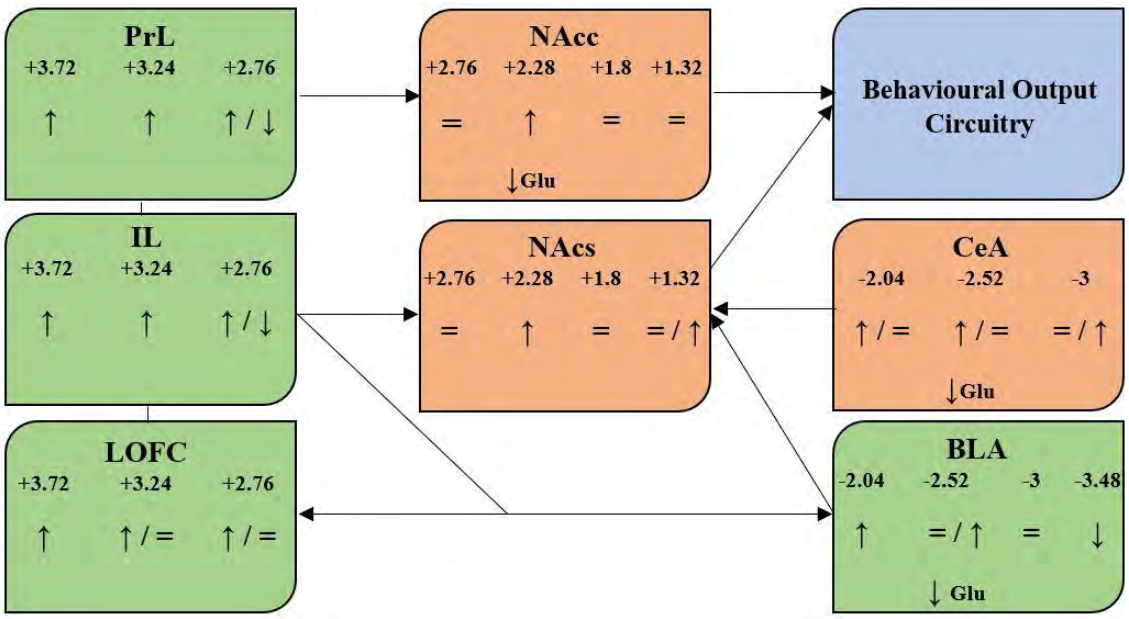

Figure 14. Neurocircuitry of AVul vs Yoked rats. Diagram depicts the astrocyte morphology and baseline glutamate activity results organised into their relevant brains regions for AVul compared to Yoked rats. Boxes represent regions, with green regions containing predominantly glutamatergic afferents, and orange containing γ-amino butyric-acid (GABA)ergic afferents. Arrows within boxes indicate the direction of any difference in astrocyte hypertrophy or glutamate activity. Arrows represent regional connections. An equal sign indicates no significant difference. Symbols following backslashes indicate an effect that was only found in one index of astrocyte hypertrophy, whereas those in front of backslashes were found in two indices. Lone symbols indicate the same effect was found in all three indices. Numbers indicate the bregma level (mm) at which the effect below was discovered. Glu = glutamate.

4.1.4 Astrocyte hypertrophy in METH addiction-vulnerable rats. It was hypothesised that AVul rats, compared to ARes and control, will demonstrate an increase in the number of astrocyte-ring intersections, nodes and longest-process length in the PrL, IL, LOFC, NAcc, NAcs, BLA, and CeA. In a subset of randomly chosen AVul, ARes and control rats (n = 2 each), Sholl analyses of astrocyte morphology suggested a global increase in astrocyte hypertrophy due to METH IVSA, with some regions demonstrating an increase in AVul rats, particularly in the mPFC and BLA.

Previous studies have demonstrated increased astrogliosis in METH-exposed rodents, operationalised as increased GFAP-expression (Granado et al., 2011; Krasnova et al., 2010b; Raineri et al., 2012; Robson et al., 2014). A recent study by Siemsen et al. (2019) demonstrated no difference in green fluorescent protein (GFP)-stained astrocyte morphology in the NAcc between short-access METH and saline IVSA trained rats following a 10-day

extinction period. This is in contradiction to the results of the present study, however there are a few differences between these studies that may explain these conflicting results. First, astrocyte morphology was only investigated in the NAcc in the study by Siemsen et al., whereas the current study investigated a number of addiction-relevant brain areas. Secondly, the current study has phenotyped rats based on addictive behaviours, and found differential effects between the phenotypes, with ARes rats demonstrating, at the majority of the bregma levels, less astrocyte hypertrophy compared to AVul rats. Siemsen et al. did not categorise their rats. Thirdly, the current study demonstrated a gradient of changes to astrocyte hypertrophy across the rostral-caudal axis of the NAcc, where more caudal regions did not show differences between AVul or ARes rats. As Siemsen et al. (2019) only measured astrocytes in more caudal areas of the NAcc, this may explain their negative findings.

4.1.5 Baseline glutamate and astrocyte-synapse connections in METH addiction-vulnerable rats. The final hypothesis posited that baseline glutamate activity would significantly and positively correlate with astrocyte-synapse connections in AVul rats in the PrL, LOFC, BLA, NAcc and NAcs, and that this correlation would be stronger and opposite in valence when compared to ARes rats. Results indicate a potential dysregulation of glutamate homeostasis in the rostral NAcc and central BLA of AVul rats, however not within the PrL, LOFC and NAcs. Astrocytes regulate glutamate neurotransmission, and this neurotransmitter has been involved in the neurocircuitry responsible for the expression of addictive behaviours (Cornish & Kalivas, 2000; Parsegian & See, 2013). In both the NAcc and BLA, there was reduced glutamate activity and a strong positive correlation between this activity and astrocyte-synapse connections, suggesting that astrocytic regulation of synaptic glutamate may be downregulated in the NAcc and BLA of AVul rats. Together, all of the current findings have significant implications for the regulation of glutamate homeostasis and reactive astrogliosis in METH-addiction.

4.2 Implications

Following from the results of this study there are two main implications to the neurobiology of METH-addiction. Firstly, addiction vulnerability may be related to dysregulation of glutamate homeostasis in the NAcc and BLA. Secondly, widespread astrocyte hypertrophy in AVul rats may be related to the exacerbation of reactive astrogliosis in METH-affected rats, particularly in the mPFC.

4.2.1 Glutamate homeostasis in the NAcc of the AVul rats within addiction neurocircuitry. In the rostral NAcc, a strong positive relationship between glutamate activity and astrocyte-synapse connections in AVul rats was found, coupled with a significant reduction in baseline glutamate activity. This reduction in baseline glutamatergic activity may reflect baseline hypoactivity of this pathway in AVul rats, which could prime these rats to dysregulation of glutamate homeostasis during relapse following re-exposure to drug-associated cues. Indeed, previous researchers have used *in-vivo* microdialysis to reveal low baseline glutamate levels in the NAc of METH short-access IVSA trained rats after 10 days of extinction (Parsegian & See, 2013). As well, Parsegian & See (2013) found that following cue-exposure, glutamate activity significantly increased, which is in line with previous research implicating glutamate transmission in the NAc in drug-relapse (Cornish & Kalivas, 2000). This may suggest that increased glutamate neurotransmission in the NAcc following cue-exposure increased METH-seeking behaviours in AVul rats.

As mentioned, coupled with low baseline glutamate activity, correlations between astrocyte-synapse colocalisation and glutamate activity suggested there was a similar decrease in astrocyte synapse connections in the rostral NAcc. This may confer further dysregulation of the astrocytic glutamate homeostasis mechanism. Siemsen et al. (2019) found that perisynaptic astrocytic processes (PAPs) had decreased contact with synapses in the NAcc of rats following METH short-access IVSA and ten days of extinction, although no

overall difference in astrocyte morphology was observed (see 4.1.4). As mentioned previously (see 1.5.1), PAPs are responsible for the majority of astrocytic glutamate reuptake and release which regulates glutamate neurotransmission (Lavialle et al., 2011). An increase in PAP-synapse contact is therefore believed to represent an increase in the ability of the astrocyte to regulate glutamate homeostasis. Although in the current study, PAPs were not measured, the changes to the number of astrocyte-synapse connections indicate that the reduced glutamate activity in the rostral NAcc may be due to withdrawal of PAPs and a reduction in glial-derived glutamate.

A potential mechanism for driving this cue-induced relapse to METH-seeking comes from relatively recent findings that astrocytic glutamate release in the NAcc reduces cocaine- and METH-seeking behaviours (Scofield et al., 2015; Siemsen et al., 2019). Scofield et al. (2015) employed an excitatory Gq-designer receptor exclusively activated by designer drugs (DREADDs) to activate astrocytes and release glial-derived glutamate in the extrasynaptic space. This reduced cue-induced relapse to cocaine-seeking via activation of mGluR2s, which regulate the pre-synaptic release of glutamate. Crucially, pharmacological and Gq-DREADD-mediated glial-glutamate release in METH IVSA-trained rats reduced cue-induced METH-seeking (Siemsen et al., 2019). Interestingly, the administration of the mGluR2/3 agonist, LY379268, has been shown to reduce cue-induced reinstatement in cocaine AVul rats (Cannella et al., 2013). These researchers also showed that this effect was mediated by mGlu2R agonism alone, suggesting that glutamate homeostasis may be specific to the addiction-vulnerable. Understanding this, it is likely that if synaptic glutamate activity is reduced at baseline and astrocytes have withdrawn from glutamatergic synapses in AVul rats, rapid efflux of PrL-derived glutamate into the synapses of NAcc MSNs would activate NAc to ventral pallidum projections which indirectly drive METH-seeking behaviours (see Figure X).

4.2.2 Glutamate homeostasis in the BLA of the AVul within the addiction neurocircuitry. In the BLA of AVul rats, there was a strong, positive correlation between glutamate activity and astrocyte-synapse connections at the rostro-central level, contrasting with strong negative correlations between these two processes in ARes and yoked rats. In the lateral amygdala, it has been shown that astrocyte-synapse connections decrease as learning-induced synaptic-strength increases, suggesting a negative relationship between astrocyte-synapse interactions and learning-induced synaptic strengthening (Ostroff, Manzur, Cain, & Ledoux, 2014). This could suggest that in the BLA of AVul rats, where there is less glutamate activity, there would be less astrocytic regulation of glutamate, whereas in ARes rats the opposite would be expected. This suggests that this system becomes dysfunctional or altered in AVul rats, whereas no such modification occurs in ARes and yoked rats. However, caution should be taken when interpreting these results, as at the rostral-most level of the BLA, AVul rats demonstrated a very strong negative correlation between glutamate activity and astrocyte-synapse connections, in contradiction to the three more-caudal levels which all demonstrated weak to strong positive correlations. It may be that this dysregulation of the baseline glutamate homeostasis in AVul rats occurs only in the central and caudal portions of the BLA, where decreased baseline glutamate was measured in AVul rats.

In the context of addiction neurocircuitry, the BLA is in a prime position to drive cue-induced METH-seeking. Indeed, previous studies have demonstrated that glutamatergic inputs from the LOFC into the BLA (Arguello et al., 2017; Lasseter, Wells, Xie, & Fuchs, 2011; Stefanik & Kalivas, 2013) mediate cue-induced cocaine-seeking. It is thought that the BLA projections to the NAc via the CeA, regulate drug-seeking behaviours and are likely responsible for cue-induced drug-seeking (Di Ciano & Everitt, 2004). This circuit is therefore potentially engaged during cue-induced relapse to METH-seeking in AVul rats, as regulatory extrasynaptic glutamatergic tone is likely reduced following the withdrawal of astrocytic

processes from synapses, facilitating hyperexcitability of these LOFC glutamatergic projections to upregulate BLA to NAc-driven drug-seeking behaviours. It must be noted however that this circuitry is yet to be tested in METH-exposed or METH-addicted animals and research is needed to test this preliminary hypothesis.

It is possible that these astrocytic processes remain somewhat preserved in the BLA of ARes rats, whereas AVul rats demonstrate a failure in the compensatory mechanisms of astrogliosis. Indeed, ARes rats had a strong negative correlation between synaptic glutamate activity and astrocyte synapse connections in the central and caudal BLA (Figure X). Concurrently, astrocyte hypertrophy in the rostral BLA was also increased in ARes rats compared to controls. This supports the idea that despite a trend for a reduction in basal BLA glutamate levels following chronic METH-exposure, when comparing ARes to controls (Figure X), astrocyte processes may have remained more available at synapses. During neurotransmission, high synaptic availability may allow for greater synaptic glutamate clearance and the release of synaptogenic and neurotrophic molecules (Bylicky, Mueller, & Day, 2018). Whereas in AVul rats, the relationship is likely reversed, as there were less astrocyte-synapse interactions and exacerbated astrocyte hypertrophy. Therefore, pathological astrogliosis in response to chronic METH-induced neurological injury may reduce the ability of astrocytes to regulate excessive glutamate neurotransmission, which is believed to drive METH-seeking behaviours (Furlong et al., 2018; Parsegian & See, 2013)

4.2.3 Astrocyte hypertrophy is exacerbated in the addiction-vulnerable. Findings from this study suggest that compensatory mechanisms attempting to re-establish a balance in glutamate homeostasis may function in ARes rats but fail in AVul rats. Astrocyte processes increasingly interact with synapses and neurons in response to CNS injury (Kim, Nabekura, & Koizumi, 2017). Therefore, if there is global hypertrophy of astrocytes in AVul rats, which has been shown in METH-addicted humans (Zhang et al., 2017), it is possible that the

compensatory astrogliosis, likely arising to protect against METH-induced neurotoxicity and glutamatergic excitotoxicity, becomes pathological. Importantly, increased GFAP-expression, a marker of the initial stages of astrogliosis, has been found up to 30 days after an experimenter-administered chronic-METH regime in rodents (Friend & Keefe, 2013). Interestingly, GFAP-expression was also found to increase following acute-METH, however chronic-METH then acute-METH after abstinence, did not exacerbate this increase in GFAP-expression. This suggests the upregulation of GFAP-expression was due to the initial chronic-METH exposure. Similarly, a more recent study found increased astrocyte hypertrophy in the parietal lobe of METH-addicts (Zhang et al., 2017), compared to controls, and linked this effect to long-term METH-abuse, rather than acute METH-use. Interestingly, they also demonstrated "fraying" of PAPs in METH-addicts, and subsequent research has found downregulation of PAPs in the NAcc of METH IVSA trained rats (Siemsen et al., 2019). This latter study however demonstrated no change in baseline astrocyte morphology or baseline glutamate reuptake. Therefore, as there was a marked increase in astrocyte hypertrophy in AVul rats compared to ARes rats in at least one level of all regions assayed, this may suggest that chronic METH-use results in persistent, stable astrogliosis that is likely a compensatory mechanism employed to regulate the neuroinflammatory and excitotoxic effects of METH-abuse, which may be exacerbated in AVul rats.

One potential mechanism that could explain the differing responses of astrocytes in AVul and ARes rats may lie in the classifications and consequences of astrogliosis. Sofroniew (2015) developed three categorises of astrogliosis, as mentioned above (see 4.1.2), with mild-moderate and Sev-1 astrogliosis the two least advanced. Mild-moderate astrogliosis corresponds to an increase in GFAP-expression and some degree of astrocyte hypertrophy. Sev-1 astrogliosis results in significant GFAP-expression and ubiquitous hypertrophy resulting in significant semi-permanent tissue reorganisation. In the context of

this study's findings, the substantial increase/exacerbation of astrocytes in various AVul brain regions may indicate severe diffuse astrogliosis, whereas the less pronounced astrogliosis observed in ARes rats may correspond to a more moderate form of astrogliosis. This distinction is crucial as the level of astrogliosis determines whether the process engaged by astrocytes are neuroprotective, usually in the mild-moderate cases (Wilhelmsson et al., 2006), or neuroinflammatory and neurotoxic, predominantly in Sev-1/2 astrogliosis (Barnabe-Heider et al., 2010; Voskuhl et al., 2009; Wanner et al., 2013).

What is still unclear from the current study, therefore, is when astrocytes hypertrophy in METH-addicted, rather than METH-exposed individuals, if this is associated with an increase in neuroinflammatory and neurotoxic processes. Astrocytes release pro-inflammatory cytokines and chemokines following CNS injury (Ramesh et al., 2013). They have also been shown to release proinflammatory cytokines, such as interleukin (ILe)-1 beta, ILe-6, and tumour necrosis factor-alpha in response to acute and prolonged METH-exposure (Gonçalves et al., 2008; Zhang et al., 2017). In contrast, during astrogliosis, astrocytes also release glial-derived neurotrophic factor (GDNF) and other growth factors (Sofroniew, 2015) which promote neuronal cell growth and prevent neurotoxicity (Rocha et al., 2012). Intriguingly, GDNF-suppressed mutant-mice have shown increased vulnerability to METH-addiction with increases in motivation to take-METH and cue-induced METH-seeking (Yan et al., 2007). Upregulation of the GDNF-gene in mice has also been shown to reduce METH IVSA and cue-induced reinstatement (Yan et al., 2013). Therefore, it may be that mild-moderate astrogliosis in ARes rats results in neuroprotective processes, whereas severe astrogliosis in AVul rats results in neurodegenerative processes. This study could have measured neuroinflammation via plasma cytokine levels to indicate whether specific pro-inflammatory cytokines were upregulated, and whether this effect was specific to AVul rats to indicate whether the observed astrogliosis in this group was neuroprotective or

neuroinflammatory. This unveils a promising avenue for future research and more importantly, a potential new treatment for METH-addiction.

4.3 Strengths, limitations and future research.

4.3.1 Measuring habitual drug-seeking in METH-addicted rats. This study employed a modified version of the addiction-phenotyping protocol (Deroche-Gamonet et al., 2004a) in an IVSA model of METH-addiction. It was the first to employ an addiction-phenotyping procedure incorporating both habitual drug-seeking (HDS) and resistance to extinction as criteria for an addiction-phenotype in a METH-exposed rat population. Using this methodology, a sub-set of rats phenotyped as AVul and ARes were able to be compared to investigate the neural substrates specifically altered in AVul rats. The methodology for this study aimed to model three distinct behaviours in a METH IVSA paradigm. Two of the three models, the cue-induced relapse model and progressive ratio model, have been repeatedly demonstrated as valid and reliable models of their respective constructs, motivation to take-METH- and cue-induced relapse to METH-seeking (Belin-Rauscent et al., 2016; Everitt et al., 2018). Interestingly, out of the n = 33 rats that undertook training for METH IVSA, only one rat met criteria for all three addictive behaviours. This suggests that a particular limitation to this paradigm may have been its ability to measure HDS in all animals, rather than just a subset.

When a rat engages in active lever pressing during the non-drug available (NDAv) periods of the HDS paradigm, this behaviour is suggestive of HDS. However, when a rat does not press the active lever during the NDAv period it is difficult to know whether the rat has learnt to attend to the cues (tone and light) which are salient during the drug-available period, or whether they have not developed HDS behaviours. Sign-tracking is a reliable predictor of the development of cue-induced relapse (Fitzpatrick et al., 2013; Robinson & Flagel, 2009; Tomie, Grimes, & Pohorecky, 2008), and as such, rats that become addicted to drugs, are

likely more attentive to the presence or absence of drug-cues. A future study may benefit from employing the Pavlovian conditioned approach task prior to METH IVSA, to determine which rats are sign-trackers and which are goal-trackers. This may provide a plausible explanation for the subset of rats that demonstrated strong cue-induced relapse behaviour but did not meet criteria for HDS. This was surprising as these behaviours have been demonstrated in cocaine-addicted rats (Belin et al., 2008; Brown et al., 2011; Deroche-Gamonet et al., 2004a; Kasanetz et al., 2010), and as cocaine is a psychostimulant like METH, cocaine-addiction shares many similarities with METH-addiction, notably high cue-reactivity (Ciccocioppo, Sanna, & Weiss, 2001; Price et al., 2010) and binge-like behaviours (Kuczenski, Segal, Melega, Lacan, & McCunney, 2009; Ward, Haney, Fischman, & Foltin, 1997). One study did however fail to demonstrate HDS and compulsive drug-seeking in their entire rat population, when undertaking an IVSA model of cocaine addiction (Waters, Moorman, Young, Feltenstein, & See, 2014). They suggest that only certain rat populations may be vulnerable to demonstrating habitual and compulsive drug-seeking behaviours which may be responsible for the smaller proportion of HDS amongst AVul rats.

4.3.2 CaMKIIa as a marker for glutamate activity at AMPARs. In this study, the marker CaMKIIa was used for indicating baseline glutamate levels as it has been repeatedly shown to regulate AMPAR activity (Herring & Nicoll, 2016; Lisman & Zhabotinsky, 2001). AMPARs are predominantly located at post-synaptic terminals and are responsible for rapid glutamatergic excitatory neurotransmission (Gouaux, 2004). CaMKIIa has been shown to increase the efficacy of AMPARs (Cai, Gu, Zhong, Ren, & Yan, 2002; Mao, Jin, Xue, Chu, & Wang, 2014). However, cocaine and morphine has been shown to interact with CaMKIIa gene expression (Liu et al., 2014; Liu, Zhang, Liu, & Yu, 2012; Wang et al., 2010), particularly in the NAc, potentially confounding the interpretation of CaMKIIa expression as a glutamate marker. The mechanism through which this upregulation occurs has not yet been

elucidated, therefore it is possible that glutamate neurotransmission in the NAc following drug and drug-cue exposure, may be responsible for this increase of CaMKIIa, as AMPA receptors are expressed on pyramidal glutamate neurons in the PFC (Baumbarger, Muhlhauser, Zhai, Yang, & Nisenbaum, 2001; Cai et al., 2002; Li, Yan, Wilson, & Swartzwelder, 2010; Myme, Sugino, Turrigiano, & Nelson, 2003; Vickers et al., 1993), pyramidal and GABA interneurons in the amygdala (Farb, Aoki, & Ledoux, 1995; Mahanty & Sah, 1998), and on GABA MSNs in the NAc (Wolf, 2010; Wolf & Ferrario, 2010). Future research may benefit, however, by measuring glutamate directly, using microdialysis, to avoid this potential confound.

4.3.3 Immunohistochemistry as a probe of neurocircuitry protein expression.

Immunohistochemistry as a tool has been used to investigate neural substrates for many decades (Brandtzaeg, 1998), however as with any technique, there are limitations to using this approach. Compared to other neurobiological assays, such as quantitative polymerase chain reaction, microarrays, proteomics and flow cytometry, immunohistochemistry does not allow for high-throughput analyses with more than three markers in a given sample. Additionally, it does not allow for measurement of *in-vivo* functional properties, such as in the case of fibre photometry or *in-vivo* microdialysis. It does, however, allow for *ex-vivo* measurements of structural populations of cells within a region and allows for the identification of intra-regional fluctuations in a given biomarker, as tissue is not homogenised. It also allows for cellular phenotyping and colocalisation analyses which are essential for all brain regions, as the CNS contains a heterogenous population of cells (Capogna, 2014; DeFelipe, 1993; Tepper et al., 2018; Walsh & Han, 2014), as well as subpopulations of cell-types. In this study, colocalisation of astrocytes and synapses allowed for an understanding of the proportion of astrocyte-synapse interactions. To investigate this

with any of the other neurobiological assays mentioned above would not be possible. This highlights the value of this technique as an essential, and effective neuroscientific tool.

4.3.4 Analytical tools and methodology for astrocyte morphology. This study employed, for the first time, a Sholl analysis technique on astrocytes in METH IVSA-trained rats with the added level of addiction-phenotype. However, only a small sample-size (n = 2 rats/group) was used for analyses of astrocyte hypertrophy, with some levels only containing n = 6 astrocytes in a group due to lack of viable sections. Similar sample sizes have been used previously (Gzielo et al., 2017) and were chosen in this study due to the substantial amount of data received from a single sample and the considerable time required for manual Sholl analyses. Importantly, as Sholl analyses were performed on only two-dimensional slices with no three-dimension reconstructions of astrocyte made, the measure of astrocyte hypertrophy employed here is likely to be conservative. Therefore, small to moderate effect sizes may be indicative of large effects. Three-dimensional analyses using open-access tools have been developed (Tavares et al., 2017), however the high-magnification confocal microscopy required, along with the subsequent detailed Sholl analyses are timely endeavours. Therefore, this data should in future be examined using confocal images to determine whether similar effect sizes are found.

4.3.5 GFAP and synapsin-I colocalisation as a measure of astrocyte-synapse connections. Also used in this study, the marker GFAP has been used extensively for analysis of astrocyte morphology due to its essential role in astrocyte structural integrity (Yang & Wang, 2015). However, it is often predominantly expressed in major astrocytic processes, to a lesser extent in the fine PAPs (Lavialle et al., 2011). Therefore, colocalisation of GFAP+ processes and synapses is limited to major processes, reducing the sensitivity of this technique. Previous research has employed green-fluorescent-protein to stain astrocyte membranes in order to more precisely quantify the number of astrocyte-synapse connections,

therefore future researchers may benefit from leveraging this technique (Scofield et al., 2016a; Siemsen et al., 2019).

4.3.6 Further future research. Two additional avenues for research may be borne from the results of this study. Firstly, an important continuation of this research would be to investigate the changes in real-time glutamatergic activity following an acute challenge, such as drug-cue exposure, in the brains of AVul rats, when compared to ARes controls. It would be expected that glutamate activity in the mPFC and NAcc would spike following exposure to drug-paired cues (Kalivas, 2009; Parsegian & See, 2013), however no research to date has investigated this in rats demonstrating significant addictive behaviours revealed through phenotyping. To relate this effect to the addiction-phenotype is crucial to forwarding understanding of the METH-addicted brain, compared to the METH-affected brain.

Secondly, in this study, it was revealed that astrocyte hypertrophy was increased throughout major regions of the addiction neurocircuitry of AVul rats, compared to ARes rats and controls. It is still unknown, however, whether addiction-vulnerability is associated with neuroprotective factors, associated with mild-moderate astrogliosis, or neuroinflammatory and neurotoxic factors associated with severe astrogliosis (Sofroniew, 2015). Markers of neuroprotective (e.g. GDNF), neuroinflammatory (e.g. IL-6), and neurotoxic (e.g. nNOS, ROS) processes should be coupled with astrocyte morphological analyses in assays of METH-addicted rat brains and/or plasma to investigate this possibility.

4.4 Conclusion

The use of addiction-phenotyping in preclinical addiction research is still relatively new, with novel models appearing year after year (Belin-Rauscent et al., 2016; Everitt et al., 2018). Here, this study was able to leverage this model to uncover a reduction in baseline glutamate in the NAcc, CeA and BLA of METH-AVul rats, as well as no change to astrocyte populations, apart from in the CeA. Crucially, this study revealed widespread increases in

astrocyte hypertrophy in major regions of addiction neurocircuitry within METH-AVul rats, suggesting a role for astrogliosis in the addiction-vulnerable phenotype. Likewise, results suggested a potential dysregulation of glutamate homeostasis in the NAcc and BLA of METH-AVul rats at baseline. Future research may benefit from employing more detailed mapping of astrocytic processes, including markers for neuroprotective and neuroinflammatory processes of astrogliosis, and measuring real-time glutamate changes to further understanding of glutamate homeostasis and neuroinflammation in addiction.

References

Abler, B., Walter, H., Erk, S., Kammerer, H., & Spitzer, M. (2006). Prediction error as a linear function of reward probability is coded in human nucleus accumbens. *NeuroImage, 31*(2), 790-795. doi:https://doi.org/10.1016/j.neuroimage.2006.01.001

Albanese, A., & Minciacchi, D. (1983). Organization of the ascending projections from the ventral tegmental area: A multiple fluorescent retrograde tracer study in the rat. *Journal of Comparative Neurology, 216*(4), 406-420. doi:10.1002/cne.902160406

Albrecht, J., Sidoryk-Wegrzynowicz, M., Zielinska, M., & Aschner, M. (2010). Roles of glutamine in neurotransmission. *Neuron Glia Biol, 6*(4), 263-276. doi:10.1017/s1740925x11000093

Allen, N. J., & Barres, B. A. (2009). Glia — more than just brain glue. *Nature, 457*, 675. doi:10.1038/457675a

Alloway, K. D., Lou, L., Nwabueze-Ogbo, F., & Chakrabarti, S. (2006). Topography of cortical projections to the dorsolateral neostriatum in rats: Multiple overlapping sensorimotor pathways. *Journal of Comparative Neurology, 499*(1), 33-48. doi:10.1002/cne.21039

American Psychiatric Association, D. S. M. T. F. (2013). *Diagnostic and statistical manual of mental disorders : DSM-5* (5th ed. ed.). Arlington, VA: American Psychiatric Association.

Araque, A., Carmignoto, G., Haydon, P. G., Oliet, S. H., Robitaille, R., & Volterra, A. (2014). Gliotransmitters travel in time and space. *Neuron, 81*(4), 728-739. doi:10.1016/j.neuron.2014.02.007

Arguello, A., Richardson, B., Hall, J., Wang, R., Hodges, M., Mitchell, M., . . . Fuchs, R. (2017). Role of a Lateral Orbital Frontal Cortex-Basolateral Amygdala Circuit in Cue-Induced Cocaine-Seeking Behavior. *Neuropsychopharmacology, 42*(3), 727-735. doi:10.1038/npp.2016.157

Asanuma, M., Miyazaki, I., Higashi, Y., Tsuji, T., & Ogawa, N. (2004). Specific Gene Expression and Possible Involvement of Inflammation in Methamphetamine-Induced Neurotoxicity. *Ann N Y Acad Sci, 1025*(1), 69-75. doi:10.1196/annals.1316.009

Atkins, A., Mashhoon, Y., & Kantak, K. (2008). Hippocampal regulation of contextual cue-induced reinstatement of cocaine-seeking behavior. *Pharmacology Biochemistry and Behavior, 90*(3), 481-491. doi:https://doi.org/10.1016/j.pbb.2008.04.007

Australian Institute of Health and Welfare. (2016). *National Drug Strategy Household Survey*. Canberra, Australia: Australian Institute of Health and Welfare

Baker, D., McFarland, K., Lake, R., Shen, H., Tang, X., Toda, S., & Kalivas, P. (2003). Neuroadaptations in cystine-glutamate exchange underlie cocaine relapse. *Nat Neurosci, 6*(7), 743-749. doi:10.1038/nn1069

Baracz, S., & Cornish, J. (2016). The neurocircuitry involved in oxytocin modulation of methamphetamine addiction. *Front Neuroendocrinol, 43*, 1-18. doi:10.1016/j.yfrne.2016.08.001

Baracz, S., Everett, N., McGregor, I., & Cornish, J. (2016). Oxytocin in the nucleus accumbens core reduces reinstatement of methamphetamine-seeking behaviour in rats. *Addiction Biology, 21*(2), 316-325. doi:10.1111/adb.12198

Barnabe-Heider, F., Goritz, C., Sabelstrom, H., Takebayashi, H., Pfrieger, F. W., Meletis, K., & Frisen, J. (2010). Origin of new glial cells in intact and injured adult spinal cord. *Cell Stem Cell, 7*(4), 470-482. doi:10.1016/j.stem.2010.07.014

Barrot, M., Olivier, J. D., Perrotti, L. I., DiLeone, R. J., Berton, O., Eisch, A. J., . . . Nestler, E. J. (2002). CREB activity in the nucleus accumbens shell controls gating of behavioral responses to emotional stimuli. *Proc Natl Acad Sci U S A, 99*(17), 11435-11440. doi:10.1073/pnas.172091899

Baumbarger, P., Muhlhauser, M., Zhai, J., Yang, C., & Nisenbaum, E. (2001). Positive Modulation of α-Amino-3-hydroxy-5-methyl-4-isoxazole Propionic Acid (AMPA) Receptors in Prefrontal Cortical Pyramidal Neurons by a Novel Allosteric Potentiator. *Journal of Pharmacology and Experimental Therapeutics, 298*(1), 86-102. Retrieved from http://jpet.aspetjournals.org/content/jpet/298/1/86.full.pdf

Beauquis, J., Pavía, P., Pomilio, C., Vinuesa, A., Podlutskaya, N., Galvan, V., & Saravia, F. (2013). Environmental enrichment prevents astroglial pathological changes in the hippocampus of APP transgenic mice, model of Alzheimer's disease. *Experimental Neurology, 239*, 28-37. doi:https://doi.org/10.1016/j.expneurol.2012.09.009

Beckstead, R. M. (1979). An autoradiographic examination of corticocortical and subcortical projections of the mediodorsal-projection (prefrontal) cortex in the rat. *Journal of Comparative Neurology, 184*(1), 43-62. doi:10.1002/cne.901840104

Belin, D., & Deroche-Gamonet, V. (2012). Responses to novelty and vulnerability to cocaine addiction: contribution of a multi-symptomatic animal model. *Cold Spring Harb Perspect Med, 2*(11). doi:10.1101/cshperspect.a011940

Belin, D., Mar, A. C., Dalley, J. W., Robbins, T. W., & Everitt, B. J. (2008). High impulsivity predicts the switch to compulsive cocaine-taking. *Science, 320*(5881), 1352-1355. doi:10.1126/science.1158136

Belin-Rauscent, A., Fouyssac, M., Bonci, A., & Belin, D. (2016). How Preclinical Models Evolved to Resemble the Diagnostic Criteria of Drug Addiction. *Biol Psychiatry, 79*(1), 39-46. doi:https://doi.org/10.1016/j.biopsych.2015.01.004

Blaha, C., Yang, C., Floresco, S., Barr, A., & Phillips, A. (1997). Stimulation of the Ventral Subiculum of the Hippocampus Evokes Glutamate Receptor-mediated Changes in Dopamine Efflux in the Rat Nucleus Accumbens. *European Journal of Neuroscience, 9*(5), 902-911. doi:10.1111/j.1460-9568.1997.tb01441.x

Bossert, J., Stern, A., Theberge, F. R., Cifani, C., Koya, E., Hope, B., & Shaham, Y. (2011). Ventral medial prefrontal cortex neuronal ensembles mediate context-induced relapse to heroin. *Nature Neuroscience, 14*(4), 420-422. doi:10.1038/nn.2758

Brandtzaeg, P. (1998). The increasing power of immunohistochemistry and immunocytochemistry. *Journal of Immunological Methods, 216*(1), 49-67. doi:https://doi.org/10.1016/S0022-1759(98)00070-2

Brog, J. S., Salyapongse, A., Deutch, A. Y., & Zahm, D. S. (1993). The patterns of afferent innervation of the core and shell in the "Accumbens" part of the rat ventral striatum: Immunohistochemical detection of retrogradely transported fluoro-gold. *Journal of Comparative Neurology, 338*(2), 255-278. doi:10.1002/cne.903380209

Brown, A., Flynn, J., Smith, D., & Dayas, C. (2011). Down-regulated striatal gene expression for synaptic plasticity-associated proteins in addiction and relapse vulnerable animals. *Int J Neuropsychopharmacol, 14*(8), 1099-1110. doi:10.1017/S1461145710001367

Burns, L., Robbins, T., & Everitt, B. (1993). Differential effects of excitotoxic lesions of the basolateral amygdala, ventral subiculum and medial prefrontal cortex on responding with conditioned reinforcement and locomotor activity potentiated by intra-accumbens infusions ofd-amphetamine. *Behav Brain Res, 55*(2), 167-183. doi:https://doi.org/10.1016/0166-4328(93)90113-5

Bylicky, M., Mueller, G., & Day, R. (2018). Mechanisms of Endogenous Neuroprotective Effects of Astrocytes in Brain Injury. *Oxidative medicine and cellular longevity, 2018*, 6501031-6501031. doi:10.1155/2018/6501031

Cai, X., Gu, Z., Zhong, P., Ren, Y., & Yan, Z. (2002). Serotonin 5-HT1A Receptors Regulate AMPA Receptor Channels through Inhibiting Ca2+/Calmodulin-dependent Kinase II in Prefrontal Cortical Pyramidal Neurons. *Journal of Biological Chemistry, 277*(39), 36553-36562. Retrieved from http://www.jbc.org/content/277/39/36553.abstract

Cameron, C. M., Murugan, M., Choi, J. Y., Engel, E. A., & Witten, I. B. (2019). Increased Cocaine Motivation Is Associated with Degraded Spatial and Temporal Representations in IL-NAc Neurons. *Neuron, 103*(1), 80-91.e87. doi:https://doi.org/10.1016/j.neuron.2019.04.015

Cannella, N., Halbout, B., Uhrig, S., Evrard, L., Corsi, M., Corti, C., . . . Spanagel, R. (2013). The mGluR2/3 agonist LY379268 induced anti-reinstatement effects in rats exhibiting addiction-like behavior. *Neuropsychopharmacology, 38*(10), 2048-2056. doi:10.1038/npp.2013.106

Cannon, C. M., & Bseikri, M. R. (2004). Is dopamine required for natural reward? *Physiol Behav, 81*(5), 741-748. doi:10.1016/j.physbeh.2004.04.020

Capogna, M. (2014). GABAergic cell type diversity in the basolateral amygdala. *Current Opinion in Neurobiology, 26*, 110-116. doi:https://doi.org/10.1016/j.conb.2014.01.006

Cardinal, R. N., Parkinson, J. A., Hall, J., & Everitt, B. J. (2002). Emotion and motivation: the role of the amygdala, ventral striatum, and prefrontal cortex. *Neuroscience & Biobehavioral Reviews, 26*(3), 321-352. doi:https://doi.org/10.1016/S0149-7634(02)00007-6

Carelli, R. M. (2002). Nucleus accumbens cell firing during goal-directed behaviors for cocaine vs. 'natural' reinforcement. *Physiol Behav, 76*(3), 379-387. doi:https://doi.org/10.1016/S0031-9384(02)00760-6

Carelli, R. M., & West, E. A. (2014). When a good taste turns bad: Neural mechanisms underlying the emergence of negative affect and associated natural reward devaluation by cocaine. *Neuropharmacology, 76 Pt B*, 360-369. doi:10.1016/j.neuropharm.2013.04.025

Carmichael, S. T., & Price, J. L. (1995). Limbic connections of the orbital and medial prefrontal cortex in macaque monkeys. *J Comp Neurol, 363*(4), 615-641. doi:10.1002/cne.903630408

Carroll, M., France, C., & Meisch, R. (1981). Intravenous self-administration of etonitazene, cocaine and phencyclidine in rats during food deprivation and satiation. *J Pharmacol Exp Ther, 217*(2), 241-247.

Cassé, F., Bardou, I., Danglot, L., Briens, A., Montagne, A., Parcq, J., . . . Docagne, F. (2012). Glutamate Controls tPA Recycling by Astrocytes, Which in Turn Influences Glutamatergic Signals. *The Journal of Neuroscience, 32*(15), 5186. doi:10.1523/JNEUROSCI.5296-11.2012

Chesworth, R., & Corbit, L. H. (2017). Recent developments in the behavioural and pharmacological enhancement of extinction of drug seeking. *Addiction Biology, 22*(1), 3-43. doi:10.1111/adb.12337

Chung, L. (2015). A Brief Introduction to the Transduction of Neural Activity into Fos Signal. *Development & reproduction, 19*(2), 61-67. doi:10.12717/DR.2015.19.2.061

Chye, Y., Mackey, S., Gutman, B., Ching, C., Batalla, A., Blaine, S., . . . Garavan, H. (2019). Subcortical surface morphometry in substance dependence: An ENIGMA addiction working group study. *Addict Biol*, e12830. doi:10.1111/adb.12830

Ciccocioppo, R., Sanna, P. P., & Weiss, F. (2001). Cocaine-predictive stimulus induces drug-seeking behavior and neural activation in limbic brain regions after multiple months

of abstinence: reversal by D(1) antagonists. *Proc Natl Acad Sci U S A, 98*(4), 1976-1981. doi:10.1073/pnas.98.4.1976

Clemens, K. J., & Holmes, N. M. (2018). An extended history of drug self-administration results in multiple sources of control over drug seeking behavior. *Prog Neuropsychopharmacol Biol Psychiatry, 87*(Pt A), 48-55. doi:10.1016/j.pnpbp.2017.11.011

Colfax, G., Santos, G., Das, M., Santos, D., Matheson, T., Gasper, J., . . . Vittinghoff, E. (2011). Mirtazapine to reduce methamphetamine use: a randomized controlled trial. *Arch Gen Psychiatry, 68*(11), 1168-1175. doi:10.1001/archgenpsychiatry.2011.124

Cornish, J. L., & Kalivas, P. W. (2000). Glutamate transmission in the nucleus accumbens mediates relapse in cocaine addiction. *J Neurosci, 20*(15), RC89. Retrieved from https://www.ncbi.nlm.nih.gov/pubmed/10899176

Courtney, K. E., & Ray, L. A. (2014). Methamphetamine: An update on epidemiology, pharmacology, clinical phenomenology, and treatment literature. *Drug and Alcohol Dependence, 143*, 11-21. doi:https://doi.org/10.1016/j.drugalcdep.2014.08.003

Cox, B., Bentzley, B., Regen-Tuero, H., See, R., Reichel, C., & Aston-Jones, G. (2017). Oxytocin Acts in Nucleus Accumbens to Attenuate Methamphetamine Seeking and Demand. *Biol Psychiatry, 81*(11), 949-958. doi:10.1016/j.biopsych.2016.11.011

Cruickshank, C., & Dyer, K. (2009). A review of the clinical pharmacology of methamphetamine. *Addiction, 104*(7), 1085-1099. doi:10.1111/j.1360-0443.2009.02564.x

Dall'Oglio, A., Gehlen, G., Achaval, M., & Rasia-Filho, A. A. (2008). Dendritic branching features of posterodorsal medial amygdala neurons of adult male and female rats: Further data based on the Golgi method. *Neurosci Lett, 430*(2), 151-156. doi:https://doi.org/10.1016/j.neulet.2007.10.051

Danbolt, N. (2001). Glutamate uptake. *Prog Neurobiol, 65*(1), 1-105. doi:10.1016/s0301-0082(00)00067-8

Darke, S., Kaye, S., & Duflou, J. (2017). Rates, characteristics and circumstances of methamphetamine-related death in Australia: a national 7-year study. *Addiction, 112*(12), 2191-2201. doi:10.1111/add.13897

Darke, S., Kaye, S., McKetin, R., & Duflou, J. (2008). Major physical and psychological harms of methamphetamine use. *Drug and Alcohol Review, 27*(3), 253-262.

Daumann, J., Koester, P., Becker, B., Wagner, D., Imperati, D., Gouzoulis-Mayfrank, E., & Tittgemeyer, M. (2011). Medial prefrontal gray matter volume reductions in users of amphetamine-type stimulants revealed by combined tract-based spatial statistics and voxel-based morphometry. *NeuroImage, 54*(2), 794-801. doi:10.1016/j.neuroimage.2010.08.065

DeFelipe, J. (1993). Neocortical Neuronal Diversity: Chemical Heterogeneity Revealed by Colocalization Studies of Classic Neurotransmitters, Neuropeptides, Calcium-binding Proteins, and Cell Surface Molecules. *Cerebral Cortex, 3*(4), 273-289. doi:10.1093/cercor/3.4.273

Degenhardt, L., Sara, G., McKetin, R., Roxburgh, A., Dobbins, T., Farrell, M., . . . Hall, W. D. (2017). Crystalline methamphetamine use and methamphetamine-related harms in Australia. *Drug Alcohol Rev, 36*(2), 160-170. doi:10.1111/dar.12426

DeJong, W. (1994). Relapse prevention: an emerging technology for promoting long-term drug abstinence. *Int J Addict, 29*(6), 681-705.

Dell, L. E., Chen, S. A., Smith, R. T., Specio, S. E., Balster, R. L., Paterson, N. E., . . . Koob, G. F. (2007). Extended Access to Nicotine Self-Administration Leads to Dependence: Circadian Measures, Withdrawal Measures, and Extinction Behavior in Rats. *Journal*

of Pharmacology and Experimental Therapeutics, 320(1), 180. doi:10.1124/jpet.106.105270

Deroche-Gamonet, V., Belin, D., & Piazza, P. (2004a). Evidence for addiction-like behavior in the rat. *Science, 305*(5686), 1014-1017. doi:10.1126/science.1099020

Deroche-Gamonet, V., Belin, D., & Piazza, P. V. (2004b). Evidence for addiction-like behavior in the rat. *Science, 305*(5686), 1014-1017. doi:10.1126/science.1099020

Di Chiara, G. (2002). Nucleus accumbens shell and core dopamine: differential role in behavior and addiction. *Behav Brain Res, 137*(1), 75-114. doi:https://doi.org/10.1016/S0166-4328(02)00286-3

Di Chiara, G., Bassareo, V., Fenu, S., De Luca, M., Spina, L., Cadoni, C., . . . Lecca, D. (2004). Dopamine and drug addiction: the nucleus accumbens shell connection. *Neuropharmacology, 47*, 227-241. doi:10.1016/j.neuropharm.2004.06.032

Di Ciano, P., & Everitt, B. J. (2004). Direct Interactions between the Basolateral Amygdala and Nucleus Accumbens Core Underlie Cocaine-Seeking Behavior by Rats. *The Journal of Neuroscience, 24*(32), 7167. doi:10.1523/JNEUROSCI.1581-04.2004

Ding, D. C. D., Gabbott, P. L. A., & Totterdell, S. (2001). Differences in the laminar origin of projections from the medial prefrontal cortex to the nucleus accumbens shell and core regions in the rat. *Brain Research, 917*(1), 81-89. doi:https://doi.org/10.1016/S0006-8993(01)02912-2

Dolenšek, J., Rupnik, M. S., & Stožer, A. (2015). Structural similarities and differences between the human and the mouse pancreas. *Islets, 7*(1), e1024405-e1024405. doi:10.1080/19382014.2015.1024405

Duvarci, S., & Pare, D. (2014). Amygdala Microcircuits Controlling Learned Fear. *Neuron, 82*(5), 966-980. doi:https://doi.org/10.1016/j.neuron.2014.04.042

Edwards, S., & Koob, G. F. (2010). Neurobiology of dysregulated motivational systems in drug addiction. *5*(3), 393-410. doi:10.2217/fnl.10.14

Elkashef, A., Vocci, F., Hanson, G., White, J., Wickes, W., & Tiihonen, J. (2008). Pharmacotherapy of methamphetamine addiction: an update. *Subst Abus*, *29*(3), 31-49. doi:10.1080/08897070802218554

Everitt, B., Cardinal, R., Parkinson, J., & Robbins, T. (2003). Appetitive behavior: impact of amygdala-dependent mechanisms of emotional learning. *Ann N Y Acad Sci, 985*, 233-250. Retrieved from https://www.ncbi.nlm.nih.gov/pubmed/12724162

Everitt, B., Giuliano, C., & Belin, D. (2018). Addictive behaviour in experimental animals: prospects for translation. *Philos Trans R Soc Lond B Biol Sci, 373*(1742). doi:10.1098/rstb.2017.0027

Everitt, B., & Robbins, T. (2013a). From the ventral to the dorsal striatum: devolving views of their roles in drug addiction. *Neurosci Biobehav Rev, 37*(9 Pt A), 1946-1954. doi:10.1016/j.neubiorev.2013.02.010

Everitt, B. J., Parkinson, J. A., Olmstead, M. C., Arroyo, M., Robledo, P., & Robbins, T. W. (1999). Associative Processes in Addiction and Reward The Role of Amygdala-Ventral Striatal Subsystems. *Ann N Y Acad Sci, 877*(1), 412-438. doi:10.1111/j.1749-6632.1999.tb09280.x

Everitt, B. J., & Robbins, T. W. (2000). Second-order schedules of drug reinforcement in rats and monkeys: measurement of reinforcing efficacy and drug-seeking behaviour. *Psychopharmacology (Berl), 153*(1), 17-30. doi:10.1007/s002130000566

Everitt, B. J., & Robbins, T. W. (2013b). From the ventral to the dorsal striatum: devolving views of their roles in drug addiction. *Neurosci Biobehav Rev, 37*(9 Pt A), 1946-1954. doi:10.1016/j.neubiorev.2013.02.010

Fallon, J. H., & Moore, R. Y. (1978). Catecholamine innervation of the basal forebrain IV. Topography of the dopamine projection to the basal forebrain and neostriatum. *Journal of Comparative Neurology, 180*(3), 545-579. doi:10.1002/cne.901800310

Farb, C., Aoki, C., & Ledoux, J. (1995). Differential localization of NMDA and AMPA receptor subunits in the lateral and basal nuclei of the amygdala: A light and electron microscopic study. *Journal of Comparative Neurology, 362*(1), 86-108. doi:10.1002/cne.903620106

Fiorillo, C., Tobler, P., & Schultz, W. (2003). Discrete coding of reward probability and uncertainty by dopamine neurons. *Science, 299*(5614), 1898-1902. doi:10.1126/science.1077349

Fischer-Smith, K. D., Houston, A. C. W., & Rebec, G. V. (2012). Differential effects of cocaine access and withdrawal on glutamate type 1 transporter expression in rat nucleus accumbens core and shell. *Neuroscience, 210*(C), 333-339. doi:10.1016/j.neuroscience.2012.02.049

Fitzpatrick, C., Gopalakrishnan, S., Cogan, E., Yager, L., Meyer, P., Lovic, V., . . . Morrow, J. (2013). Variation in the Form of Pavlovian Conditioned Approach Behavior among Outbred Male Sprague-Dawley Rats from Different Vendors and Colonies: Sign-Tracking vs. Goal-Tracking. *PLoS One, 8*(10), e75042. doi:10.1371/journal.pone.0075042

Frank, M. G. (2013). Astroglial regulation of sleep homeostasis. *Current Opinion in Neurobiology, 23*(5), 812-818. doi:10.1016/j.conb.2013.02.009

Friend, D., & Keefe, K. (2013). Glial reactivity in resistance to methamphetamine-induced neurotoxicity. *J Neurochem, 125*(4), 566-574. doi:10.1111/jnc.12201

Fuchs, R. A., Evans, K. A., Parker, M. P., & See, R. E. (2004). Differential involvement of orbitofrontal cortex subregions in conditioned cue-induced and cocaine-primed

reinstatement of cocaine seeking in rats. *The Journal of neuroscience : the official journal of the Society for Neuroscience, 24*(29), 6600-6610. doi:10.1523/JNEUROSCI.1924-04.2004

Fuchs, R. A., Higginbotham, J. A., & Hansen, E. J. (2019). Chapter 2 - Animal Models of Addiction. In M. Torregrossa (Ed.), *Neural Mechanisms of Addiction* (pp. 3-22): Academic Press.

Funk, D., Coen, K., Tamadon, S., Hope, B. T., Shaham, Y., & Lê, A. D. (2016). Role of Central Amygdala Neuronal Ensembles in Incubation of Nicotine Craving. *The Journal of Neuroscience, 36*(33), 8612. doi:10.1523/JNEUROSCI.1505-16.2016

Furlong, T., Corbit, L., Brown, R., & Balleine, B. (2018). Methamphetamine promotes habitual action and alters the density of striatal glutamate receptor and vesicular proteins in dorsal striatum. *Addiction Biology, 23*(3), 857-867. doi:10.1111/adb.12534

Garcia, A. F., Nakata, K. G., & Ferguson, S. M. (2018). Viral strategies for targeting cortical circuits that control cocaine-taking and cocaine-seeking in rodents. *Pharmacology, Biochemistry and Behavior, 174*, 33-41. doi:10.1016/j.pbb.2017.05.009

Gipson, C., Reissner, K., Kupchik, Y., Smith, A., Stankeviciute, N., Hensley-Simon, M., & Kalivas, P. (2013). Reinstatement of nicotine seeking is mediated by glutamatergic plasticity. *Proceedings of the National Academy of Sciences, 110*(22), 9124. doi:10.1073/pnas.1220591110

Goldstein, R., & Volkow, N. (2002). Drug Addiction and Its Underlying Neurobiological Basis: Neuroimaging Evidence for the Involvement of the Frontal Cortex. *American Journal of Psychiatry, 159*(10), 1642-1652.

Goldstein, R., & Volkow, N. (2011a). Dysfunction of the prefrontal cortex in addiction: neuroimaging findings and clinical implications. *Nature Reviews Neuroscience, 12*(11), 652-669. doi:10.1038/nrn3119

Goldstein, R. Z., & Volkow, N. D. (2011b). Dysfunction of the prefrontal cortex in addiction: neuroimaging findings and clinical implications. *Nature Reviews Neuroscience, 12*(11), 652-669. doi:10.1038/nrn3119

Gonçalves, J., Martins, T., Ferreira, R., Milhazes, N., Borges, F., Ribeiro, C., . . . Silva, A. (2008). Methamphetamine-Induced Early Increase of IL-6 and TNF-α mRNA Expression in the Mouse Brain. *Ann N Y Acad Sci, 1139*(1), 103-111. doi:10.1196/annals.1432.043

Gouaux, E. (2004). Structure and function of AMPA receptors. *The Journal of Physiology, 554*(2), 249-253. doi:10.1113/jphysiol.2003.054320

Gourley, S., & Taylor, J. (2016). Going and stopping: dichotomies in behavioral control by the prefrontal cortex. *Nat Neurosci, 19*(5), 656-664. doi:10.1038/nn.4275

Granado, N., Lastres-Becker, I., Ares-Santos, S., Oliva, I., Martin, E., Cuadrado, A., & Moratalla, R. (2011). Nrf2 deficiency potentiates methamphetamine-induced dopaminergic axonal damage and gliosis in the striatum. *Glia, 59*(12), 1850-1863. doi:10.1002/glia.21229

Greenlund, L., Deckwerth, T., & Johnson, E. (1995). Superoxide dismutase delays neuronal apoptosis: A role for reactive oxygen species in programmed neuronal death. *Neuron, 14*(2), 303-315. doi:https://doi.org/10.1016/0896-6273(95)90287-2

Groenewegen, H. J., & Russchen, F. T. (1984). Organization of the efferent projections of the nucleus accumbens to pallidal, hypothalamic, and mesencephalic structures: A tracing and immunohistochemical study in the cat. *Journal of Comparative Neurology, 223*(3), 347-367. doi:10.1002/cne.902230303

Gzielo, K., Kielbinski, M., Ploszaj, J., Janeczko, K., Gazdzinski, S., & Setkowicz, Z. (2017). Long-Term Consumption of High-Fat Diet in Rats: Effects on Microglial and

Astrocytic Morphology and Neuronal Nitric Oxide Synthase Expression. *Cellular and Molecular Neurobiology, 37*(5), 783-789. doi:10.1007/s10571-016-0417-5

Haber, S. N. (2014). The place of dopamine in the cortico-basal ganglia circuit. *Neuroscience, 282*, 248-257. doi:https://doi.org/10.1016/j.neuroscience.2014.10.008

Haber, S. N., & Knutson, B. (2010). The Reward Circuit: Linking Primate Anatomy and Human Imaging. *Neuropsychopharmacology, 35*(1), 4-26. doi:10.1038/npp.2009.129

Haber, S. N., Kunishio, K., Mizobuchi, M., & Lynd-Balta, E. (1995). The orbital and medial prefrontal circuit through the primate basal ganglia. *J Neurosci, 15*(7 Pt 1), 4851-4867.

Halpin, L. E., Collins, S. A., & Yamamoto, B. K. (2014). Neurotoxicity of methamphetamine and 3,4-methylenedioxymethamphetamine. *Life Sci, 97*(1), 37-44. doi:10.1016/j.lfs.2013.07.014

Hamani, C., SaintCyr, J., Fraser, J., Kaplitt, M., & Lozano, A. (2004). The subthalamic nucleus in the context of movement disorders. *Brain, 127*(1), 4-20. doi:10.1093/brain/awh029

Hao, Y., Martin-Fardon, R., & Weiss, F. (2010). Behavioral and Functional Evidence of Metabotropic Glutamate Receptor 2/3 and Metabotropic Glutamate Receptor 5 Dysregulation in Cocaine-Escalated Rats: Factor in the Transition to Dependence. *Biol Psychiatry, 68*(3), 240-248. doi:https://doi.org/10.1016/j.biopsych.2010.02.011

Hartig, S. M. (2013). Basic Image Analysis and Manipulation in ImageJ. *Current Protocols in Molecular Biology, 102*(1), 14.15.11-14.15.12. doi:10.1002/0471142727.mb1415s102

Heidbreder, C. A., & Groenewegen, H. J. (2003). The medial prefrontal cortex in the rat: evidence for a dorso-ventral distinction based upon functional and anatomical characteristics. In (Vol. 27, pp. 555-579).

Herring, B., & Nicoll, R. (2016). Long-Term Potentiation: From CaMKII to AMPA Receptor Trafficking. *Annual Review of Physiology, 78*(1), 351-365. doi:10.1146/annurev-physiol-021014-071753

Hol, E., & Pekny, M. (2015). Glial fibrillary acidic protein (GFAP) and the astrocyte intermediate filament system in diseases of the central nervous system. *Curr Opin Cell Biol, 32*, 121-130. doi:10.1016/j.ceb.2015.02.004

Hoover, W. B., & Vertes, R. P. (2007). Anatomical analysis of afferent projections to the medial prefrontal cortex in the rat. *Brain Structure and Function, 212*(2), 149-179. doi:10.1007/s00429-007-0150-4

Hu, J., Ferreira, A., & Van Eldik, L. (1997). S100β Induces Neuronal Cell Death Through Nitric Oxide Release from Astrocytes. *J Neurochem, 69*(6), 2294-2301. doi:10.1046/j.1471-4159.1997.69062294.x

Hyman, S. E., Malenka, R. C., & Nestler, E. J. (2006). Neural mechanisms of addiction: the role of reward-related learning and memory. *Annu Rev Neurosci, 29*, 565-598. doi:10.1146/annurev.neuro.29.051605.113009

Jadhav, K. S., Peterson, V. L., Halfon, O., Ahern, G., Fouhy, F., Stanton, C., . . . Boutrel, B. (2018). Gut microbiome correlates with altered striatal dopamine receptor expression in a model of compulsive alcohol seeking. *Neuropharmacology, 141*, 249-259. doi:https://doi.org/10.1016/j.neuropharm.2018.08.026

Janak, P. H., & Tye, K. M. (2015). From circuits to behaviour in the amygdala. *Nature, 517*(7534), 284-292. doi:10.1038/nature14188

Jay, T. M. (2003). Dopamine: a potential substrate for synaptic plasticity and memory mechanisms. *Prog Neurobiol, 69*(6), 375-390. doi:https://doi.org/10.1016/S0301-0082(03)00085-6

Jedynak, J. P., Uslaner, J. M., Esteban, J. A., & Robinson, T. E. (2007). Methamphetamine-induced structural plasticity in the dorsal striatum. *European Journal of Neuroscience, 25*(3), 847-853. doi:10.1111/j.1460-9568.2007.05316.x

Kalivas, P., & Volkow, N. (2005). The Neural Basis of Addiction: A Pathology of Motivation and Choice. *American Journal of Psychiatry, 162*(8), 1403-1413. doi:10.1176/appi.ajp.162.8.1403

Kalivas, P. W. (2000). A role for glutamate transmission in addiction to psychostimulants. *Addict Biol, 5*(3), 325-329. doi:10.1111/j.1369-1600.2000.tb00199.x

Kalivas, P. W. (2009). The glutamate homeostasis hypothesis of addiction. *Nat Rev Neurosci, 10*(8), 561-572. doi:10.1038/nrn2515

Kasanetz, F., Deroche-Gamonet, V., Berson, N., Balado, E., Lafourcade, M., Manzoni, O., & Piazza, P. (2010). Transition to addiction is associated with a persistent impairment in synaptic plasticity. *Science (New York, N.Y.), 328*(5986), 1709. doi:10.1126/science.1187801

Kau, K. S., Madayag, A., Mantsch, J. R., Grier, M. D., Abdulhameed, O., & Baker, D. A. (2008). Blunted cystine–glutamate antiporter function in the nucleus accumbens promotes cocaine-induced drug seeking. *Neuroscience, 155*(2), 530-537. doi:10.1016/j.neuroscience.2008.06.010

Keitz, M., Martin-Soelch, C., & Leenders, K. L. (2003). Reward processing in the brain: a prerequisite for movement preparation? *Neural plasticity, 10*(1-2), 121.

Kim, J., Perry, C., Luikinga, S., Zbukvic, I., Brown, R., & Lawrence, A. (2015). Extinction of a cocaine-taking context that protects against drug-primed reinstatement is dependent on the metabotropic glutamate 5 receptor. *Addiction Biology, 20*(3), 482-489. doi:10.1111/adb.12142

Kim, S., Nabekura, J., & Koizumi, S. (2017). Astrocyte-mediated synapse remodeling in the pathological brain. *Glia, 65*(11), 1719-1727. doi:10.1002/glia.23169

Knackstedt, L. A., LaRowe, S., Mardikian, P., Malcolm, R., Upadhyaya, H., Hedden, S., . . . Kalivas, P. W. (2009). The Role of Cystine-Glutamate Exchange in Nicotine Dependence in Rats and Humans. *Biological Psychiatry, 65*(10), 841-845. doi:https://doi.org/10.1016/j.biopsych.2008.10.040

Koella, W. (1981). GABA systems and behavior. *Advances in biochemical psychopharmacology, 29*, 11-21. Retrieved from https://www.scopus.com/inward/record.uri?eid=2-s2.0-0019400665&partnerID=40&md5=2c2c4d8e76a23fbdb08551e7c5e37111

Konova, A. B., Parvaz, M. A., Bernstein, V., Zilverstand, A., Moeller, S. J., Delgado, M. R., . . . Goldstein, R. Z. (2019). Neural mechanisms of extinguishing drug and pleasant cue associations in human addiction: role of the VMPFC. *Addiction Biology, 24*(1), 88-99. doi:10.1111/adb.12545

Koob, G. (2005). The neurocircuitry of addiction: Implications for treatment. *Clinical Neuroscience Research, 5*(2-4), 89-101. doi:10.1016/j.cnr.2005.08.005

Koob, G., & Le Moal, M. (2001). Drug Addiction, Dysregulation of Reward, and Allostasis. *Neuropsychopharmacology, 24*(2), 97-129. doi:10.1016/S0893-133X(00)00195-0

Koob, G., & Volkow, N. (2016). Neurobiology of addiction: a neurocircuitry analysis. *The Lancet Psychiatry, 3*(8), 760-773. doi:10.1016/S2215-0366(16)00104-8

Koob, G., & Volkow, N. D. (2010). Neurocircuitry of addiction. *Neuropsychopharmacology, 35*(1), 217-238. doi:10.1038/npp.2009.110

Koob, G. F., & Weiss, F. (1992). Neuropharmacology of cocaine and ethanol dependence. *Recent Dev Alcohol, 10*, 201-233. Retrieved from https://www.ncbi.nlm.nih.gov/pubmed/1350359

Koya, E., Uejima, J., Wihbey, K., Bossert, J., Hope, B. T., & Shaham, Y. (2009). Role of ventral medial prefrontal cortex in incubation of cocaine craving. *Neuropharmacology, 56 Suppl 1*, 177-185. doi:10.1016/j.neuropharm.2008.04.022

Krasnova, I., Justinova, Z., Ladenheim, B., Jayanthi, S., McCoy, M., Barnes, C., . . . Cadet, J. (2010a). Methamphetamine Self-Administration Is Associated with Persistent Biochemical Alterations in Striatal and Cortical Dopaminergic Terminals in the Rat. *PLoS One, 5*(1), e8790. doi:10.1371/journal.pone.0008790

Krasnova, I. N., & Cadet, J. L. (2009). Methamphetamine toxicity and messengers of death. *Brain Research Reviews, 60*(2), 379-407. doi:https://doi.org/10.1016/j.brainresrev.2009.03.002

Krasnova, I. N., Justinova, Z., & Cadet, J. L. (2016). Methamphetamine addiction: involvement of CREB and neuroinflammatory signaling pathways. *Psychopharmacology, 233*(10), 1945-1962. doi:10.1007/s00213-016-4235-8

Krasnova, I. N., Justinova, Z., Ladenheim, B., Jayanthi, S., McCoy, M. T., Barnes, C., . . . Cadet, J. L. (2010b). Methamphetamine Self-Administration Is Associated with Persistent Biochemical Alterations in Striatal and Cortical Dopaminergic Terminals in the Rat. *PLoS One, 5*(1), e8790. doi:10.1371/journal.pone.0008790

Krettek, J., & Price, J. (1978). A description of the amygdaloid complex in the rat and cat with observations on intra-amygdaloid axonal connections. *Journal of Comparative Neurology, 178*(2), 255-279. doi:10.1002/cne.901780205

Kuczenski, R., Segal, D., Melega, W., Lacan, G., & McCunney, S. (2009). Human Methamphetamine Pharmacokinetics Simulated in the Rat: Behavioral and Neurochemical Effects of a 72-h Binge. *Neuropsychopharmacology, 34*(11), 2430-2441. doi:10.1038/npp.2009.73

Larsson, M. (2017). Non-canonical heterogeneous cellular distribution and co-localization of CaMKIIα and CaMKIIβ in the spinal superficial dorsal horn. *Brain Structure and Function*. doi:10.1007/s00429-017-1566-0

Lasseter, H., Wells, A., Xie, X., & Fuchs, R. (2011). Interaction of the Basolateral Amygdala and Orbitofrontal Cortex is Critical for Drug Context-Induced Reinstatement of Cocaine-Seeking Behavior in Rats. *Neuropsychopharmacology, 36*(3), 711-720. doi:10.1038/npp.2010.209

Lavialle, M., Aumann, G., Anlauf, E., Pröls, F., Arpin, M., & Derouiche, A. (2011). Structural plasticity of perisynaptic astrocyte processes involves ezrin and metabotropic glutamate receptors. *Proceedings of the National Academy of Sciences, 108*(31), 12915. doi:10.1073/pnas.1100957108

LeDoux, J. (2007). The amygdala. *Current biology : CB, 17*(20), R868-874. doi:10.1016/j.cub.2007.08.005

Li, Q., Yan, H., Wilson, W., & Swartzwelder, H. (2010). Modulation of NMDA and AMPA-mediated synaptic transmission by CB1 receptors in frontal cortical pyramidal cells. *Brain Research, 1342*, 127-137. doi:https://doi.org/10.1016/j.brainres.2010.04.029

Li, X., Zeric, T., Kambhampati, S., Bossert, J. M., & Shaham, Y. (2015). The Central Amygdala Nucleus is Critical for Incubation of Methamphetamine Craving. *Neuropsychopharmacology, 40*(5), 1297-1306. doi:10.1038/npp.2014.320

Limpens, J. H., Damsteegt, R., Broekhoven, M. H., Voorn, P., & Vanderschuren, L. J. (2015). Pharmacological inactivation of the prelimbic cortex emulates compulsive reward seeking in rats. *Brain Res, 1628*(Pt A), 210-218. doi:10.1016/j.brainres.2014.10.045

Lisman, J., & Zhabotinsky, A. (2001). A Model of Synaptic Memory: A CaMKII/PP1 Switch that Potentiates Transmission by Organizing an AMPA Receptor Anchoring

Assembly. *Neuron, 31*(2), 191-201. doi:https://doi.org/10.1016/S0896-6273(01)00364-6

Liu, X., Liu, Y., Zhong, P., Wilkinson, B., Qi, J., Olsen, C., . . . Liu, Q. (2014). CaMKII Activity in the Ventral Tegmental Area Gates Cocaine-Induced Synaptic Plasticity in the Nucleus Accumbens. *Neuropsychopharmacology, 39*(4), 989-999. doi:10.1038/npp.2013.299

Liu, Z., Zhang, J., Liu, X., & Yu, L. (2012). Inhibition of CaMKII activity in the nucleus accumbens shell blocks the reinstatement of morphine-seeking behavior in rats. *Neurosci Lett, 518*(2), 167-171. doi:https://doi.org/10.1016/j.neulet.2012.05.003

Lominac, K. D., McKenna, C. L., Schwartz, L. M., Ruiz, P. N., Wroten, M. G., Miller, B. W., . . . Szumlinski, K. K. (2014). Mesocorticolimbic monoamine correlates of methamphetamine sensitization and motivation. *Front Syst Neurosci, 8*(MAY), 70. doi:10.3389/fnsys.2014.00070

Lominac, K. D., Quadir, S. G., Barrett, H. M., McKenna, C. L., Schwartz, L. M., Ruiz, P. N., . . . Szumlinski, K. K. (2016). Prefrontal glutamate correlates of methamphetamine sensitization and preference. *Eur J Neurosci, 43*(5), 689-702. doi:10.1111/ejn.13159

London, E. D., Kohno, M., Morales, A. M., & Ballard, M. E. (2015). Chronic methamphetamine abuse and corticostriatal deficits revealed by neuroimaging. *Brain Research, 1628*, 174-185. doi:https://doi.org/10.1016/j.brainres.2014.10.044

Lu, L., Uejima, J., Gray, S., Bossert, J., & Shaham, Y. (2007). Systemic and Central Amygdala Injections of the mGluR2/3 Agonist LY379268 Attenuate the Expression of Incubation of Cocaine Craving. *Biol Psychiatry, 61*(5), 591-598. doi:https://doi.org/10.1016/j.biopsych.2006.04.011

Lu, Y., Sareddy, G. R., Wang, J., Wang, R., Li, Y., Dong, Y., . . . Brann, D. W. (2019). Neuron-Derived Estrogen Regulates Synaptic Plasticity and Memory. *The Journal of Neuroscience, 39*(15), 2792-2809. doi:10.1523/jneurosci.1970-18.2019

Mackey, S., Allgaier, N., Chaarani, B., Spechler, P., Orr, C., Bunn, J., . . . Garavan, H. (2019). Mega-Analysis of Gray Matter Volume in Substance Dependence: General and Substance-Specific Regional Effects. *Am J Psychiatry, 176*(2), 119-128. doi:10.1176/appi.ajp.2018.17040415

Mahanty, N., & Sah, P. (1998). Calcium-permeable AMPA receptors mediate long-term potentiation in interneurons in the amygdala. *Nature, 394*(6694), 683-687. doi:10.1038/29312

Malarkey, E., & Parpura, V. (2008). Mechanisms of glutamate release from astrocytes. *Neurochem Int, 52*(1-2), 142-154. doi:10.1016/j.neuint.2007.06.005

Maldonado-Irizarry, C., Swanson, C., & Kelley, A. (1995). Glutamate receptors in the nucleus accumbens shell control feeding behavior via the lateral hypothalamus. *The Journal of Neuroscience, 15*(10), 6779. doi:10.1523/JNEUROSCI.15-10-06779.1995

Malvaez, M., & Wassum, K. (2018). Regulation of habit formation in the dorsal striatum. *Current Opinion in Behavioral Sciences, 20*, 67-74. doi:https://doi.org/10.1016/j.cobeha.2017.11.005

Mao, L. M., Jin, D. Z., Xue, B., Chu, X. P., & Wang, J. Q. (2014). Phosphorylation and regulation of glutamate receptors by CaMKII. *Sheng Li Xue Bao, 66*(3), 365-372.

Mash, D. (2016). Excited Delirium and Sudden Death: A Syndromal Disorder at the Extreme End of the Neuropsychiatric Continuum. *Front Physiol, 7*, 435. doi:10.3389/fphys.2016.00435

Maurice, N., Deniau, J., Glowinski, J., & Thierry, A. (1998a). Relationships between the Prefrontal Cortex and the Basal Ganglia in the Rat: Physiology of the

Corticosubthalamic Circuits. *Journal of Neuroscience, 18*(22), 9539-9546. doi:10.1080/009841098158467

Maurice, N., Deniau, J. M., Glowinski, J., & Thierry, A. M. (1998b). Relationships between the Prefrontal Cortex and the Basal Ganglia in the Rat: Physiology of the Corticosubthalamic Circuits. *Journal of Neuroscience, 18*(22), 9539-9546. doi:10.1080/009841098158467

McDonald, A. J. (1991). Organization of amygdaloid projections to the prefrontal cortex and associated striatum in the rat. *Neuroscience, 44*(1), 1-14. doi:10.1016/0306-4522(91)90247-L

McDonald, A. J., Mascagni, F., & Guo, L. (1996). Projections of the medial and lateral prefrontal cortices to the amygdala: a Phaseolus vulgaris leucoagglutinin study in the rat. *Neuroscience, 71*(1), 55-75. doi:https://doi.org/10.1016/0306-4522(95)00417-3

McFarland, K., Lapish, C., & Kalivas, P. (2003). Prefrontal Glutamate Release into the Core of the Nucleus Accumbens Mediates Cocaine-Induced Reinstatement of Drug-Seeking Behavior. *The Journal of Neuroscience, 23*(8), 3531. doi:10.1523/JNEUROSCI.23-08-03531.2003

McGeorge, A. J., & Faull, R. L. M. (1989). The organization of the projection from the cerebral cortex to the striatum in the rat. *Neuroscience, 29*(3), 503-537. doi:https://doi.org/10.1016/0306-4522(89)90128-0

McKetin, R., Lubman, D., Baker, A., Dawe, S., & Ali, R. L. (2013). Dose-related psychotic symptoms in chronic methamphetamine users: evidence from a prospective longitudinal study. *JAMA Psychiatry, 70*(3), 319-324. doi:10.1001/jamapsychiatry.2013.283

McNamee, D., Liljeholm, M., Zika, O., & Doherty, J. P. (2015). Characterizing the Associative Content of Brain Structures Involved in Habitual and Goal-Directed

Actions in Humans: A Multivariate fMRI Study. *The Journal of Neuroscience, 35*(9), 3764. doi:10.1523/JNEUROSCI.4677-14.2015

Medvedev, N., Popov, V., Henneberger, C., Kraev, I., Rusakov, D., & Stewart, M. (2014). Glia selectively approach synapses on thin dendritic spines. *Philos Trans R Soc Lond B Biol Sci, 369*(1654), 20140047. doi:10.1098/rstb.2014.0047

Meil, W., & See, R. (1997). Lesions of the basolateral amygdala abolish the ability of drug associated cues to reinstate responding during withdrawal from self-administered cocaine. *Behav Brain Res, 87*(2), 139-148. doi:https://doi.org/10.1016/S0166-4328(96)02270-X

Mestas, J., & Hughes, C. C. W. (2004). Of Mice and Not Men: Differences between Mouse and Human Immunology. *The Journal of Immunology, 172*(5), 2731. doi:10.4049/jimmunol.172.5.2731

Milad, M., Wright, C., Orr, S., Pitman, R., Quirk, G., & Rauch, S. (2007). Recall of Fear Extinction in Humans Activates the Ventromedial Prefrontal Cortex and Hippocampus in Concert. *Biol Psychiatry, 62*(5), 446-454. doi:10.1016/j.biopsych.2006.10.011

Montaron, M. F., Deniau, J. M., Menetrey, A., Glowinski, J., & Thierry, A. M. (1996). Prefrontal cortex inputs of the nucleus accumbens-nigro-thalamic circuit. *Neuroscience, 71*(2), 371-382. doi:10.1016/0306-4522(95)00455-6

Moorman, D. E., James, M. H., McGlinchey, E. M., & Aston-Jones, G. (2015). Differential roles of medial prefrontal subregions in the regulation of drug seeking. *Brain Research, 1628*, 130-146. doi:https://doi.org/10.1016/j.brainres.2014.12.024

Morley, K., Cornish, J., Faingold, A., Wood, K., & Haber, P. (2017). Pharmacotherapeutic agents in the treatment of methamphetamine dependence. *Expert Opin Investig Drugs, 26*(5), 563-578. doi:10.1080/13543784.2017.1313229

Moussawi, K., & Kalivas, P. (2010). Group II metabotropic glutamate receptors (mGlu2/3) in drug addiction. *Eur J Pharmacol, 639*(1-3), 115-122. doi:10.1016/j.ejphar.2010.01.030

Myme, C., Sugino, K., Turrigiano, G., & Nelson, S. (2003). The NMDA-to-AMPA Ratio at Synapses Onto Layer 2/3 Pyramidal Neurons Is Conserved Across Prefrontal and Visual Cortices. *Journal of Neurophysiology, 90*(2), 771-779. doi:10.1152/jn.00070.2003

Nash, B., Thomson, C., Linington, C., Arthur, A., McClure, J., McBride, M., & Barnett, S. (2011). Functional duality of astrocytes in myelination. *J Neurosci, 31*(37), 13028-13038. doi:10.1523/jneurosci.1449-11.2011

Nevin, J. A. (2012). Resistance to extinction and behavioral momentum. *Behavioural Processes, 90*(1), 89-97. doi:https://doi.org/10.1016/j.beproc.2012.02.006

Oberheim, N., Goldman, S., & Nedergaard, M. (2012). Heterogeneity of astrocytic form and function. *Methods in molecular biology (Clifton, N.J.), 814*, 23-45. doi:10.1007/978-1-61779-452-0_3

Oliveira, J. F., Sardinha, V. M., Guerra-Gomes, S., Araque, A., & Sousa, N. (2015). Do stars govern our actions? Astrocyte involvement in rodent behavior. *Trends Neurosci, 38*(9), 535-549. doi:10.1016/j.tins.2015.07.006

Ongur, D., An, X., & Price, J. L. (1998). Prefrontal cortical projections to the hypothalamus in macaque monkeys. *J Comp Neurol, 401*(4), 480-505.

Ongur, D., & Price, J. (2000). The Organization of Networks within the Orbital and Medial Prefrontal Cortex of Rats, Monkeys and Humans. *Cerebral Cortex, 10*(3), 206-219. doi:10.1093/cercor/10.3.206

Osborne, M., & Olive, M. (2008). A role for mGluR5 receptors in intravenous methamphetamine self-administration. *Ann N Y Acad Sci, 1139*, 206-211. doi:10.1196/annals.1432.034

Ostroff, L., Manzur, M., Cain, C., & Ledoux, J. (2014). Synapses lacking astrocyte appear in the amygdala during consolidation of pavlovian threat conditioning. *Journal of Comparative Neurology, 522*(9), 2152-2163. doi:10.1002/cne.23523

Panenka, W., Procyshyn, R., Lecomte, T., MacEwan, G., Flynn, S., Honer, W., & Barr, A. (2013). Methamphetamine use: a comprehensive review of molecular, preclinical and clinical findings. *Drug Alcohol Depend, 129*(3), 167-179. doi:10.1016/j.drugalcdep.2012.11.016

Panlilio, L., & Goldberg, S. (2007). Self-administration of drugs in animals and humans as a model and an investigative tool. *Addiction, 102*(12), 1863-1870.

Papadimitriou, D., Xanthos, T., Dontas, I., Lelovas, P., & Perrea, D. (2008). The use of mice and rats as animal models for cardiopulmonary resuscitation research. *Laboratory Animals, 42*(3), 265-276. doi:10.1258/la.2007.006035

Pape, H., & Pare, D. (2010). Plastic Synaptic Networks of the Amygdala for the Acquisition, Expression, and Extinction of Conditioned Fear. *Physiological Reviews, 90*(2), 419-463. doi:10.1152/physrev.00037.2009

Parpura, V., Heneka, M. T., Montana, V., Oliet, S. H. R., Schousboe, A., Haydon, P. G., . . . Verkhratsky, A. (2012). Glial cells in (patho)physiology. *J Neurochem, 121*(1), 4-27. doi:10.1111/j.1471-4159.2012.07664.x

Parpura, V., & Zorec, R. (2010). Gliotransmission: Exocytotic release from astrocytes. *Brain Research Reviews, 63*(1), 83-92. doi:https://doi.org/10.1016/j.brainresrev.2009.11.008

Parsegian, A., & See, R. (2013). Dysregulation of Dopamine and Glutamate Release in the Prefrontal Cortex and Nucleus Accumbens Following Methamphetamine Self-

Administration and During Reinstatement in Rats. *Neuropsychopharmacology, 39*(4), 811. doi:10.1038/npp.2013.231

Perea, G., Navarrete, M., & Araque, A. (2009). Tripartite synapses: astrocytes process and control synaptic information. *Trends Neurosci, 32*(8), 421-431. doi:10.1016/j.tins.2009.05.001

Perez-Costas, E., Melendez-Ferro, M., & Roberts, R. C. (2010). Basal ganglia pathology in schizophrenia: dopamine connections and anomalies. *J Neurochem, 113*(2), 287-302. doi:10.1111/j.1471-4159.2010.06604.x

Peters, J., LaLumiere, R. T., & Kalivas, P. W. (2008). Infralimbic Prefrontal Cortex Is Responsible for Inhibiting Cocaine Seeking in Extinguished Rats. *The Journal of Neuroscience, 28*(23), 6046. doi:10.1523/JNEUROSCI.1045-08.2008

Piazza, P. V., & Deroche-Gamonet, V. (2013). A multistep general theory of transition to addiction. *Psychopharmacology (Berl), 229*(3), 387-413. doi:10.1007/s00213-013-3224-4

Pitkänen, A., Pikkarainen, M., Nurminen, N., & Ylinen, A. (2000). Reciprocal Connections between the Amygdala and the Hippocampal Formation, Perirhinal Cortex, and Postrhinal Cortex in Rat: A Review. *Ann N Y Acad Sci, 911*(1), 369-391. doi:10.1111/j.1749-6632.2000.tb06738.x

Pitkänen, A., Stefanacci, L., Farb, C., Go, G., Ledoux, J., & Amaral, D. (1995). Intrinsic connections of the rat amygdaloid complex: Projections originating in the lateral nucleus. *Journal of Comparative Neurology, 356*(2), 288-310. doi:10.1002/cne.903560211

Pomierny-Chamiolo, L., Miszkiel, J., Frankowska, M., Pomierny, B., Niedzielska, E., Smaga, I., . . . Filip, M. (2015). Withdrawal from Cocaine Self-administration and Yoked Cocaine Delivery Dysregulates Glutamatergic mGlu 5 and NMDA Receptors in the

Rat Brain. *Neurodegeneration, Neuroregeneration, Neurotrophic Action, and Neuroprotection, 27*(3), 246-258. doi:10.1007/s12640-014-9502-z

Pompey, S. N., Michaely, P., & Luby-Phelps, K. (2013). Quantitative Fluorescence Co-localization to Study Protein–Receptor Complexes. In M. A. Williams & T. Daviter (Eds.), *Protein-Ligand Interactions: Methods and Applications* (pp. 439-453). Totowa, NJ: Humana Press.

Price, K., Saladin, M., Baker, N., Tolliver, B., DeSantis, S., McRae-Clark, A., & Brady, K. (2010). Extinction of drug cue reactivity in methamphetamine-dependent individuals. *Behaviour Research and Therapy, 48*(9), 860-865. doi:https://doi.org/10.1016/j.brat.2010.05.010

Quirk, G., & Mueller, D. (2007). Neural Mechanisms of Extinction Learning and Retrieval. *Neuropsychopharmacology, 33*, 56. doi:10.1038/sj.npp.1301555

Rahman, S., & McBride, W. J. (2002). Involvement of GABA and cholinergic receptors in the nucleus accumbens on feedback control of somatodendritic dopamine release in the ventral tegmental area. *J Neurochem, 80*(4), 646-654. doi:10.1046/j.0022-3042.2001.00739.x

Raineri, M., Gonzalez, B., Goitia, B., Garcia-Rill, E., Krasnova, I., Cadet, J., . . . Bisagno, V. (2012). Modafinil abrogates methamphetamine-induced neuroinflammation and apoptotic effects in the mouse striatum. *PLoS One, 7*(10), e46599. doi:10.1371/journal.pone.0046599

Ramesh, G., MacLean, A., & Philipp, M. (2013). Cytokines and Chemokines at the Crossroads of Neuroinflammation, Neurodegeneration, and Neuropathic Pain. *Mediators of Inflammation, 2013*(2013), 480739. doi:10.1155/2013/480739

Ransohoff, R., & Brown, M. (2012). Innate immunity in the central nervous system. *Journal of Clinical Investigation, 122*(4), 1164-1171. doi:10.1172/JCI58644

Reep, R., Corwin, J., & King, V. (1996). Neuronal connections of orbital cortex in rats: topography of cortical and thalamic afferents. *Experimental Brain Research, 111*(2), 215-232. doi:10.1007/BF00227299

Rezaei, F., Emami, M., Zahed, S., Morabbi, M., Farahzadi, M., & Akhondzadeh, S. (2015). Sustained-release methylphenidate in methamphetamine dependence treatment: a double-blind and placebo-controlled trial. *DARU Journal of Pharmaceutical Sciences, 23*(1). doi:10.1186/s40199-015-0092-y

Rezaei, F., Ghaderi, E., Mardani, R., Hamidi, S., & Hassanzadeh, K. (2016). Topiramate for the management of methamphetamine dependence: a pilot randomized, double-blind, placebo-controlled trial. *Fundam Clin Pharmacol, 30*(3), 282-289. doi:10.1111/fcp.12178

Richardson, N., & Roberts, D. (1996). Progressive ratio schedules in drug self-administration studies in rats: a method to evaluate reinforcing efficacy. *J Neurosci Methods, 66*(1), 1-11. Retrieved from https://www.ncbi.nlm.nih.gov/pubmed/8794935

Robbins, T. (1976). Relationship between reward-enhancing and stereotypical effects of psychomotor stimulant drugs. *Nature, 264*(5581), 57-59. doi:10.1038/264057a0

Robinson, T., & Berridge, K. (2008). Review. The incentive sensitization theory of addiction: some current issues. *Philos Trans R Soc Lond B Biol Sci, 363*(1507), 3137-3146. doi:10.1098/rstb.2008.0093

Robinson, T., & Flagel, S. (2009). Dissociating the Predictive and Incentive Motivational Properties of Reward-Related Cues Through the Study of Individual Differences. *Biol Psychiatry, 65*(10), 869-873. doi:https://doi.org/10.1016/j.biopsych.2008.09.006

Robinson, T. E., & Berridge, K. C. (1993). The neural basis of drug craving: an incentive-sensitization theory of addiction. *Brain Res Brain Res Rev, 18*(3), 247-291. doi:10.1016/0165-0173(93)90013-P

Robinson, T. E., & Kolb, B. (1997). Persistent structural modifications in nucleus accumbens and prefrontal cortex neurons produced by previous experience with amphetamine. *J Neurosci, 17*(21), 8491-8497. Retrieved from https://www.ncbi.nlm.nih.gov/pubmed/9334421

Robson, M., Turner, R., Naser, Z., McCurdy, C., O'Callaghan, J., Huber, J., & Matsumoto, R. (2014). SN79, a sigma receptor antagonist, attenuates methamphetamine-induced astrogliosis through a blockade of OSMR/gp130 signaling and STAT3 phosphorylation. *Experimental Neurology, 254*, 180-189. doi:10.1016/j.expneurol.2014.01.020

Rocha, A., & Kalivas, P. W. (2010). Role of the prefrontal cortex and nucleus accumbens in reinstating methamphetamine seeking. *European Journal of Neuroscience, 31*(5), 903-909. doi:10.1111/j.1460-9568.2010.07134.x

Rocha, S., Cristovão, A., Campos, F., Fonseca, C., & Baltazar, G. (2012). Astrocyte-derived GDNF is a potent inhibitor of microglial activation. *Neurobiology of Disease, 47*(3), 407-415. doi:10.1016/j.nbd.2012.04.014

Roitman, M. F., Wheeler, R. A., Wightman, R. M., & Carelli, R. M. (2008). Real-time chemical responses in the nucleus accumbens differentiate rewarding and aversive stimuli. *Nature Neuroscience, 11*(12), 1376-1377. doi:10.1038/nn.2219

Rose, M., & Grant, J. (2008). Pharmacotherapy for methamphetamine dependence: a review of the pathophysiology of methamphetamine addiction and the theoretical basis and efficacy of pharmacotherapeutic interventions. *Annals of clinical psychiatry : official journal of the American Academy of Clinical Psychiatrists, 20*(3), 145. doi:10.1080/10401230802177656

Rothman, R., Baumann, M., Dersch, C., Romero, D., Rice, K., Carroll, F., & Partilla, J. (2001). Amphetamine-type central nervous system stimulants release norepinephrine more potently than they release dopamine and serotonin. *Synapse, 39*(1), 32-41.

Royer, S., Martina, M., & Paré, D. (1999). An Inhibitory Interface Gates Impulse Traffic between the Input and Output Stations of the Amygdala. *The Journal of Neuroscience, 19*(23), 10575. doi:10.1523/JNEUROSCI.19-23-10575.1999

Rubio, F. J., Quintana-Feliciano, R., Warren, B. L., Li, X., Witonsky, K. F. R., Valle, F. S. D., . . . Hope, B. T. (2019). Prelimbic cortex is a common brain area activated during cue-induced reinstatement of cocaine and heroin seeking in a polydrug self-administration rat model. *Eur J Neurosci, 49*(2), 165-178. doi:10.1111/ejn.14203

Rusakov, D. (2001). The Role of Perisynaptic Glial Sheaths in Glutamate Spillover and Extracellular Ca2+ Depletion. *Biophysical Journal, 81*(4), 1947-1959. doi:https://doi.org/10.1016/S0006-3495(01)75846-8

Russchen, F. T., Bakst, I., Amaral, D. G., & Price, J. L. (1985). The amygdalostriatal projections in the monkey. An anterograde tracing study. *Brain Research, 329*(1-2), 241-257. doi:10.1016/0006-8993(85)90530-X

Salgado, S., & Kaplitt, M. (2015a). The Nucleus Accumbens: A Comprehensive Review. *Stereotact Funct Neurosurg, 93*(2), 75-93. doi:10.1159/000368279

Salgado, S., & Kaplitt, M. G. (2015b). The Nucleus Accumbens: A Comprehensive Review. *Stereotact Funct Neurosurg, 93*(2), 75-93. doi:10.1159/000368279

Sampedro-Piquero, P., De Bartolo, P., Petrosini, L., Zancada-Menendez, C., Arias, J. L., & Begega, A. (2014). Astrocytic plasticity as a possible mediator of the cognitive improvements after environmental enrichment in aged rats. *Neurobiology of Learning and Memory, 114*, 16-25. doi:https://doi.org/10.1016/j.nlm.2014.04.002

Sari, Y., & Sreemantula, S. N. (2012). Neuroimmunophilin GPI-1046 reduces ethanol consumption in part through activation of GLT1 in alcohol-preferring rats. *Neuroscience, 227*, 327-335. doi:10.1016/j.neuroscience.2012.10.007

Saur, L., Baptista, P. P. A., de Senna, P. N., Paim, M. F., Nascimento, P. d., Ilha, J., . . . Xavier, L. L. (2014). Physical exercise increases GFAP expression and induces morphological changes in hippocampal astrocytes. *Brain Structure and Function, 219*(1), 293-302. doi:10.1007/s00429-012-0500-8

Savander, V., Go, G., Ledoux, J., & Pitkänen, A. (1995). Intrinsic connections of the rat amygdaloid complex: Projections originating in the basal nucleus. *Journal of Comparative Neurology, 361*(2), 345-368. doi:10.1002/cne.903610211

Schoenbaum, G., Roesch, M., & Stalnaker, T. (2006). Orbitofrontal cortex, decision-making and drug addiction. *Trends in Neurosciences*, 116-124.

Schultz, W. (1998). Predictive Reward Signal of Dopamine Neurons. In W. Schultz (Ed.), (Vol. 80, pp. 1-27).

Schwendt, M., Reichel, C., & See, R. (2012). Extinction-dependent alterations in corticostriatal mGluR2/3 and mGluR7 receptors following chronic methamphetamine self-administration in rats. *PLoS One, 7*(3), e34299. doi:10.1371/journal.pone.0034299

Scofield, M., Boger, H., Smith, R., Li, H., Haydon, P., & Kalivas, P. (2015). Gq-DREADD Selectively Initiates Glial Glutamate Release and Inhibits Cue-induced Cocaine Seeking. *Biol Psychiatry, 78*(7), 441-451. doi:https://doi.org/10.1016/j.biopsych.2015.02.016

Scofield, M., Li, H., Siemsen, B., Healey, K., Tran, P., Woronoff, N., . . . Reissner, K. (2016a). Cocaine Self-Administration and Extinction Leads to Reduced Glial Fibrillary Acidic Protein Expression and Morphometric Features of Astrocytes in the

Nucleus Accumbens Core. *Biol Psychiatry, 80*(3), 207-215. doi:10.1016/j.biopsych.2015.12.022

Scofield, M. D. (2018). Exploring the Role of Astroglial Glutamate Release and Association With Synapses in Neuronal Function and Behavior. *Biol Psychiatry, 84*(11), 778-786. doi:10.1016/j.biopsych.2017.10.029

Scofield, M. D., Li, H., Siemsen, B. M., Healey, K. L., Tran, P. K., Woronoff, N., . . . Reissner, K. J. (2016b). Cocaine Self-Administration and Extinction Leads to Reduced Glial Fibrillary Acidic Protein Expression and Morphometric Features of Astrocytes in the Nucleus Accumbens Core. *Biological Psychiatry, 80*(3), 207-215. doi:10.1016/j.biopsych.2015.12.022

See, R. E., Kruzich, P. J., & Grimm, J. W. (2001). Dopamine, but not glutamate, receptor blockade in the basolateral amygdala attenuates conditioned reward in a rat model of relapse to cocaine-seeking behavior. *Psychopharmacology, 154*(3), 301-310. doi:10.1007/s002130000636

Sellings, L., & Clarke, P. (2003). Segregation of Amphetamine Reward and Locomotor Stimulation between Nucleus Accumbens Medial Shell and Core. *The Journal of Neuroscience, 23*(15), 6295. doi:10.1523/JNEUROSCI.23-15-06295.2003

Shah, A., Kumar, S., Simon, S. D., Singh, D. P., & Kumar, A. (2013). HIV gp120- and methamphetamine-mediated oxidative stress induces astrocyte apoptosis via cytochrome P450 2E1. *Cell death & disease, 4*(10), e850-e850. doi:10.1038/cddis.2013.374

Shen, H., Scofield, M., Boger, H., Hensley, M., & Kalivas, P. (2014). Synaptic Glutamate Spillover Due to Impaired Glutamate Uptake Mediates Heroin Relapse. *The Journal of Neuroscience, 34*(16), 5649. doi:10.1523/JNEUROSCI.4564-13.2014

Siemsen, B., Reichel, C., Leong, K., Garcia-Keller, C., Gipson, C., Spencer, S., . . . Scofield, M. (2019). Effects of Methamphetamine Self-Administration and Extinction on Astrocyte Structure and Function in the Nucleus Accumbens Core. *Neuroscience, 406*, 528-541. doi:https://doi.org/10.1016/j.neuroscience.2019.03.040

Smith, R., Lobo, M., Spencer, S., & Kalivas, P. (2013). Cocaine-induced adaptations in D1 and D2 accumbens projection neurons (a dichotomy not necessarily synonymous with direct and indirect pathways). *Current Opinion in Neurobiology, 23*(4), 546-552. doi:10.1016/j.conb.2013.01.026

Smith, R. J., & Laiks, L. S. (2018). Behavioral and neural mechanisms underlying habitual and compulsive drug seeking. *Prog Neuropsychopharmacol Biol Psychiatry, 87*(Pt A), 11-21. doi:10.1016/j.pnpbp.2017.09.003

Sofroniew, M. (2015). Astrogliosis. *Cold Spring Harbor Perspectives in Biology, 7*(2). Retrieved from http://cshperspectives.cshlp.org/content/7/2/a020420.abstract

Spencer, S., Scofield, M., & Kalivas, P. W. (2016). The good and bad news about glutamate in drug addiction. *J Psychopharmacol, 30*(11), 1095-1098. doi:10.1177/0269881116655248

Stefanik, M., & Kalivas, P. (2013). Optogenetic dissection of basolateral amygdala projections during cue-induced reinstatement of cocaine seeking. *Frontiers in Behavioral Neuroscience, 7*, 213. Retrieved from https://www.frontiersin.org/article/10.3389/fnbeh.2013.00213

Tavares, G., Martins, M., Correia, J. S., Sardinha, V. M., Guerra-Gomes, S., das Neves, S. P., . . . Oliveira, J. F. (2017). Employing an open-source tool to assess astrocyte tridimensional structure. *Brain Structure and Function, 222*(4), 1989-1999. doi:10.1007/s00429-016-1316-8

Tepper, J., Koós, T., Ibanez-Sandoval, O., Tecuapetla, F., Faust, T., & Assous, M. (2018). Heterogeneity and Diversity of Striatal GABAergic Interneurons: Update 2018. *Frontiers in Neuroanatomy, 12*, 91. Retrieved from https://www.frontiersin.org/article/10.3389/fnana.2018.00091

Thomas, D. M., & Kuhn, D. M. (2005). Attenuated microglial activation mediates tolerance to the neurotoxic effects of methamphetamine. *J Neurochem, 92*(4), 790-797. doi:10.1111/j.1471-4159.2004.02906.x

Thompson, P. M., Hayashi, K. M., Simon, S. L., Geaga, J. A., Hong, M. S., Sui, Y., . . . London, E. D. (2004). Structural abnormalities in the brains of human subjects who use methamphetamine. *J Neurosci, 24*(26), 6028-6036. doi:10.1523/jneurosci.0713-04.2004

Tobias, M. C., O'Neill, J., Hudkins, M., Bartzokis, G., Dean, A. C., & London, E. D. (2010). White-matter abnormalities in brain during early abstinence from methamphetamine abuse. *Psychopharmacology, 209*(1), 13-24. doi:10.1007/s00213-009-1761-7

Tomie, A., Grimes, K., & Pohorecky, L. (2008). Behavioral characteristics and neurobiological substrates shared by Pavlovian sign-tracking and drug abuse. *Brain Research Reviews, 58*(1), 121-135. doi:https://doi.org/10.1016/j.brainresrev.2007.12.003

Torres, O., Jayanthi, S., Ladenheim, B., McCoy, M., Krasnova, I., & Cadet, J. (2017). Compulsive methamphetamine taking under punishment is associated with greater cue-induced drug seeking in rats. *Behav Brain Res, 326*, 265-271. doi:10.1016/j.bbr.2017.03.009

Tricomi, E., Balleine, B., & O'Doherty, J. (2009). A specific role for posterior dorsolateral striatum in human habit learning. *Eur J Neurosci, 29*(11), 2225-2232. doi:10.1111/j.1460-9568.2009.06796.x

Ungless, M. (2004). Dopamine: the salient issue. *Trends in Neurosciences, 27*(12), 702-706. doi:https://doi.org/10.1016/j.tins.2004.10.001

United Nations Office on Drugs and Crime. (2016). *World Drug Report.* Retrieved from http://www.unodc.org/wdr2015/

United Nations Office on Drugs and Crime. (2018). *World Drug Report 2018* (2). Retrieved from

Van Bockstaele, E. J., & Pickel, V. M. (1995). GABA-containing neurons in the ventral tegmental area project to the nucleus accumbens in rat brain. *Brain Research, 682*(1-2), 215-221. doi:10.1016/0006-8993(95)00334-M

Vanderschuren, L., Di Ciano, P., & Everitt, B. (2005). Involvement of the dorsal striatum in cue-controlled cocaine seeking. *J Neurosci, 25*(38), 8665-8670. doi:10.1523/JNEUROSCI.0925-05.2005

Verkhratsky, A., & Parpura, V. (2016). Astrogliopathology in neurological, neurodevelopmental and psychiatric disorders. *Neurobiology of Disease, 85*, 254-261. doi:10.1016/j.nbd.2015.03.025

Vickers, J., Huntley, G., Edwards, A., Moran, T., Rogers, S., Heinemann, S., & Morrison, J. (1993). Quantitative localization of AMPA/kainate and kainate glutamate receptor subunit immunoreactivity in neurochemically identified subpopulations of neurons in the prefrontal cortex of the macaque monkey. *The Journal of Neuroscience, 13*(7), 2982. doi:10.1523/JNEUROSCI.13-07-02982.1993

Volkow, N. D., Fowler, J. S., & Wang, G.-J. (2003). The addicted human brain: insights from imaging studies. *The Journal of Clinical Investigation, 111*(10), 1444-1451. doi:10.1172/JCI18533

Volkow, N. D., & Morales, M. (2015). The Brain on Drugs: From Reward to Addiction. *Cell, 162*(4), 712-725. doi:10.1016/j.cell.2015.07.046

Voskuhl, R., Peterson, R., Song, B., Ao, Y., Morales, L., Tiwari-Woodruff, S., & Sofroniew, M. (2009). Reactive astrocytes form scar-like perivascular barriers to leukocytes during adaptive immune inflammation of the CNS. *J Neurosci, 29*(37), 11511-11522. doi:10.1523/jneurosci.1514-09.2009

Wagner, F. (2002). From First Drug Use to Drug Dependence Developmental Periods of Risk for Dependence upon Marijuana, Cocaine, and Alcohol. *Neuropsychopharmacology, 26*(4), 479-488. doi:10.1016/s0893-133x(01)00367-0

Wall, Nicholas R., De La Parra, M., Callaway, Edward M., & Kreitzer, Anatol C. (2013). Differential Innervation of Direct- and Indirect-Pathway Striatal Projection Neurons. *Neuron, 79*(2), 347-360. doi:https://doi.org/10.1016/j.neuron.2013.05.014

Wallis, J. D. (2011). Cross-species studies of orbitofrontal cortex and value-based decision-making. *Nature Neuroscience, 15*(1), 13-19. doi:10.1038/nn.2956

Walsh, J., & Han, M. (2014). The heterogeneity of ventral tegmental area neurons: Projection functions in a mood-related context. *Neuroscience, 282*, 101-108. doi:https://doi.org/10.1016/j.neuroscience.2014.06.006

Wang, G., Shi, J., Chen, N., Xu, L., Li, J., Li, P., . . . Lu, L. (2013). Effects of length of abstinence on decision-making and craving in methamphetamine abusers. *PLoS One, 8*(7), e68791. doi:10.1371/journal.pone.0068791

Wang, L., Lv, Z., Hu, Z., Sheng, J., Hui, B., Sun, J., & Ma, L. (2010). Chronic cocaine-induced H3 acetylation and transcriptional activation of CaMKIIalpha in the nucleus accumbens is critical for motivation for drug reinforcement. *Neuropsychopharmacology, 35*(4), 913-928. doi:10.1038/npp.2009.193

Wanner, I., Anderson, M., Song, B., Levine, J., Fernandez, A., Gray-Thompson, Z., . . . Sofroniew, M. (2013). Glial scar borders are formed by newly proliferated, elongated astrocytes that interact to corral inflammatory and fibrotic cells via STAT3-dependent

mechanisms after spinal cord injury. *J Neurosci, 33*(31), 12870-12886. doi:10.1523/jneurosci.2121-13.2013

Ward, A., Haney, M., Fischman, M., & Foltin, R. (1997). Binge cocaine self-administration in humans: intravenous cocaine. *Psychopharmacology, 132*(4), 375-381. doi:10.1007/s002130050358

Warr, O., Takahashi, M., & Attwell, D. (1999). Modulation of extracellular glutamate concentration in rat brain slices by cystine-glutamate exchange. *The Journal of Physiology, 514 (Pt 3)*(Pt 3), 783-793. doi:10.1111/j.1469-7793.1999.783ad.x

Wassum, K. M., & Izquierdo, A. (2015). The basolateral amygdala in reward learning and addiction. *Neurosci Biobehav Rev, 57*, 271-283. doi:10.1016/j.neubiorev.2015.08.017

Waters, R. P., Moorman, D. E., Young, A. B., Feltenstein, M. W., & See, R. E. (2014). Assessment of a proposed "three-criteria" cocaine addiction model for use in reinstatement studies with rats. *Psychopharmacology (Berl), 231*(16), 3197-3205. doi:10.1007/s00213-014-3497-2

Weeks, J. (1961). *Self-maintained morphine "addiction": a method for chronic programmed intravenous injection in unrestrained rats.* Paper presented at the Fed. Proc.

Whitelaw, R., Markou, A., Robbins, T., & Everitt, B. (1996). Excitotoxic lesions of the basolateral amygdala impair the acquisition of cocaine-seeking behaviour under a second-order schedule of reinforcement. *Psychopharmacology, 127*(1), 213-224. doi:10.1007/BF02805996

Wilhelmsson, U., Bushong, E., Price, D. L., Smarr, B. L., Phung, V., Terada, M., . . . Pekny, M. (2006). Redefining the concept of reactive astrocytes as cells that remain within their unique domains upon reaction to injury. *Proc Natl Acad Sci U S A, 103*(46), 17513-17518. doi:10.1073/pnas.0602841103

Williams, D. J., Crossman, A. R., & Slater, P. (1977). The efferent projections of the nucleus accumbens in the rat. *Brain Research, 130*(2), 217-227. doi:10.1016/0006-8993(77)90271-2

Williams, S., Sullivan, R., Scott, H., Finkelstein, D., Colditz, P., Lingwood, B., . . . Pow, D. (2005). Glial glutamate transporter expression patterns in brains from multiple mammalian species. *Glia, 49*(4), 520-541. doi:10.1002/glia.20139

Wolf, M. (2010). Regulation of AMPA receptor trafficking in the nucleus accumbens by dopamine and cocaine. *Neurotox Res, 18*(3-4), 393-409. doi:10.1007/s12640-010-9176-0

Wolf, M. E., & Ferrario, C. R. (2010). AMPA receptor plasticity in the nucleus accumbens after repeated exposure to cocaine. *Neuroscience & Biobehavioral Reviews, 35*(2), 185-211. doi:https://doi.org/10.1016/j.neubiorev.2010.01.013

Xi, Z., Baker, D., Shen, H., Carson, D., & Kalivas, P. (2002). Group II Metabotropic Glutamate Receptors Modulate Extracellular Glutamate in the Nucleus Accumbens. *Journal of Pharmacology and Experimental Therapeutics, 300*(1), 162. doi:10.1124/jpet.300.1.162

Yager, L., Garcia, A., Wunsch, A., & Ferguson, S. (2015). The ins and outs of the striatum: role in drug addiction. *Neuroscience, 301*, 529-541. doi:10.1016/j.neuroscience.2015.06.033

Yan, Y., Miyamoto, Y., Nitta, A., Muramatsu, S., Ozawa, K., Yamada, K., & Nabeshima, T. (2013). Intrastriatal gene delivery of GDNF persistently attenuates methamphetamine self-administration and relapse in mice. *International Journal of Neuropsychopharmacology, 16*(7), 1559-1567. doi:10.1017/S1461145712001575

Yan, Y., Yamada, K., Niwa, M., Nagai, T., Nitta, A., & Nabeshima, T. (2007). Enduring vulnerability to reinstatement of methamphetamine-seeking behavior in glial cell line-

derived neurotrophic factor mutant mice. *The FASEB Journal, 21*(9), 1994-2004. doi:10.1096/fj.06-7772com

Yang, C., & Mogenson, G. (1984). Electrophysiological responses of neurones in the nucleus accumbens to hippocampal stimulation and the attenuation of the excitatory responses by the mesolimbic dopaminergic system. *Brain Research, 324*(1), 69-84. doi:10.1016/0006-8993(84)90623-1

Yang, C. R., & Mogenson, G. J. (1989). Ventral pallidal neuronal responses to dopamine receptor stimulation in the nucleus accumbens. *Brain Research, 489*(2), 237-246. doi:10.1016/0006-8993(89)90856-1

Yang, M. H., Jung, M. S., Lee, M. J., Yoo, K. H., Yook, Y. J., Park, E. Y., . . . Park, J. H. (2008). Gene expression profiling of the rewarding effect caused by methamphetamine in the mesolimbic dopamine system. *Mol Cells, 26*(2), 121-130. Retrieved from https://www.ncbi.nlm.nih.gov/pubmed/18594179

Yang, X., Wang, Y., Li, Q., Zhong, Y., Chen, L., Du, Y., . . . Yan, J. (2018). The Main Molecular Mechanisms Underlying Methamphetamine- Induced Neurotoxicity and Implications for Pharmacological Treatment. *Front Mol Neurosci, 11*, 186. doi:10.3389/fnmol.2018.00186

Yang, Z., & Wang, K. (2015). Glial fibrillary acidic protein: from intermediate filament assembly and gliosis to neurobiomarker. *Trends in Neurosciences, 38*(6), 364-374. doi:https://doi.org/10.1016/j.tins.2015.04.003

Yashiro, K., & Philpot, B. (2008). Regulation of NMDA receptor subunit expression and its implications for LTD, LTP, and metaplasticity. *Neuropharmacology, 55*(7), 1081-1094. doi:10.1016/j.neuropharm.2008.07.046

Young, A. M. J. (2004). Increased extracellular dopamine in nucleus accumbens in response to unconditioned and conditioned aversive stimuli: studies using 1 min microdialysis

in rats. *J Neurosci Methods, 138*(1), 57-63. doi:https://doi.org/10.1016/j.jneumeth.2004.03.003

Zahm, D. S., & Heimer, L. (1993). Specificity in the efferent projections of the nucleus accumbens in the rat: Comparison of the rostral pole projection patterns with those of the core and shell. *Journal of Comparative Neurology, 327*(2), 220-232. doi:10.1002/cne.903270205

Zhang, T., Yanagida, J., Kamii, H., Wada, S., Domoto, M., Sasase, H., . . . Kaneda, K. (2019). Glutamatergic neurons in the medial prefrontal cortex mediate the formation and retrieval of cocaine-associated memories in mice. *Addict Biol*. doi:10.1111/adb.12723

Zhang, Z., Gong, Q., Feng, X., Zhang, D., & Li, Q. (2017). Astrocytic clasmatodendrosis in the cerebral cortex of methamphetamine abusers. *Forensic Sciences Research, 2*(3), 144. doi:10.1080/20961790.2017.1280890

Zorick, T., Rad, D., Rim, C., & Tsuang, J. (2008). An overview of methamphetamine-induced psychotic syndromes. *Addictive Disorders & Their Treatment, 7*(3), 143-156.